

Supplementary Material

Synthesis, Reactivity and Antimicrobial Activity of a Series of 2-Arylamino-1,3-Selenazoles.

Julia Kuchar ¹, Katharina Reinhold ¹, Vera Rösgen ¹, Nils Nöthling ², Christian W. Lehmann ² and Fabian Mohr ^{1,*}

¹ Anorganische Chemie, Fakultät für Mathematik und Naturwissenschaften, Bergische Universität Wuppertal, Gaußstr. 20, 42119 Wuppertal, Germany.

² Max-Planck-Institut für Kohlenforschung, Kaiser-Wilhelm-Platz 1, 45470 Mülheim an der Ruhr, Germany.

Contents

Figures S 1-S 124. Proton, carbon and selenium NMR spectra of the compounds.

Table S 1. Crystallographic and refinement details.

Experimental details of the X-ray structure determinations

Experimental details of the biological studies

Results of the NCI 60 screening

Compound 2a

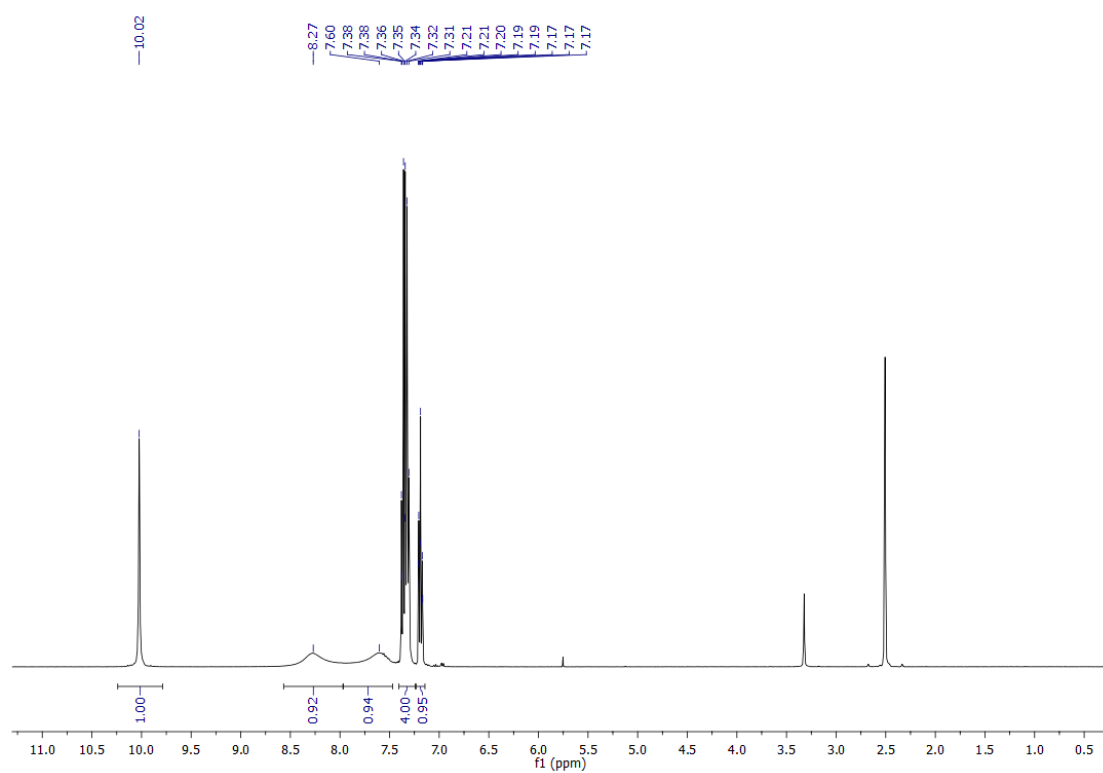


Figure S 1: ¹H-NMR (400 MHz, DMSO- d_6) of compound 2a

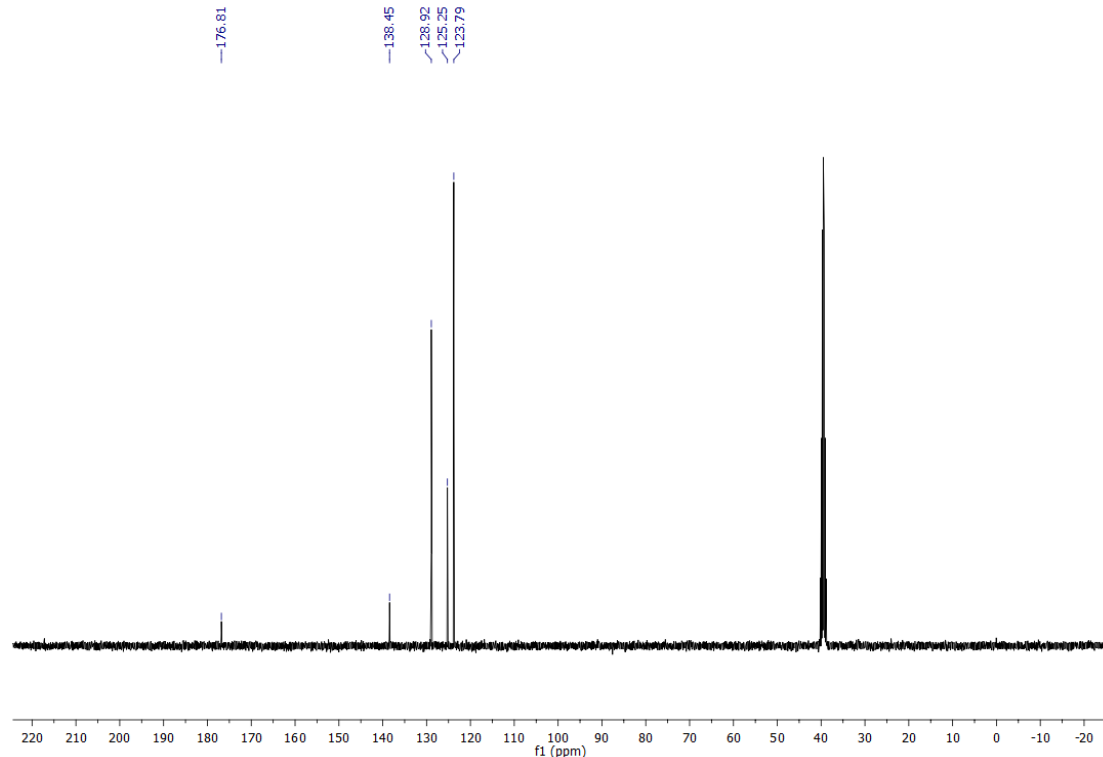


Figure S 2: ¹³C-NMR (101 MHz, DMSO- d_6) of compound 2a

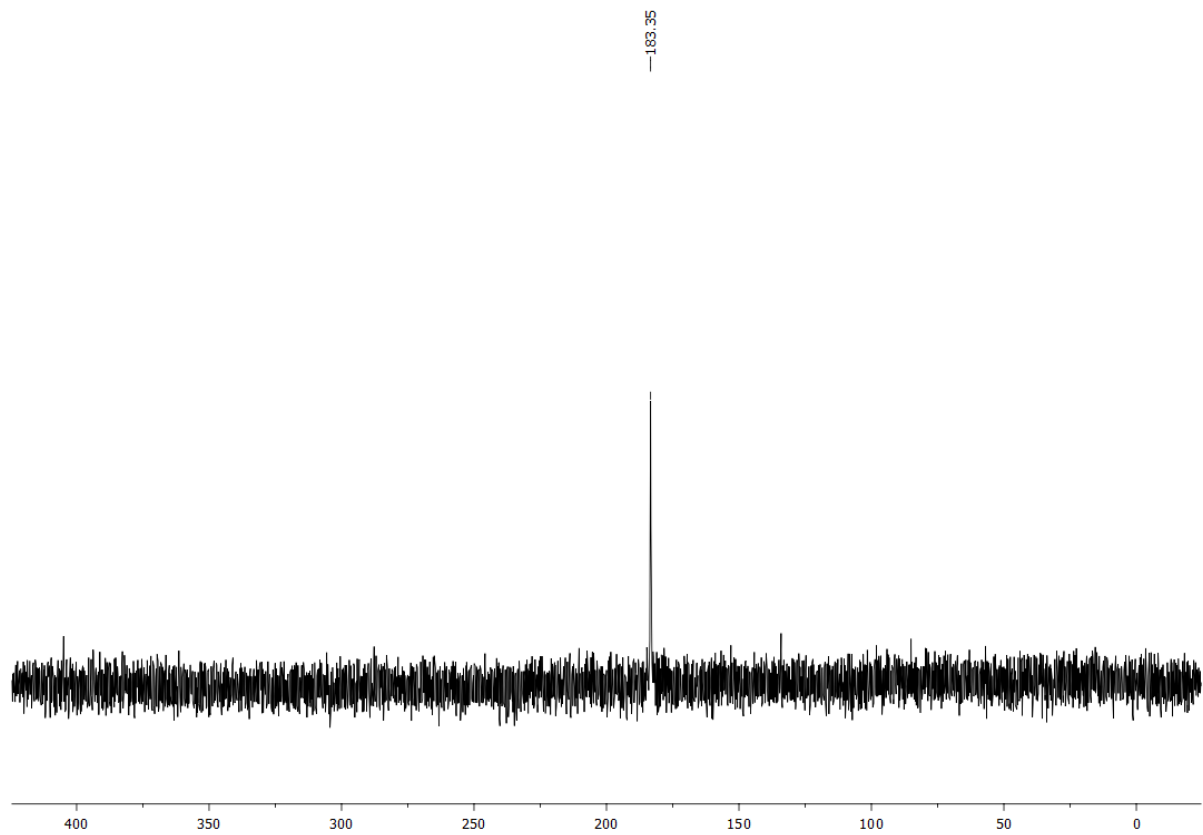


Figure S 3: ^{77}Se -NMR (76 MHz, MeOD, 248 K) of compound 2a

Compound 2b

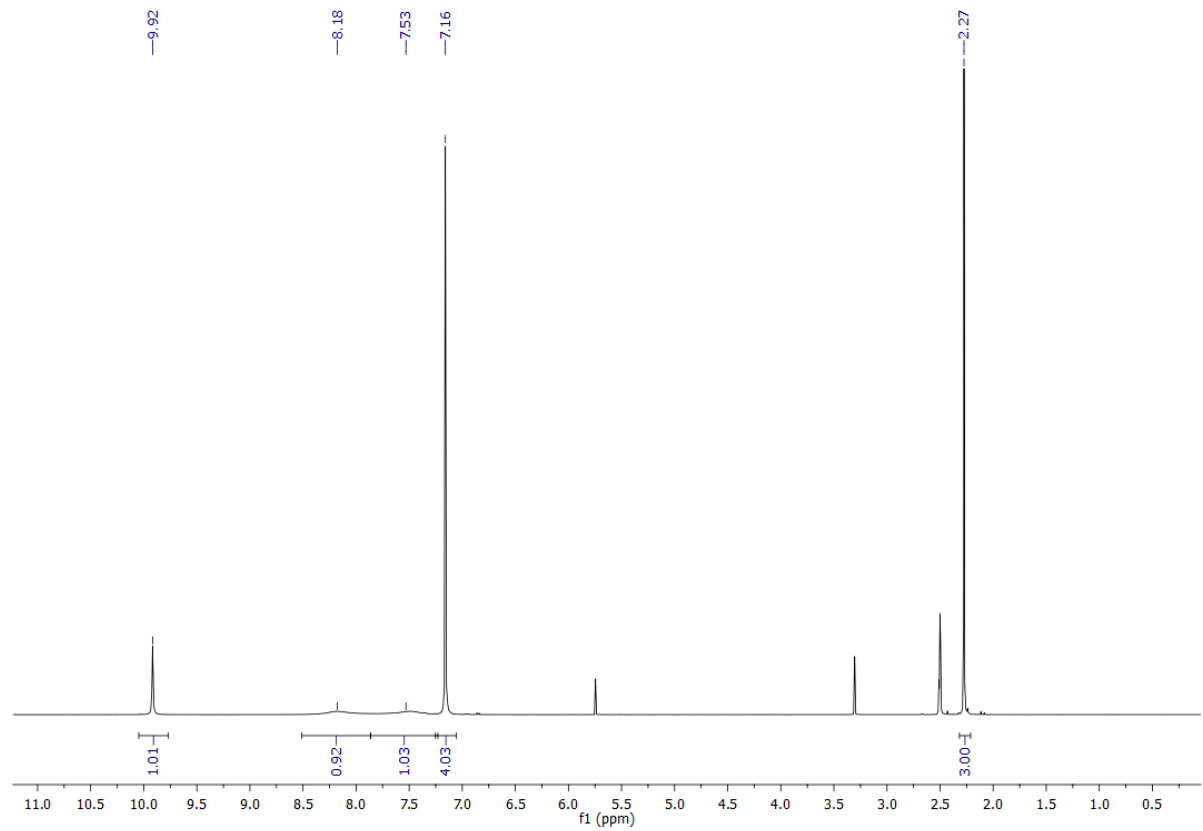


Figure S 4: ^1H -NMR (400 MHz, DMSO- d_6) of compound 2b

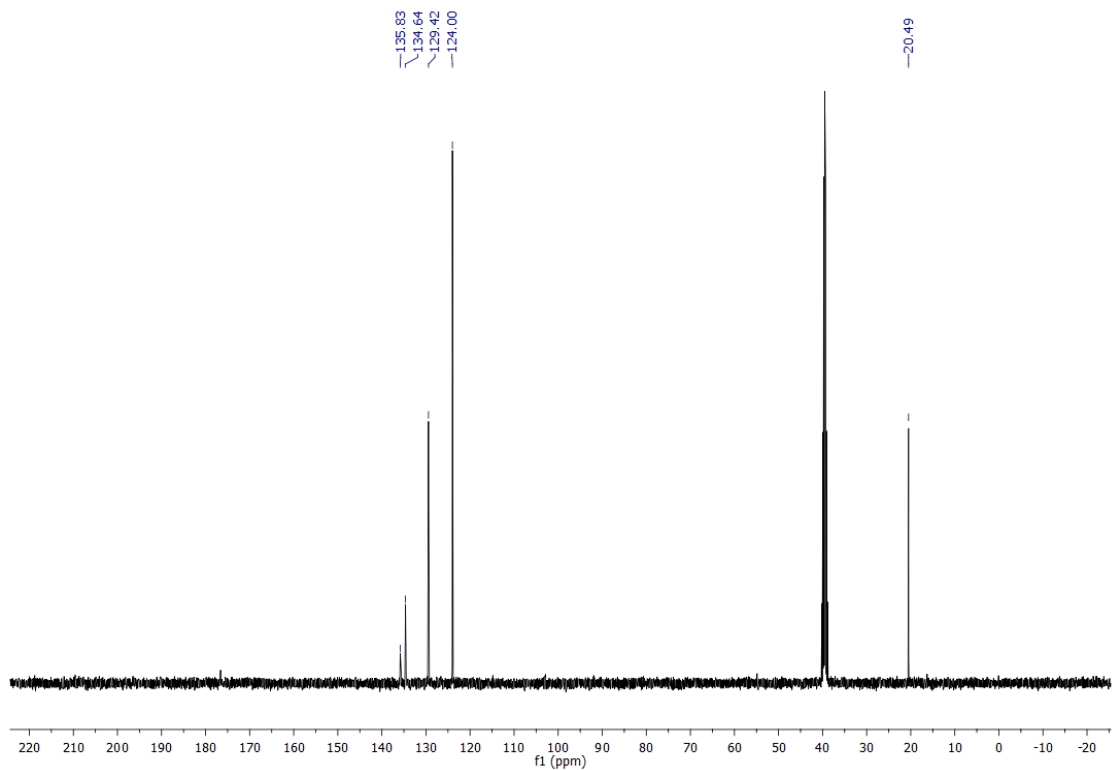


Figure S 5: ^{13}C -NMR (101 MHz, $\text{DMSO}-d_6$) of compound 2b

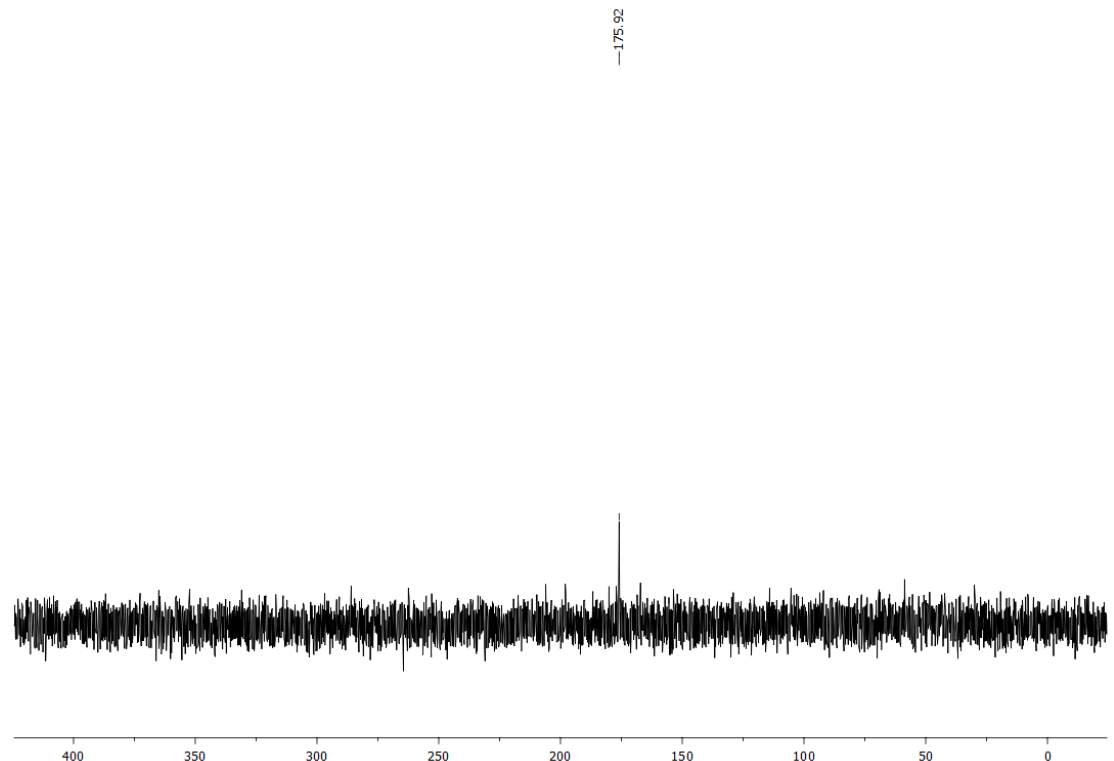


Figure S 6: ^{77}Se -NMR (76 MHz, MeOD , 248K) of compound 2b

Compound 2c

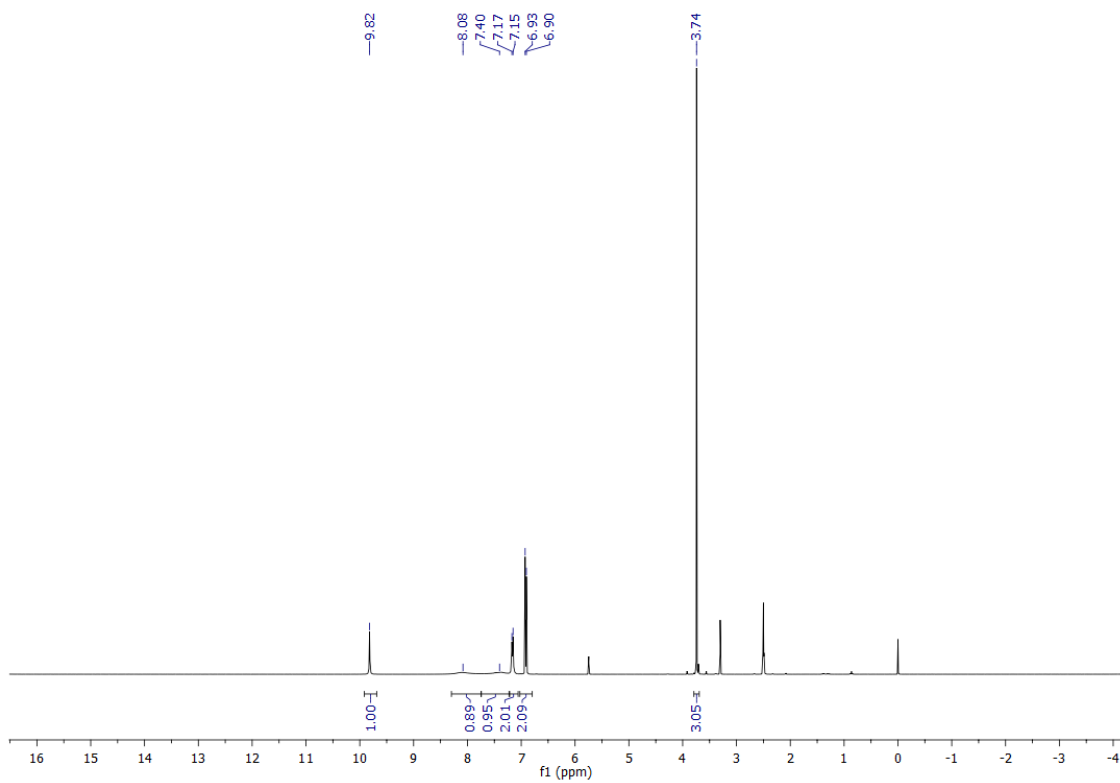


Figure S 7: ¹H-NMR (600 MHz, DMSO- d_6) of compound 2c

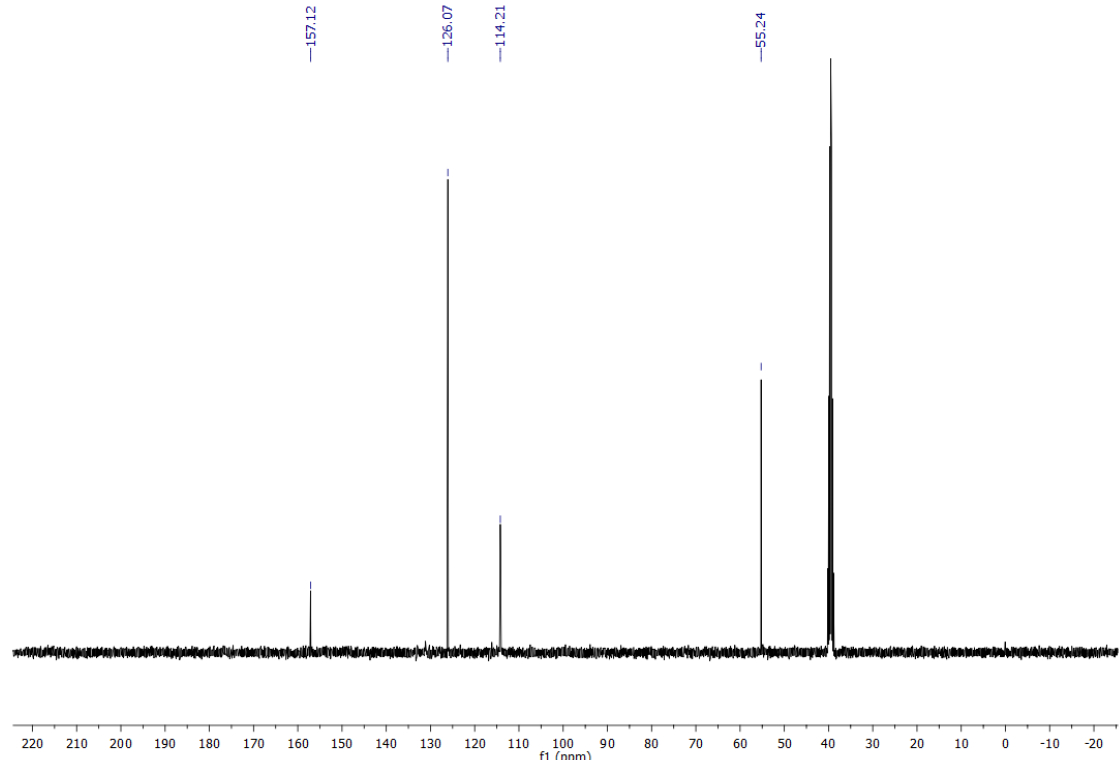


Figure S 8: ¹³C-NMR (151 MHz, DMSO- d_6) of compound 2c

Compound 3

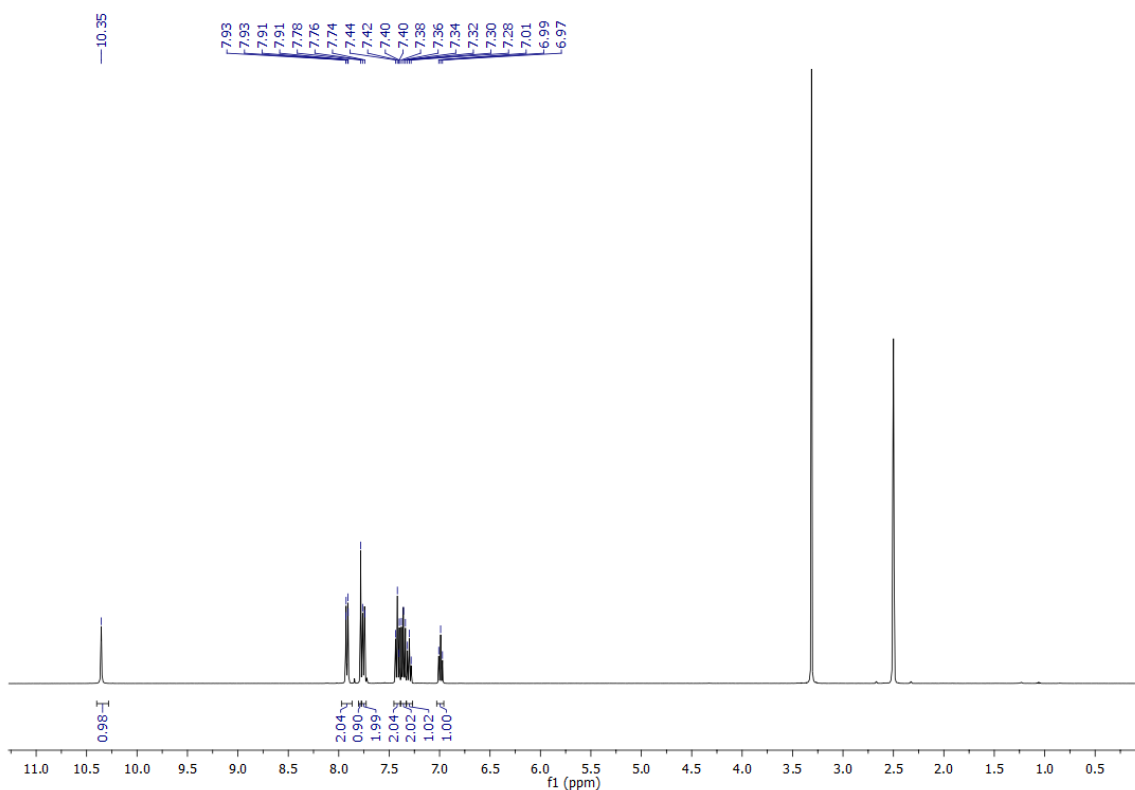


Figure S 9: ¹H-NMR (400 MHz, DMSO- d_6) of compound 3

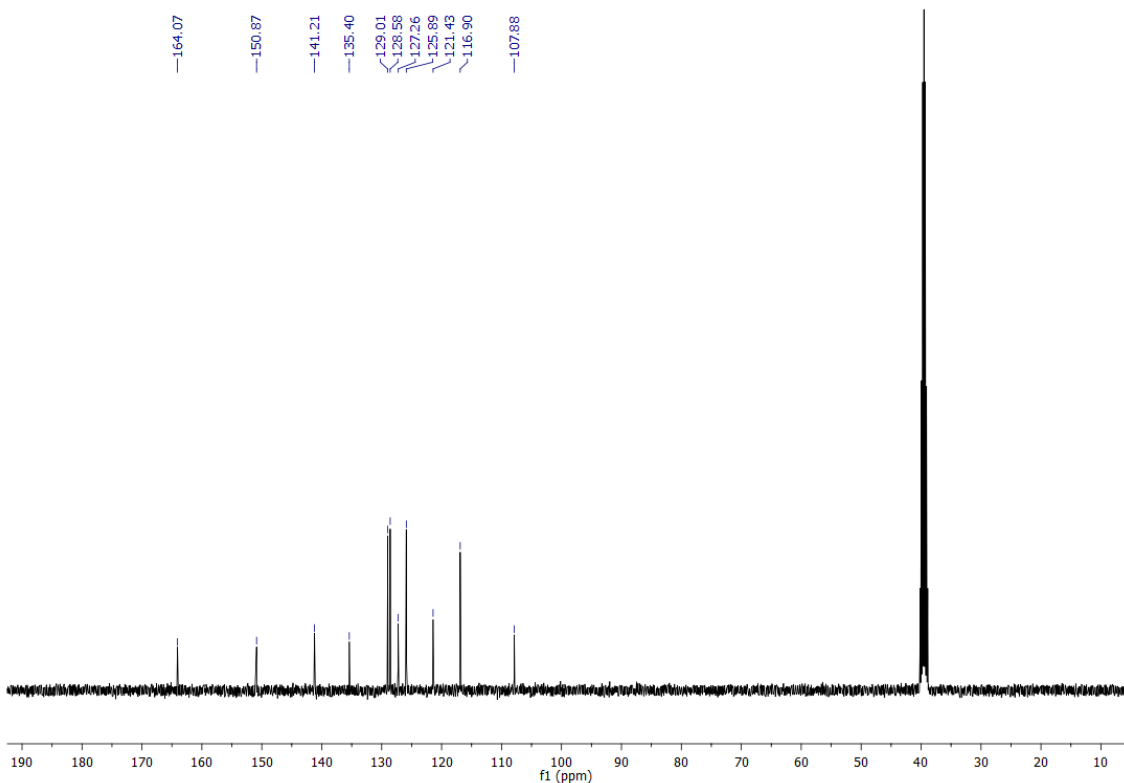


Figure S 10: ¹³C-NMR (101 MHz, DMSO- d_6) of compound 3

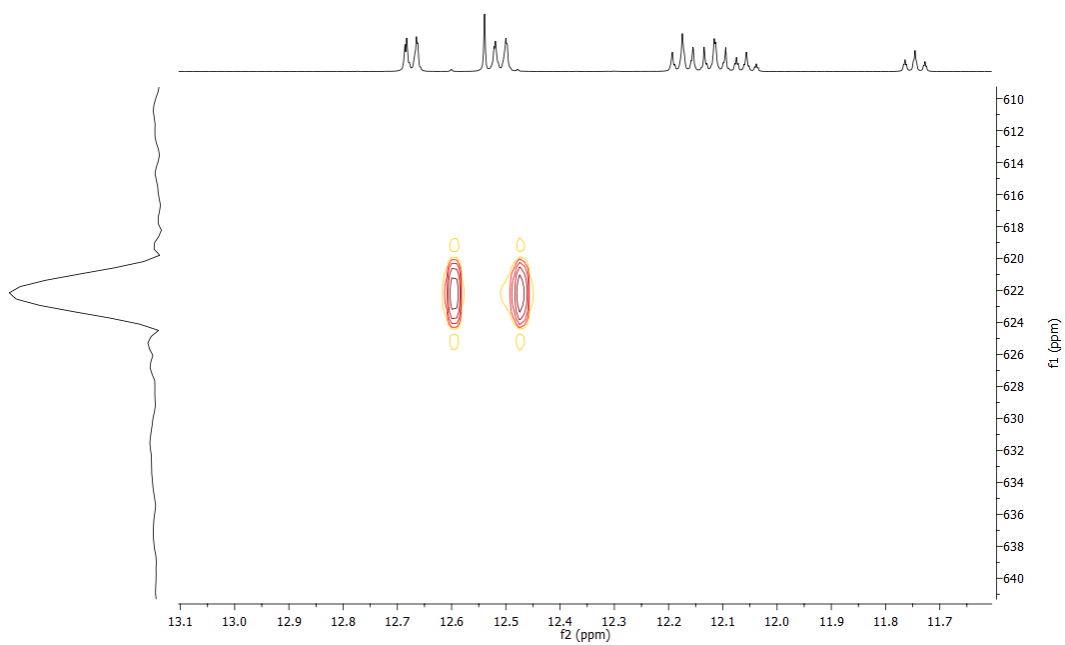


Figure S 11: ^1H - ^{77}Se -HMBC (400 MHz, 76 MHz, $\text{DMSO}-d_6$) of compound 3

Compound 4

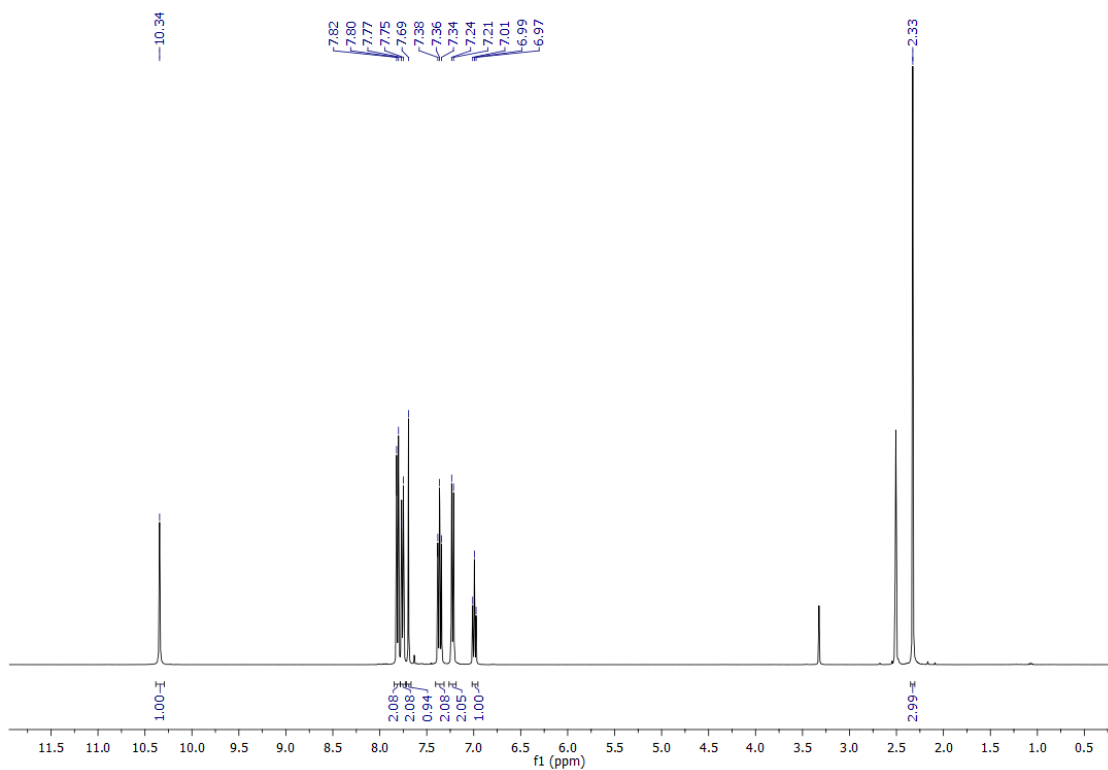


Figure S 12: ^1H -NMR (400 MHz, $\text{DMSO}-d_6$) of compound 4

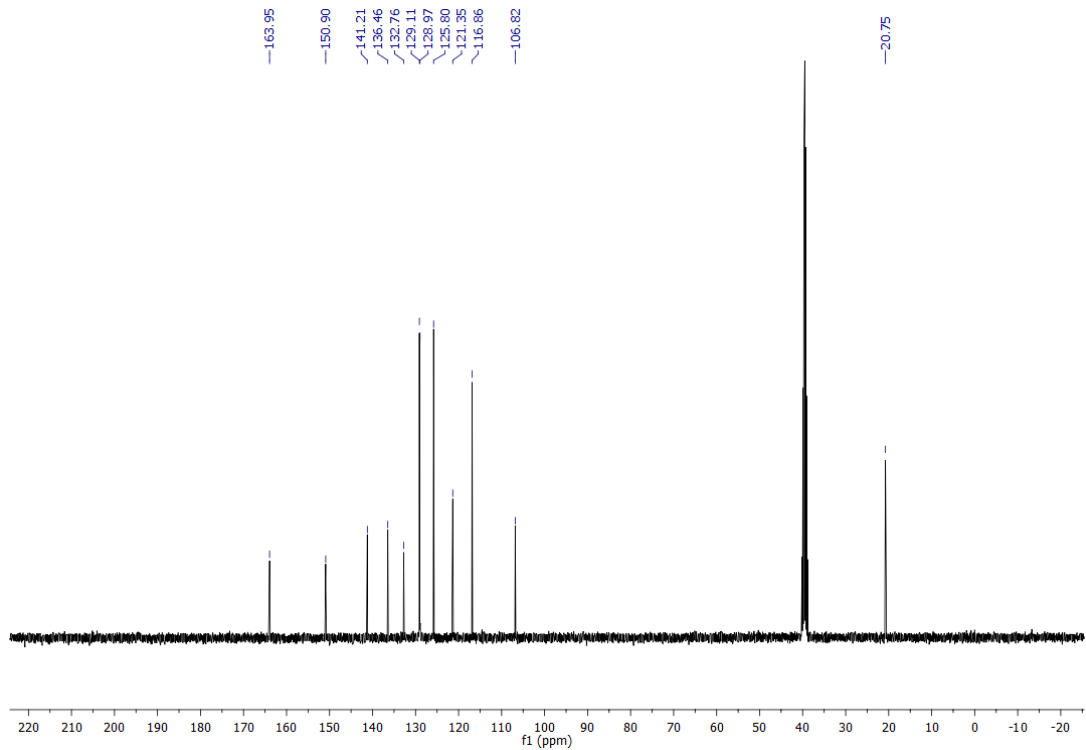


Figure S 13: ^{13}C -NMR (101 MHz, DMSO-d_6) of compound 4

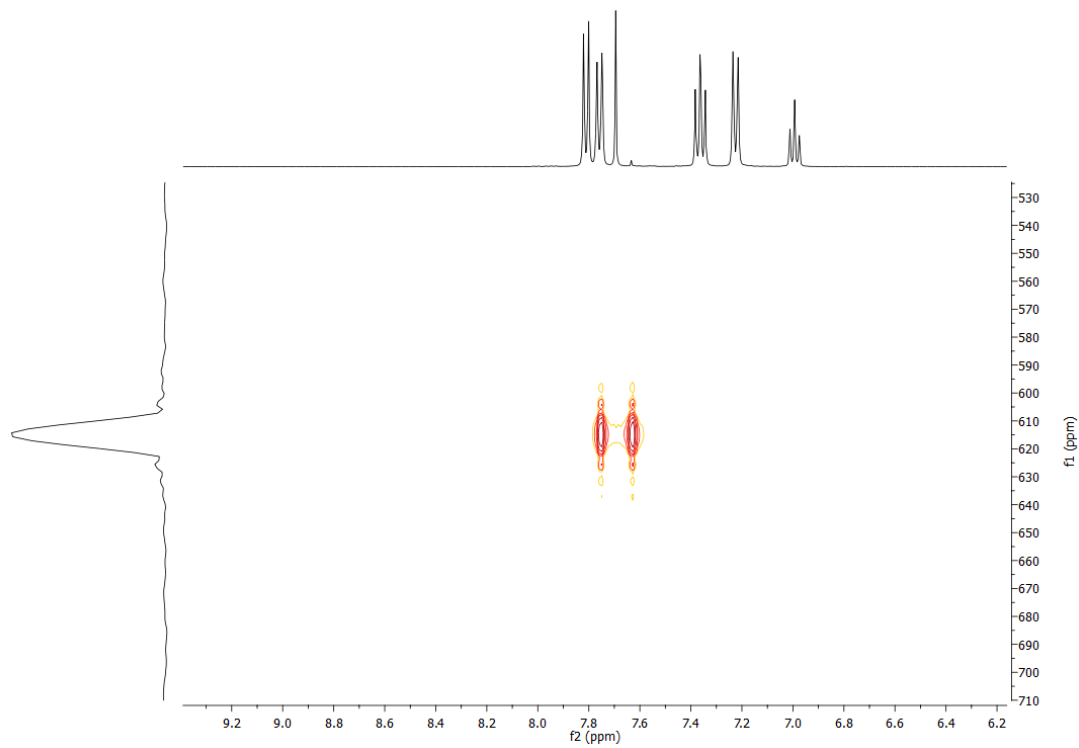
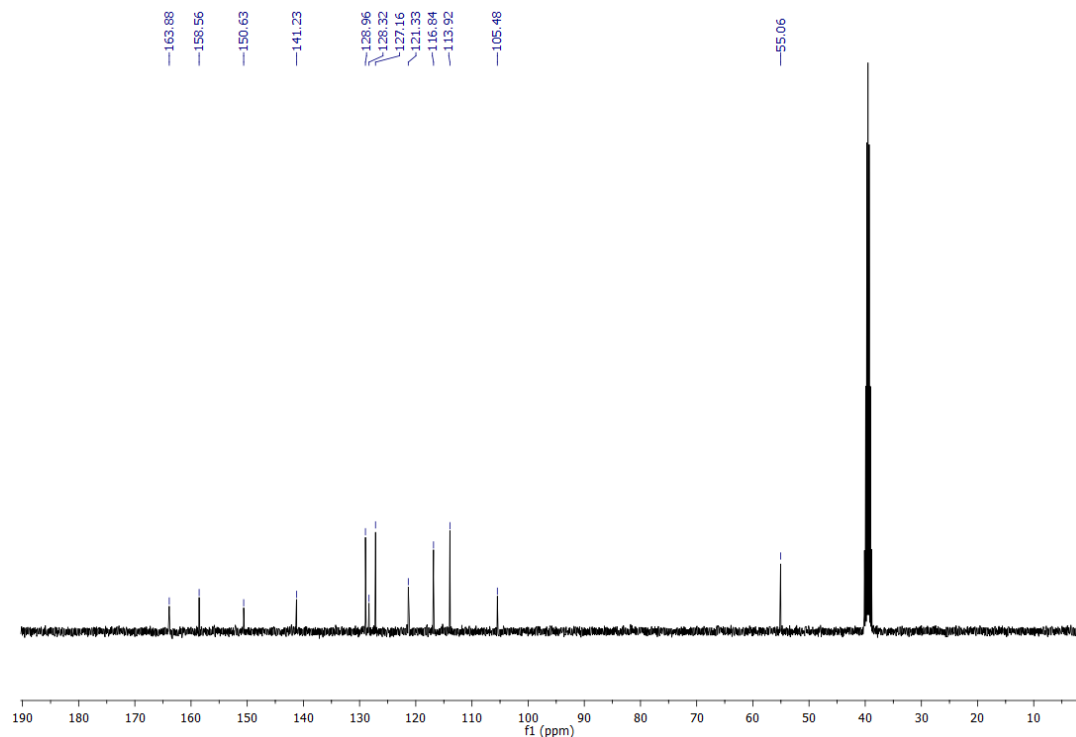
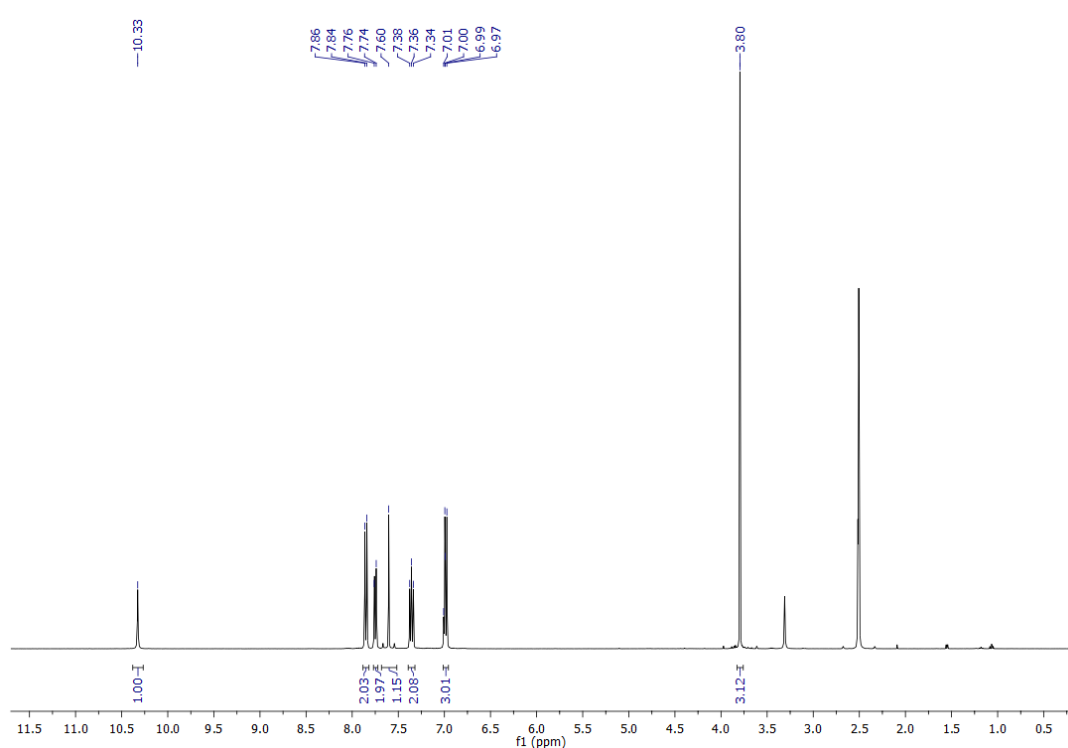


Figure S 14: ^1H - ^{77}Se -HMBC (400 MHz, 76 MHz, DMSO-d_6) of compound 4

Compound 5



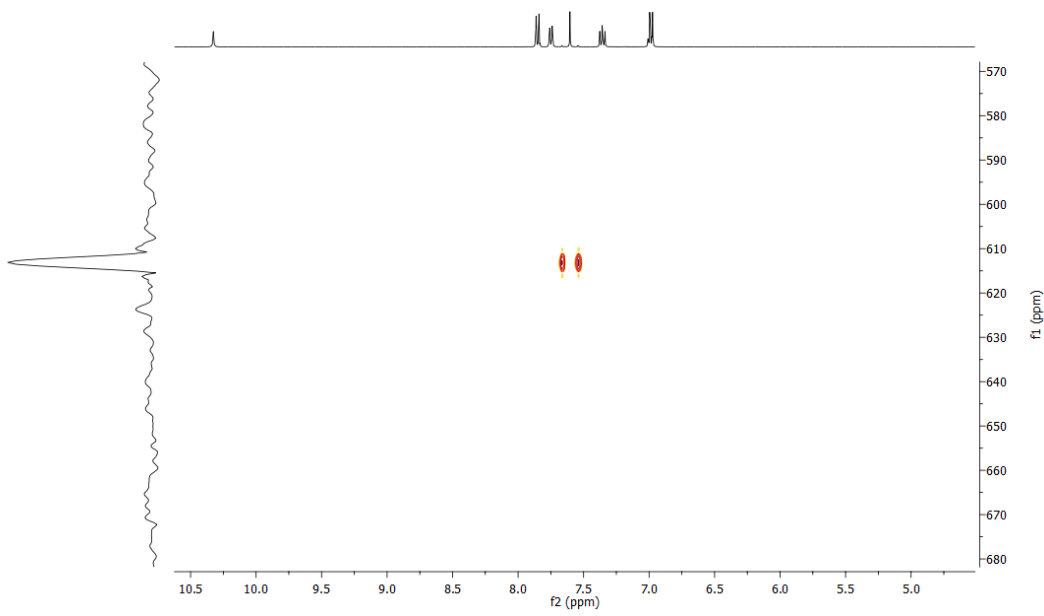


Figure S 17: ^1H - ^{77}Se -HMBC (400 MHz, 76 MHz, DMSO- d_6) of compound 5

Compound 6

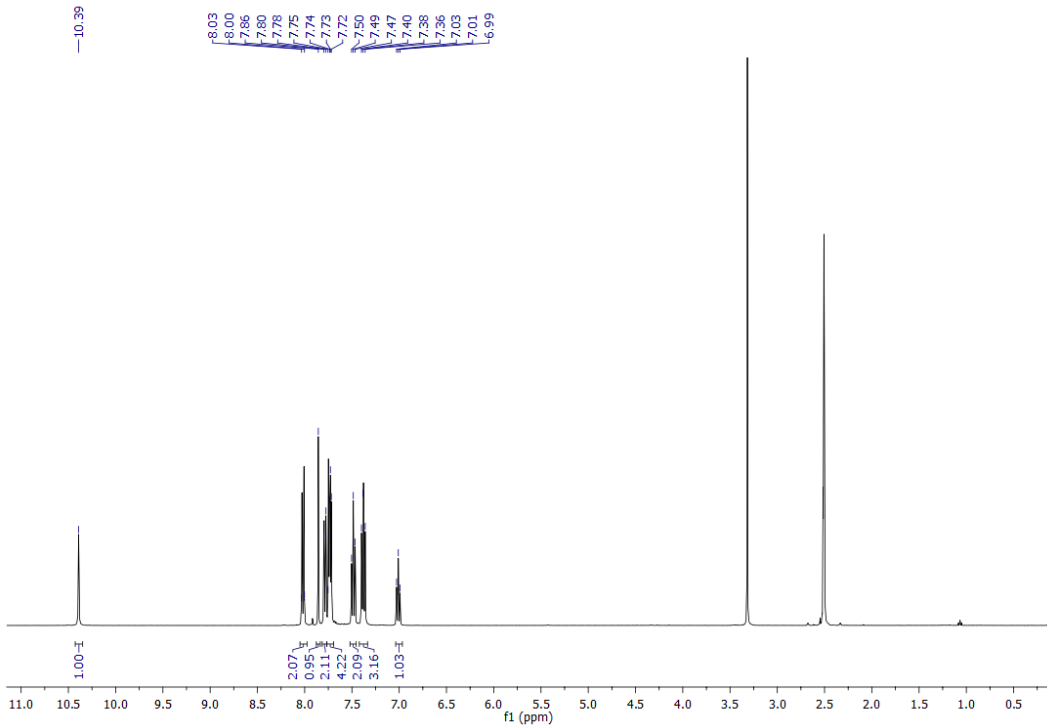


Figure S 18: ^1H -NMR (400 MHz, DMSO- d_6) of compound 6

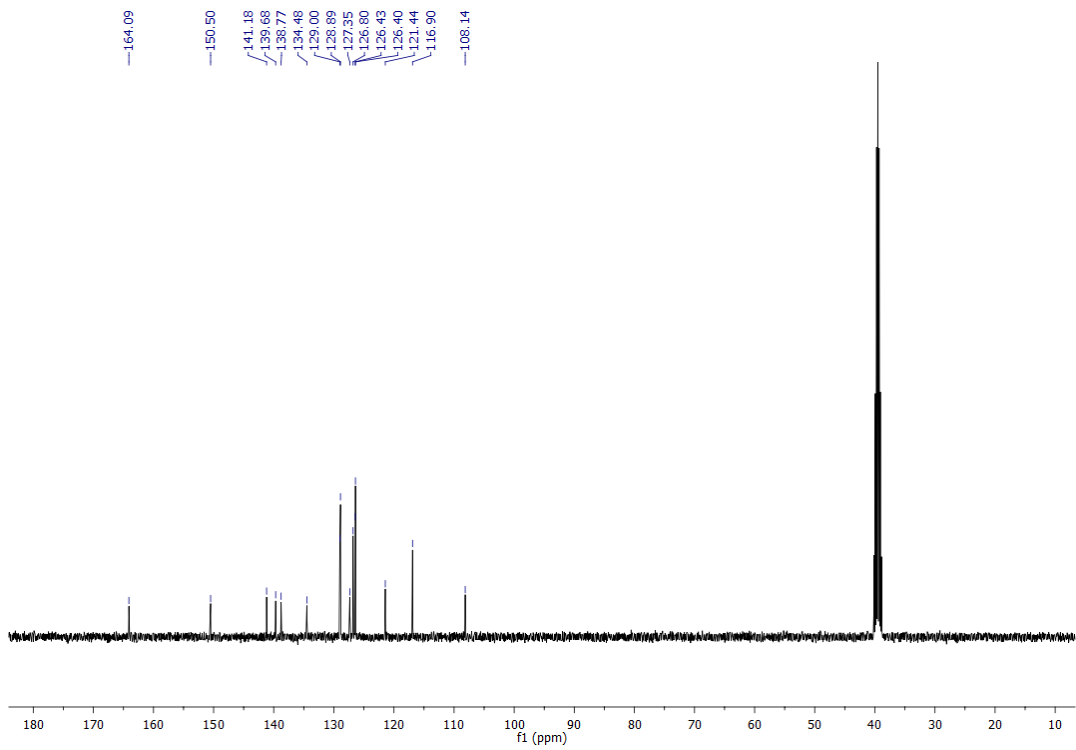


Figure S 19: ^{13}C -NMR (101 MHz, $\text{DMSO}-d_6$) of compound 6

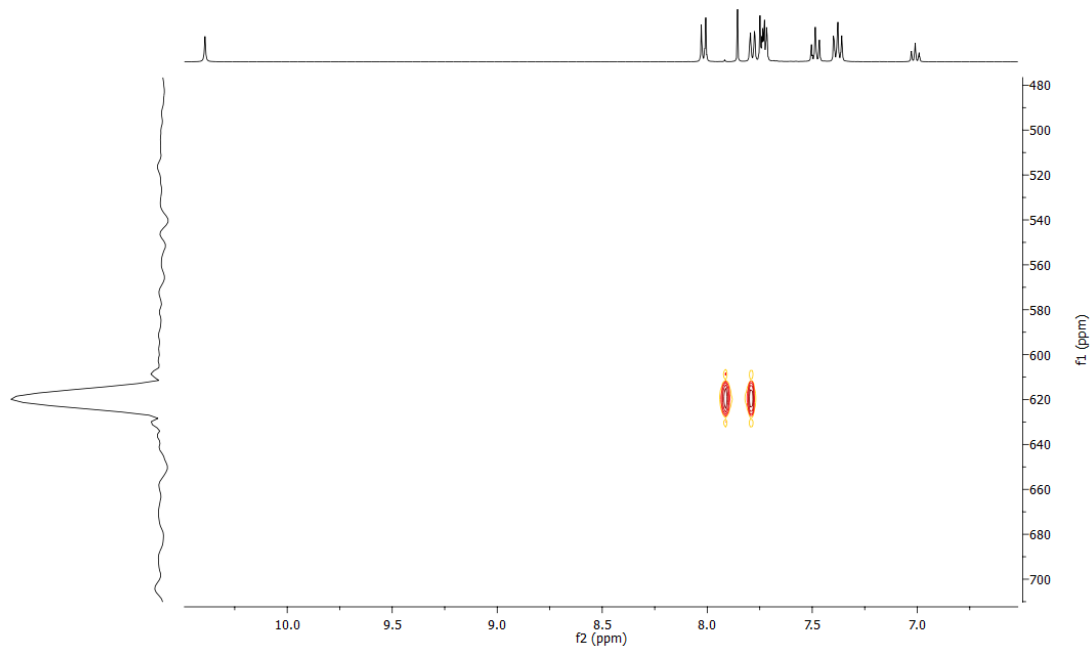


Figure S 20: ^1H - ^{77}Se -HMBC (400 MHz, 76 MHz, $\text{DMSO}-d_6$) of compound 6

Compound 7

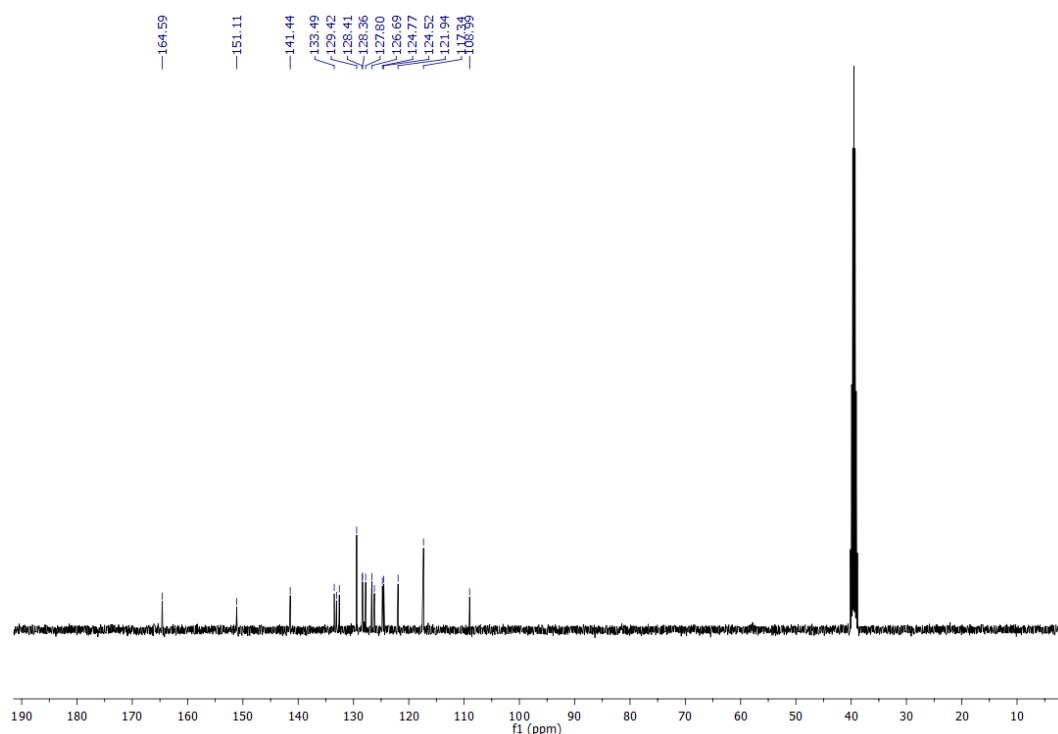
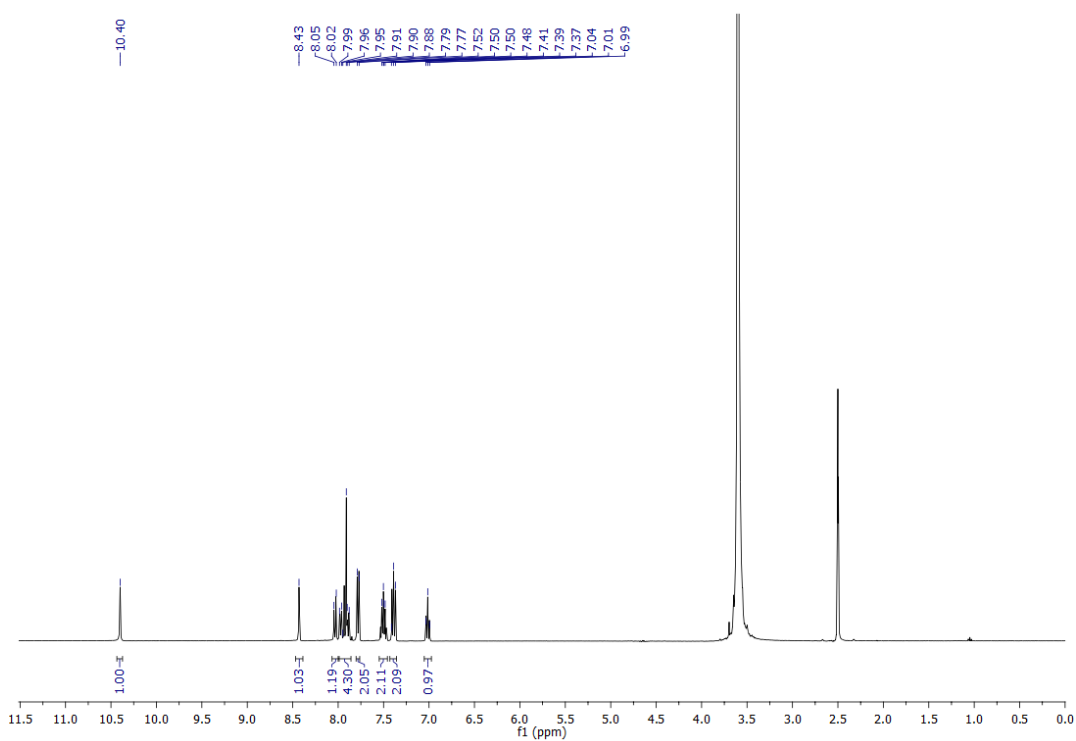


Figure S 22: ^{13}C -NMR (101 MHz, $\text{DMSO}-d_6$) of compound 7

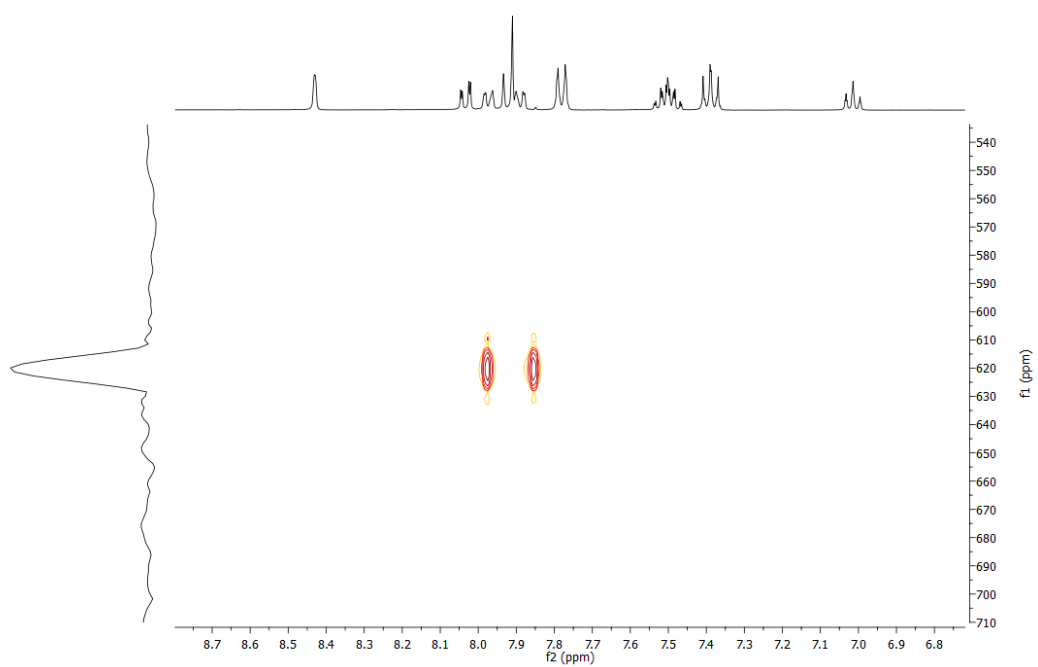


Figure S 23: ^1H - ^{77}Se -HMBC (400 MHz, 76 MHz, $\text{DMSO}-d_6$) of compound 7

Compound 8

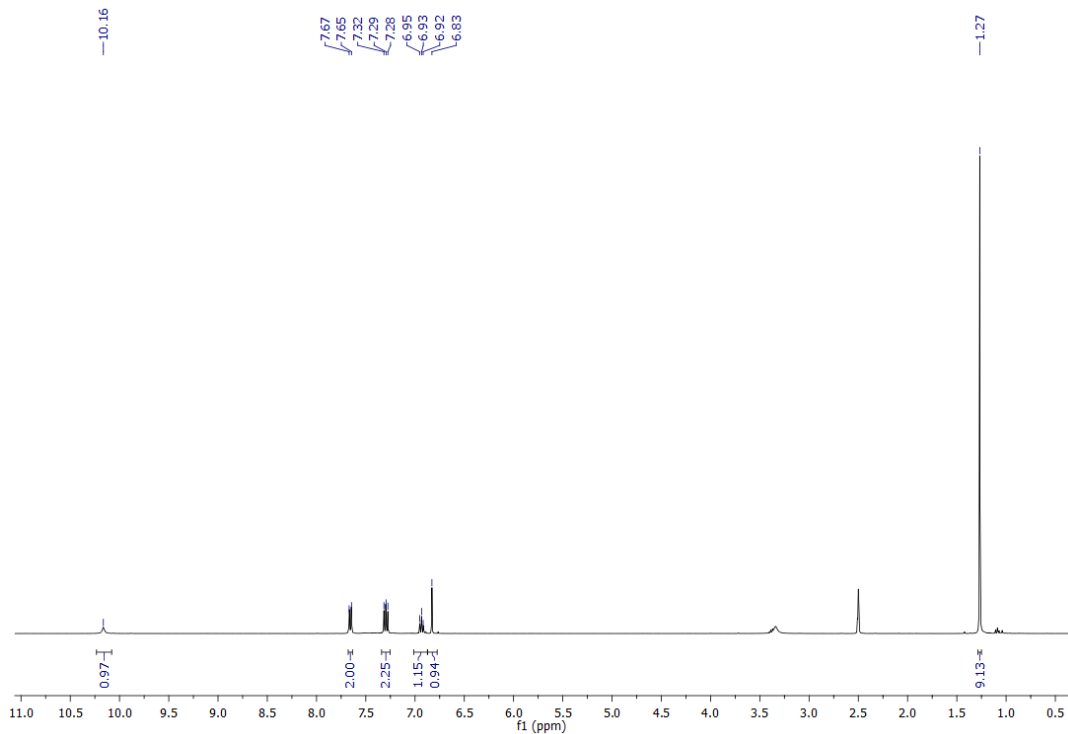


Figure S 24: ^1H -NMR (400 MHz, $\text{DMSO}-d_6$) of compound 8

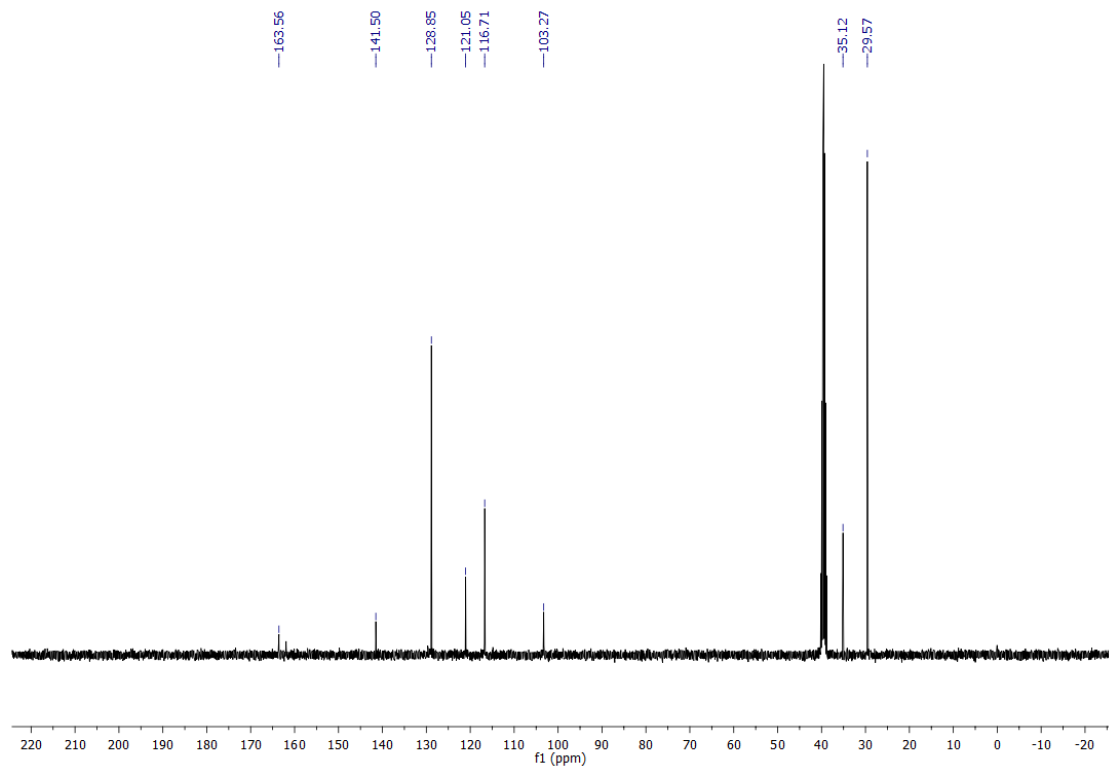


Figure S 25: ^{13}C -NMR (101 MHz, $\text{DMSO}-d_6$) of compound 8

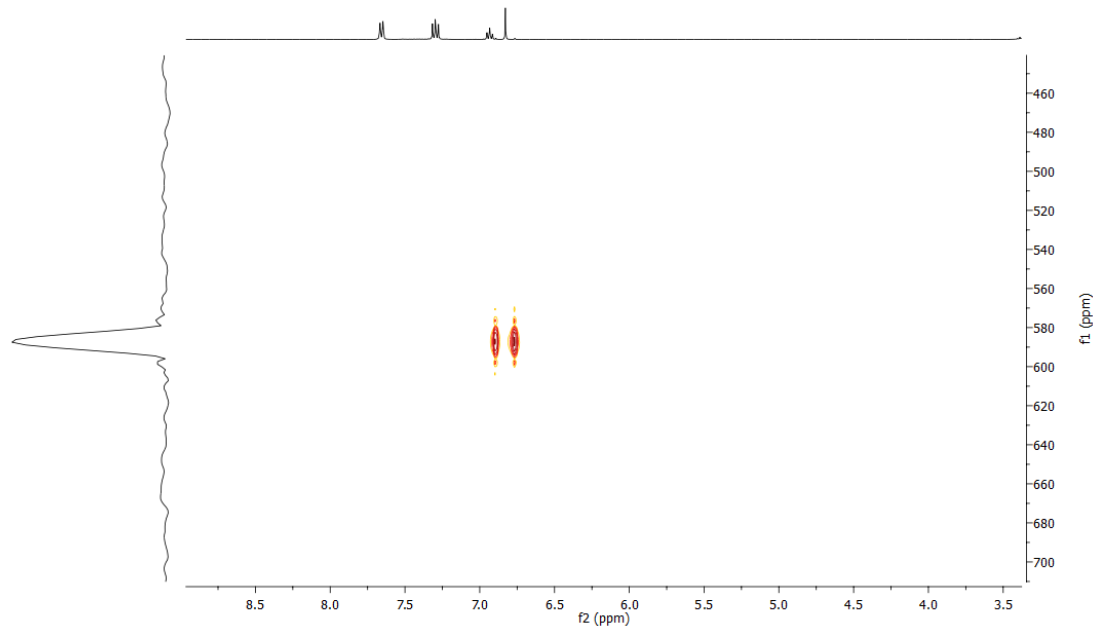


Figure S 26: ^1H - ^{77}Se -HMBC (400 MHz, 76 MHz, $\text{DMSO}-d_6$) of compound 8

Compound 9

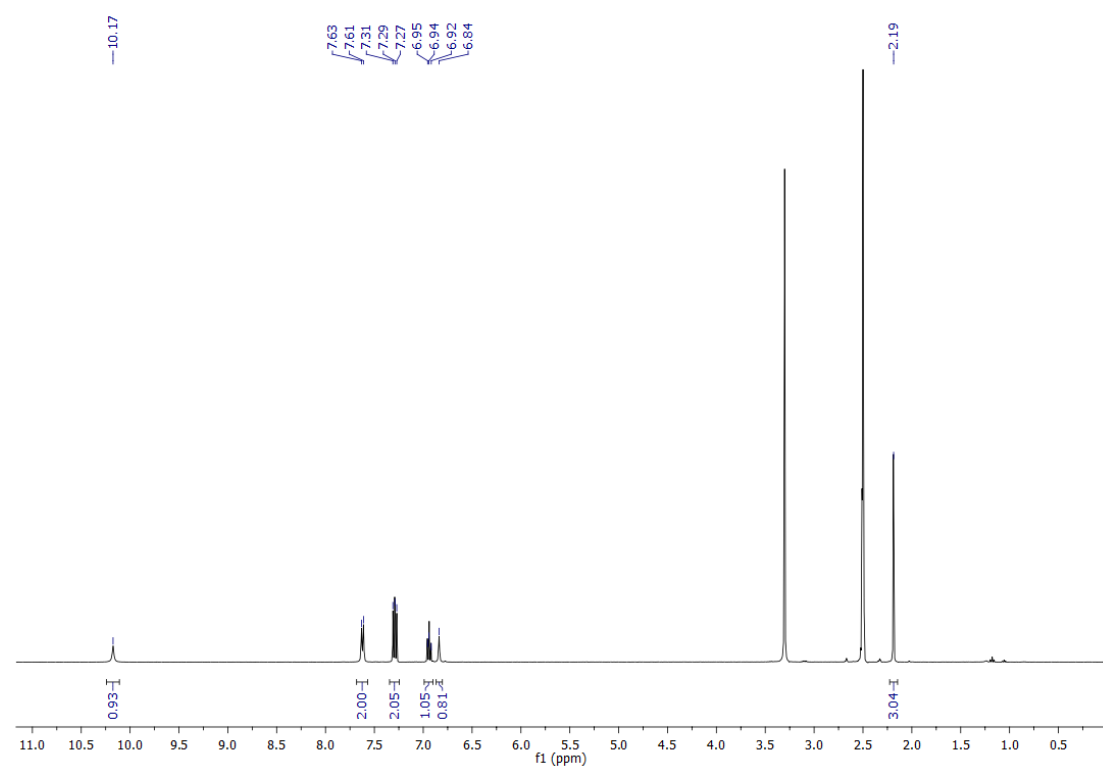


Figure S 27: ¹H-NMR (400 MHz, $\text{DMSO}-d_6$) of compound 9

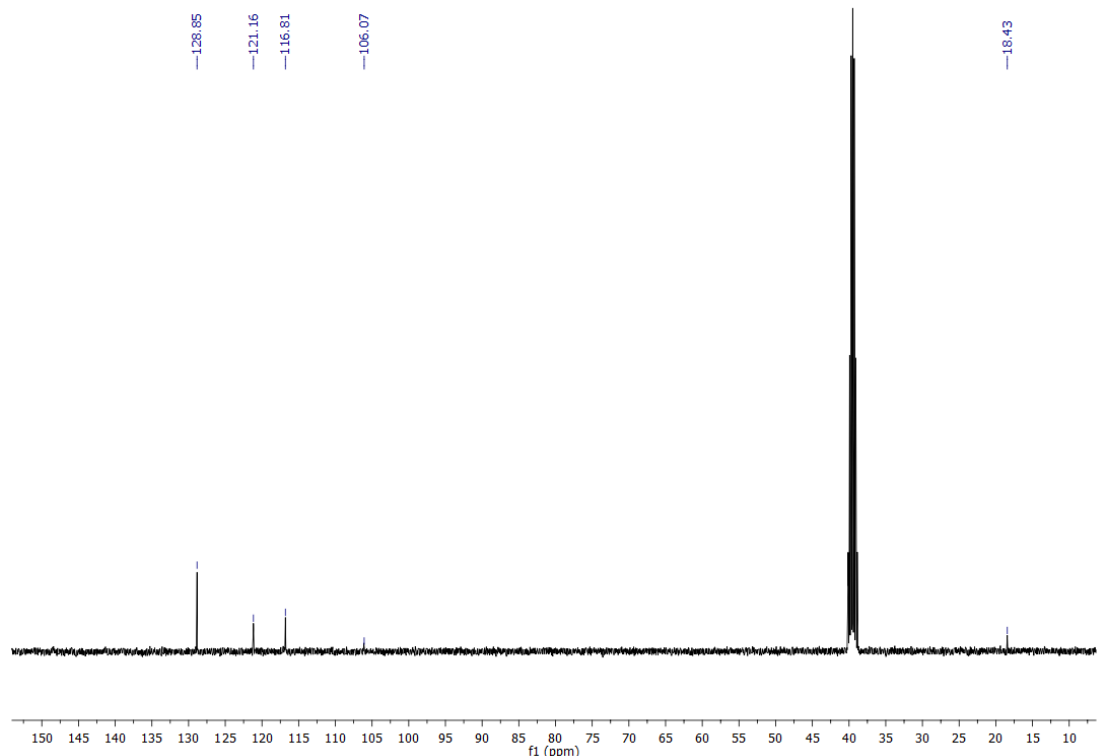


Figure S 28: ¹³C-NMR (101 MHz, $\text{DMSO}-d_6$) of compound 9

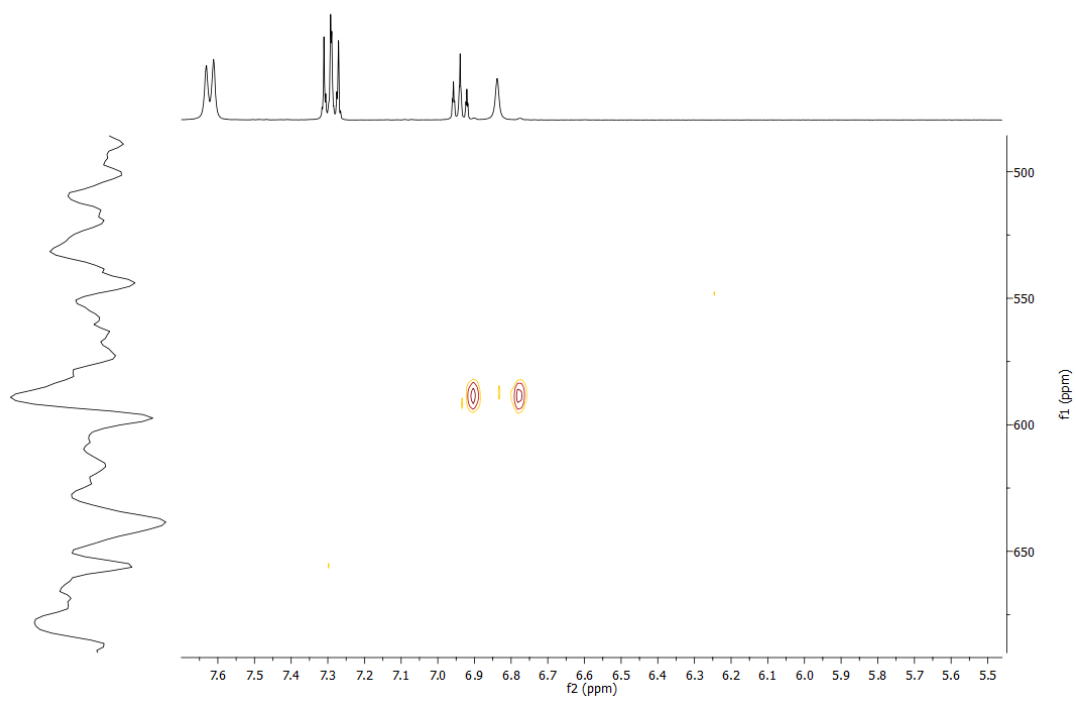


Figure S 29: ^1H - ^{77}Se -HMBC (400 MHz, 76 MHz, $\text{DMSO}-d_6$) of compound 9

Compound 10

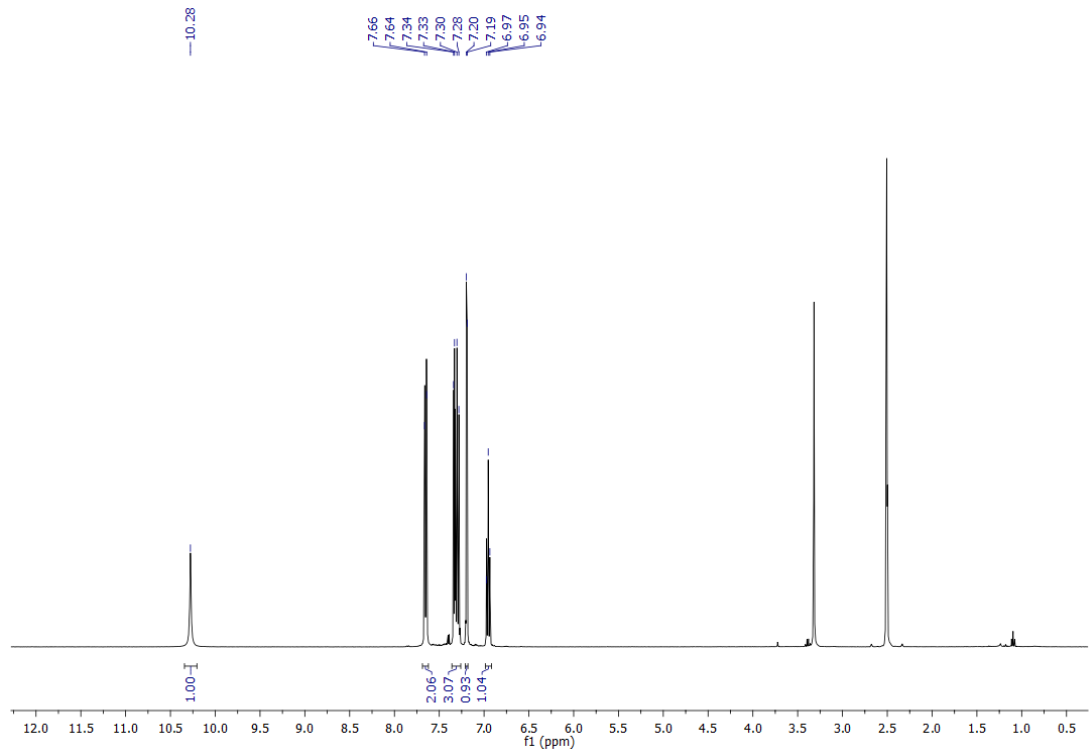


Figure S 30: ^1H -NMR (400 MHz, $\text{DMSO}-d_6$) of compound 10

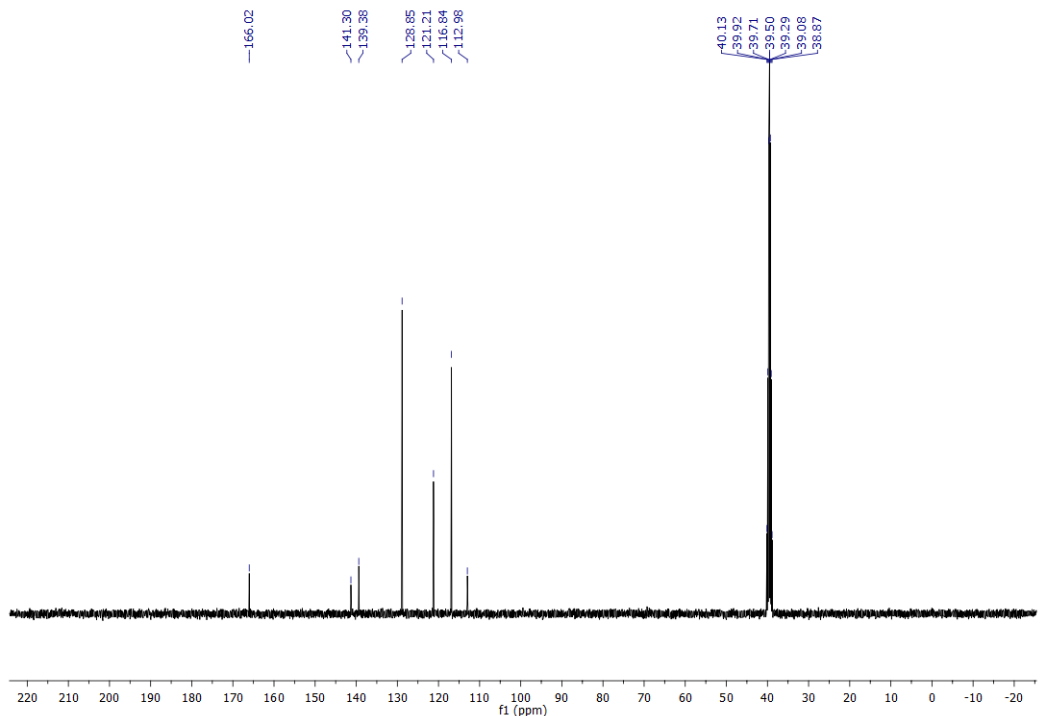


Figure S 31: ^{13}C -NMR (101 MHz, DMSO- d_6) of compound 10

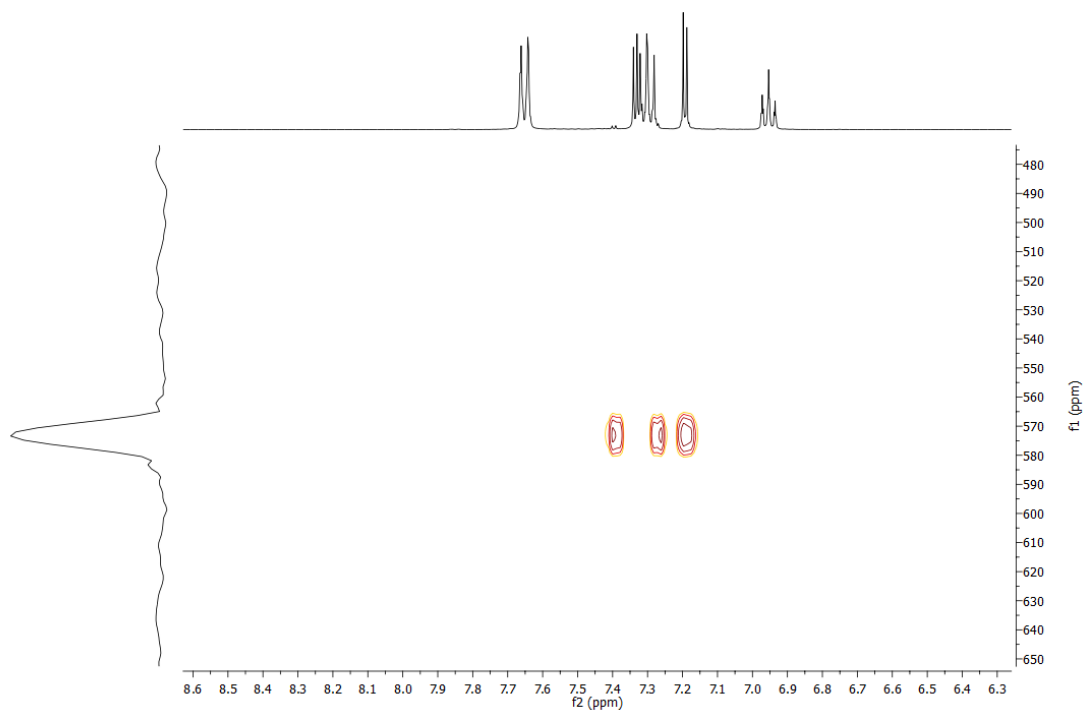


Figure S 32: ^1H - ^{77}Se -HMBC (400 MHz, 76 MHz, DMSO- d_6) of compound 10

Compound 11

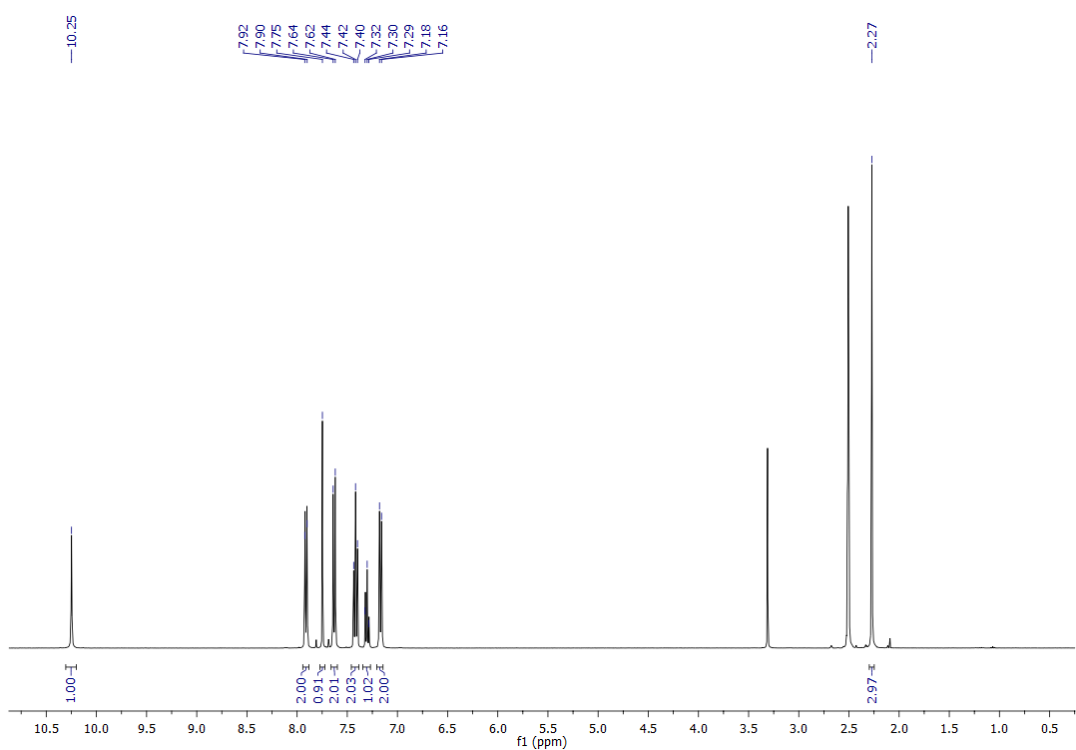


Figure S 33

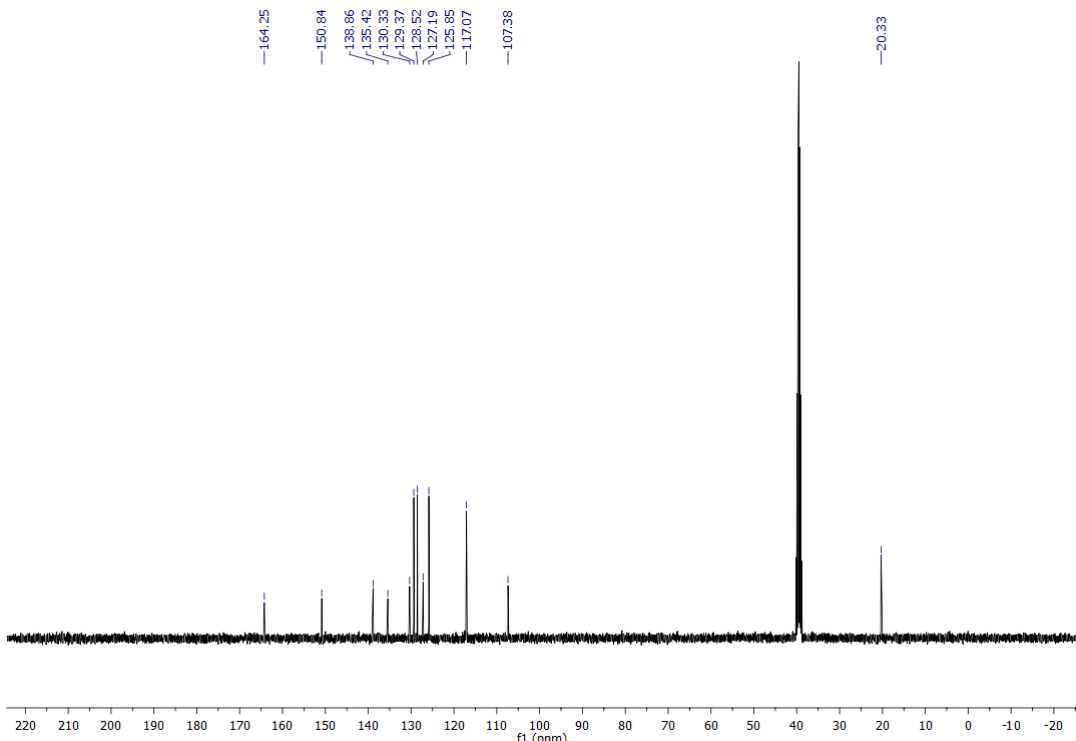


Figure S 34: ¹³C-NMR (101 MHz, DMSO- d_6) of compound 11

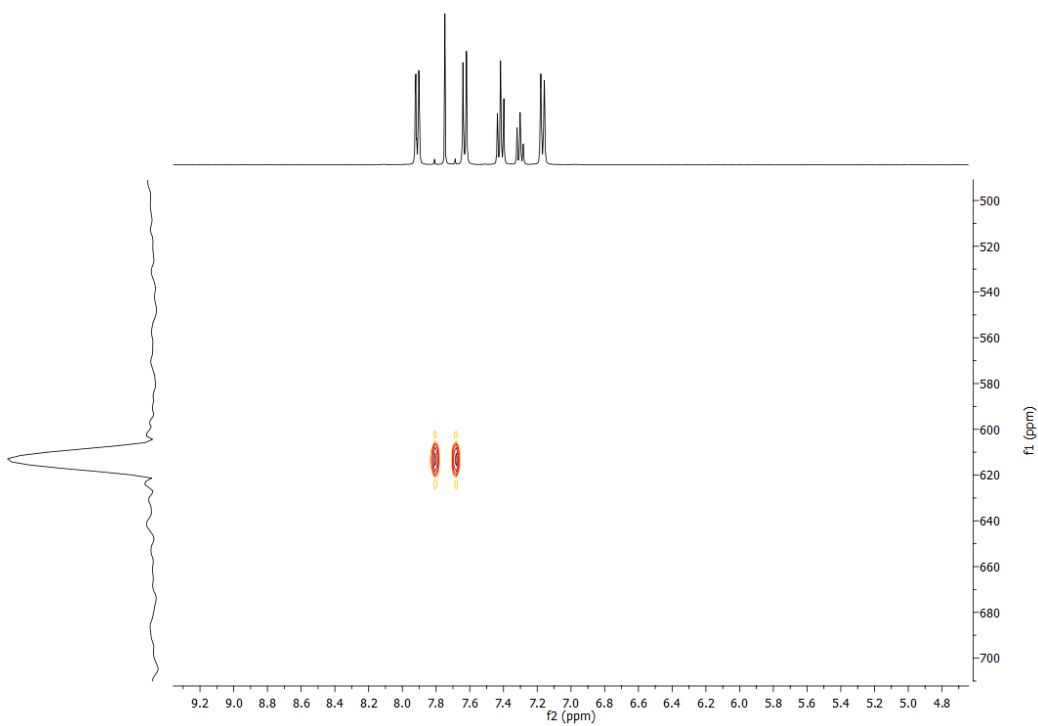


Figure S 35: ^1H - ^{77}Se -HMBC (400 MHz, 76 MHz, $\text{DMSO}-d_6$) of compound 11

Compound 12

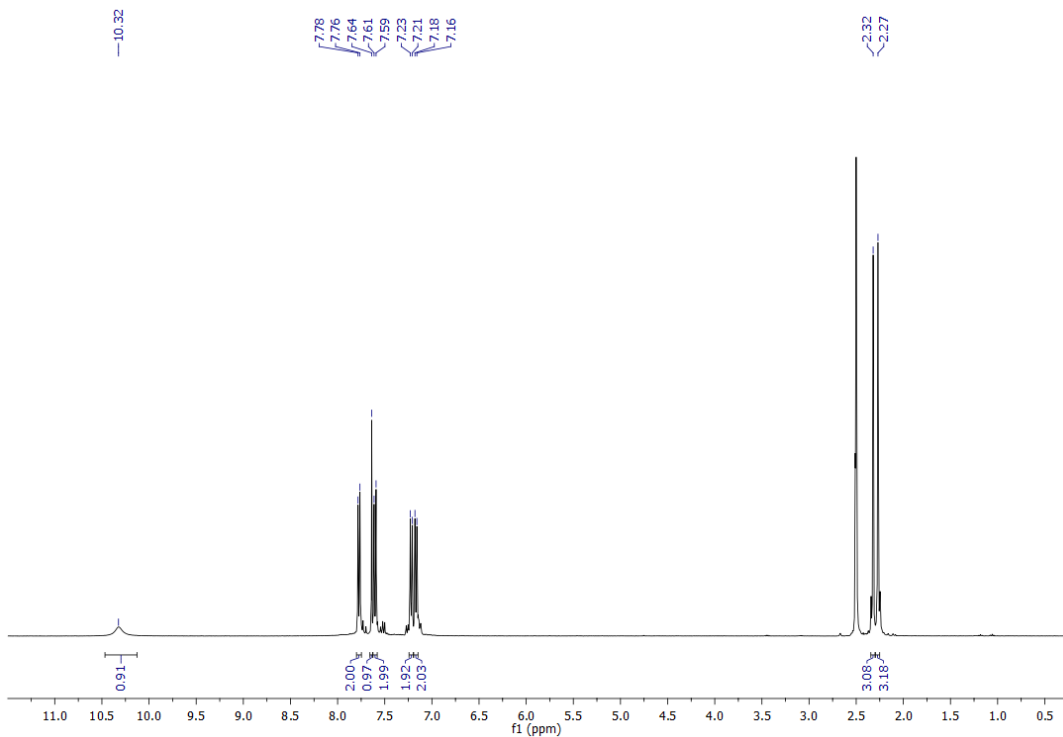


Figure S 36: ^1H -NMR (400 MHz, $\text{DMSO}-d_6$) of compound 12

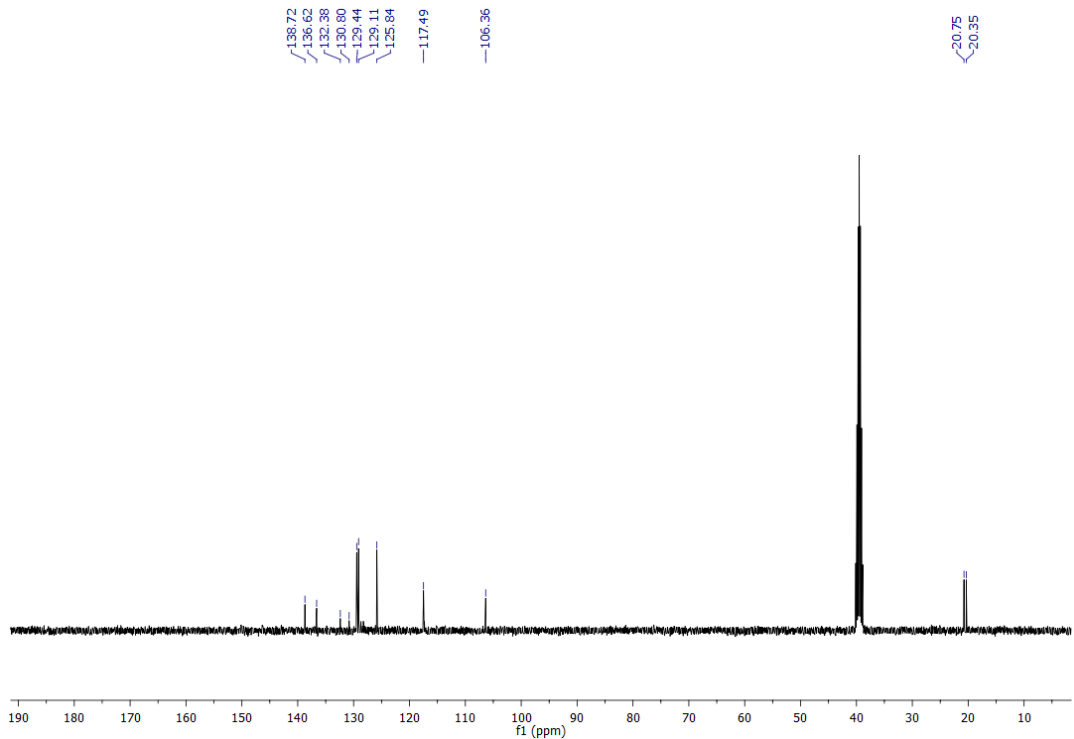


Figure S 37: ^{13}C -NMR (101 MHz, $\text{DMSO}-d_6$) of compound 12

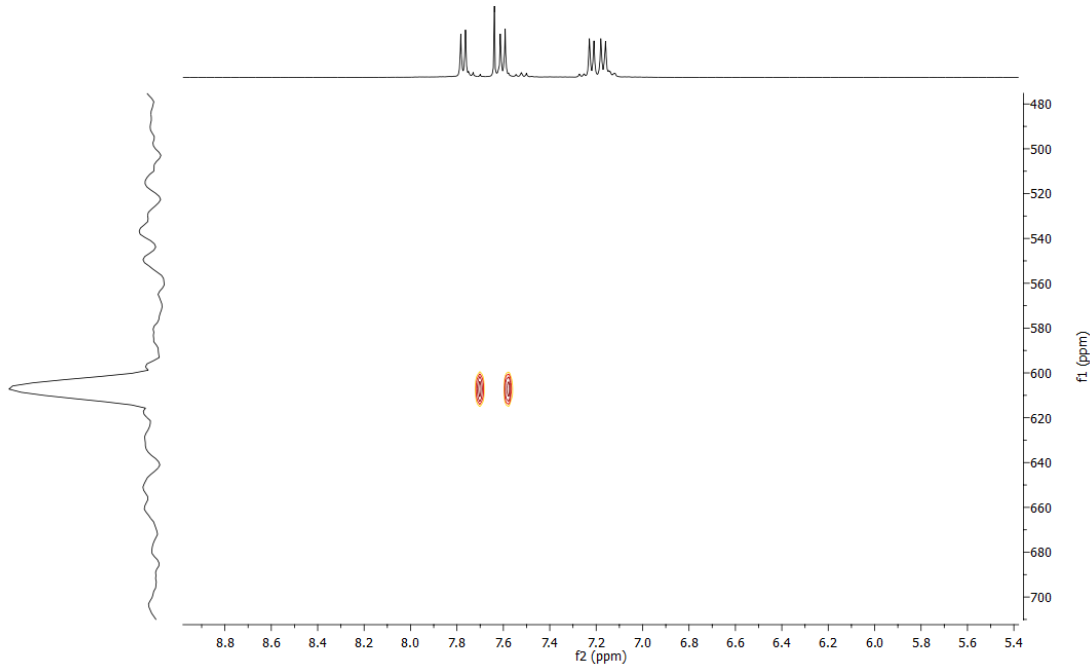


Figure S 38: ^1H - ^{77}Se -HMBC (400 MHz, 76 MHz, $\text{DMSO}-d_6$) of compound 12

Compound 13

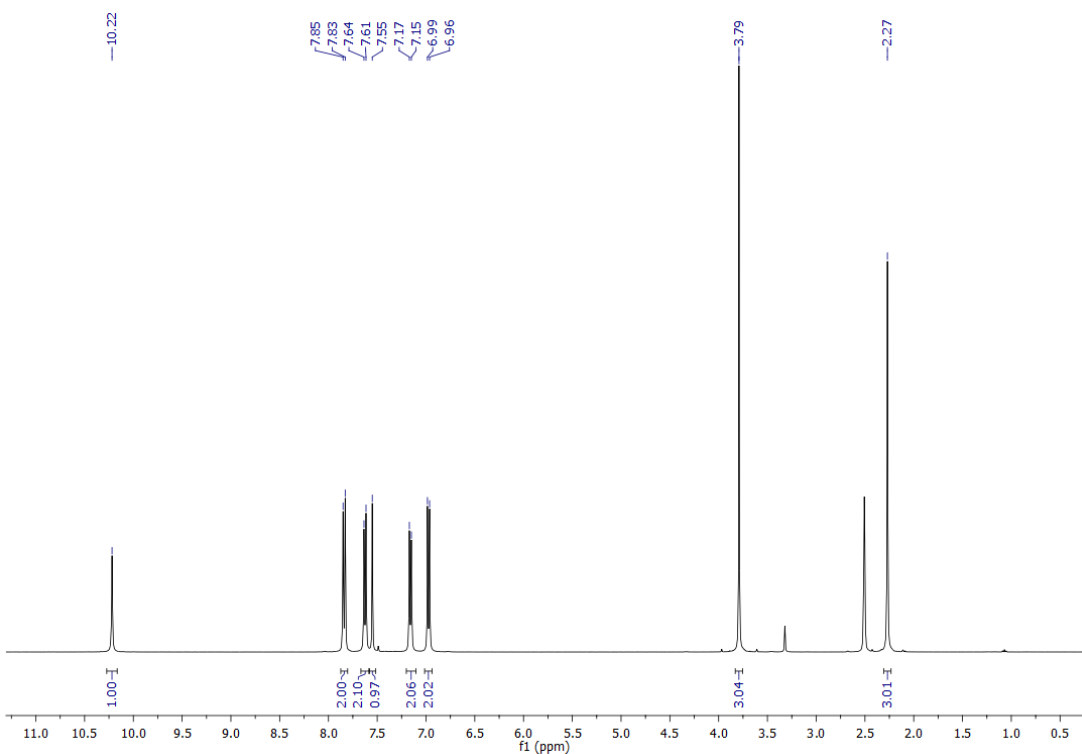


Figure S 39: ¹H-NMR (400 MHz, DMSO- d_6) of compound 13

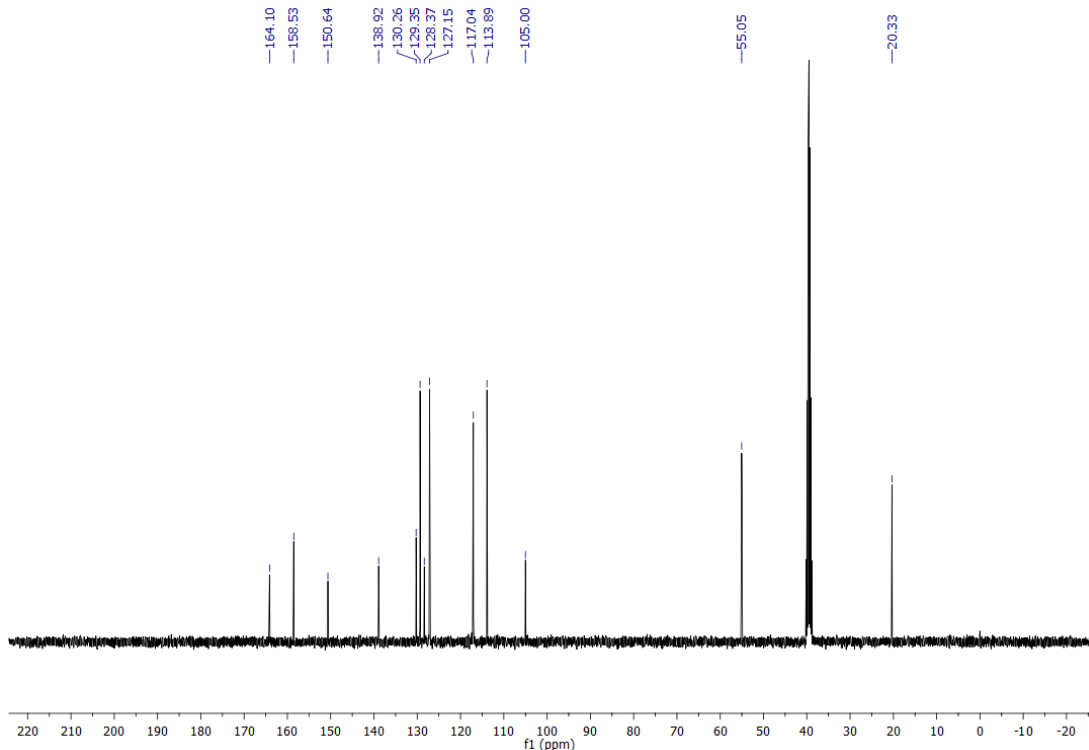


Figure S 40: ¹³C-NMR (101 MHz, DMSO- d_6) of compound 13

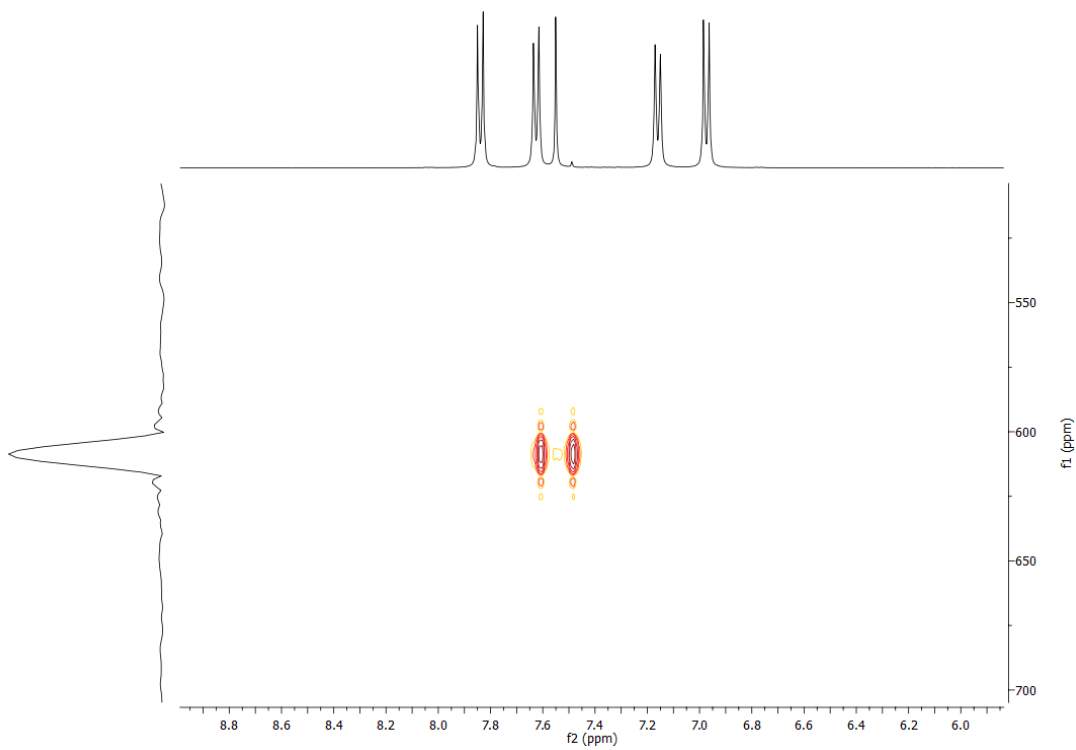


Figure S 41: ^1H - ^{77}Se -HMBC (400 MHz, 76 MHz, $\text{DMSO}-d_6$) of compound 13

Compound 14

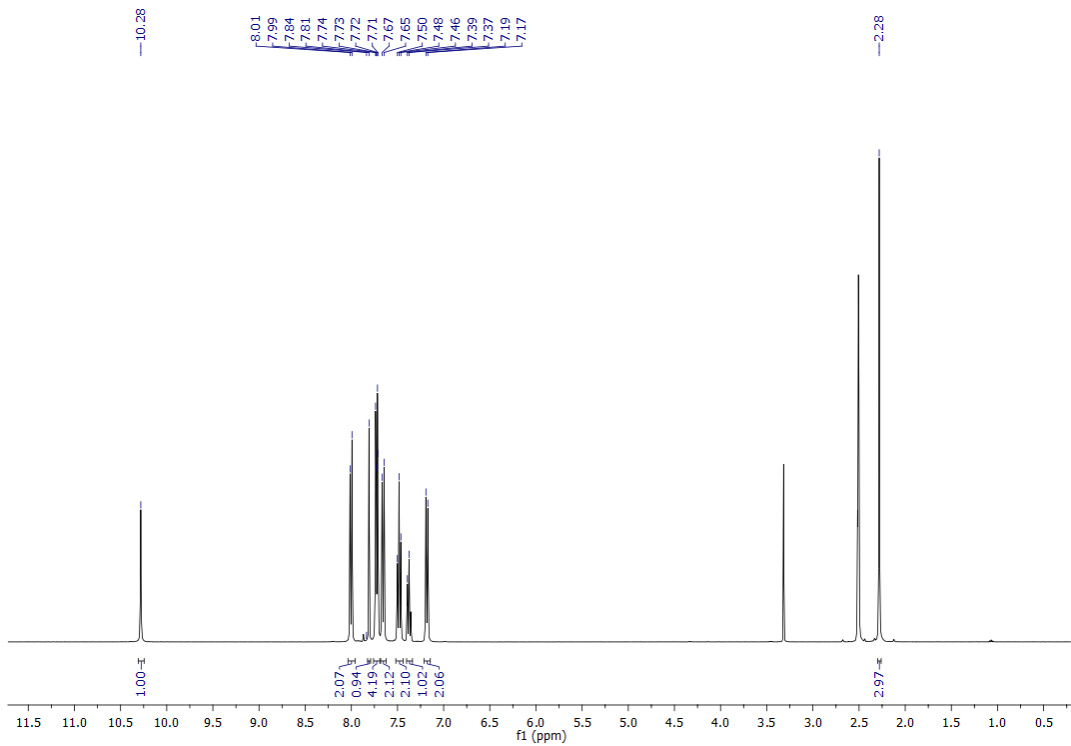


Figure S 42: ^1H -NMR (400 MHz, $\text{DMSO}-d_6$) of compound 14

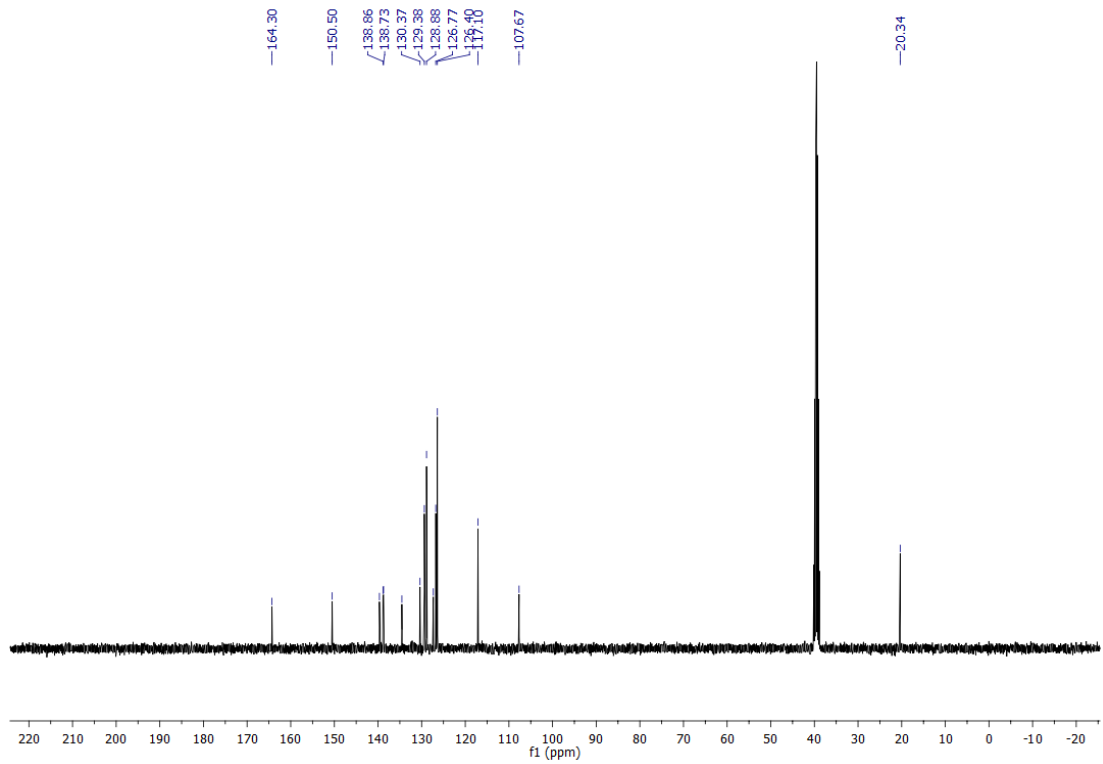


Figure S 43: ^{13}C -NMR (101 MHz, DMSO- d_6) of compound 14

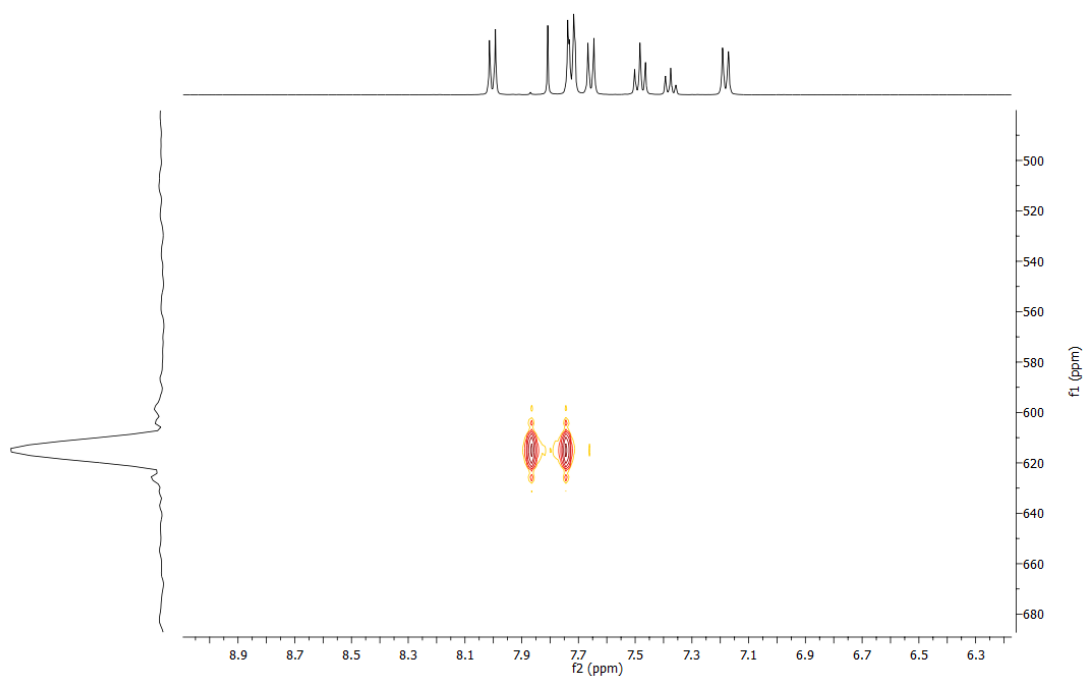


Figure S 44: ^1H - ^{77}Se -HMBC (400 MHz, 76 MHz, DMSO- d_6) of compound 14

Compound 15

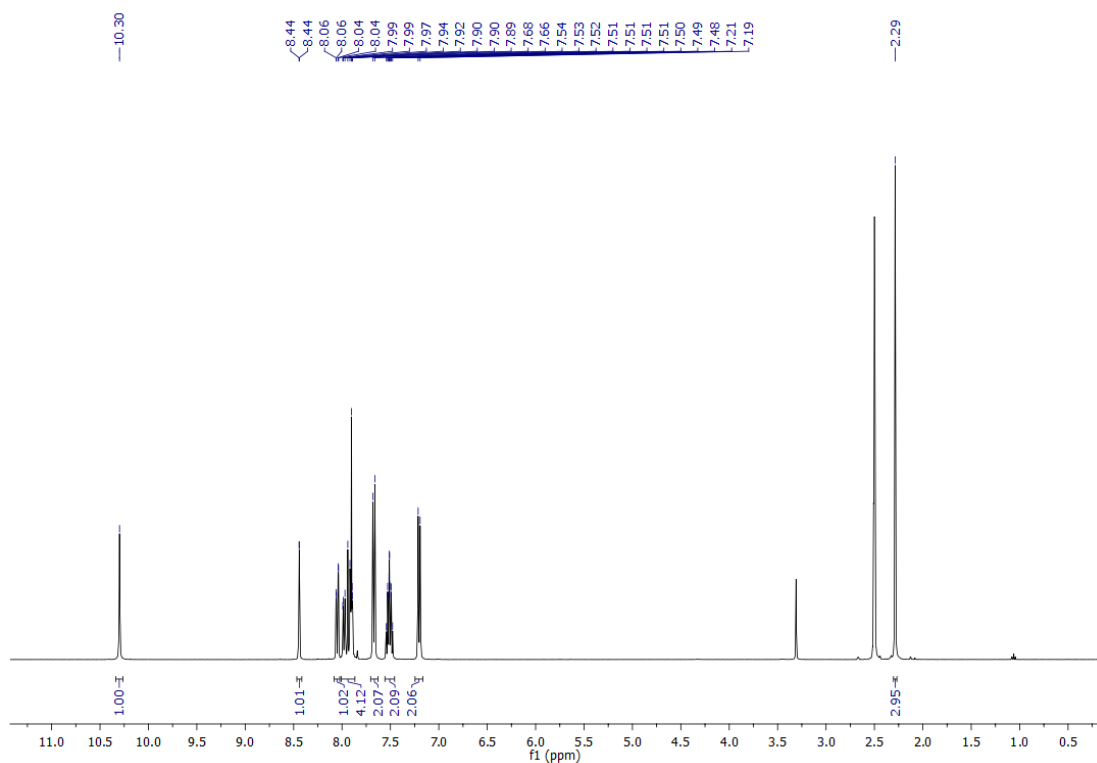


Figure S 45: ¹H-NMR (400 MHz, DMSO- d_6) of compound 15

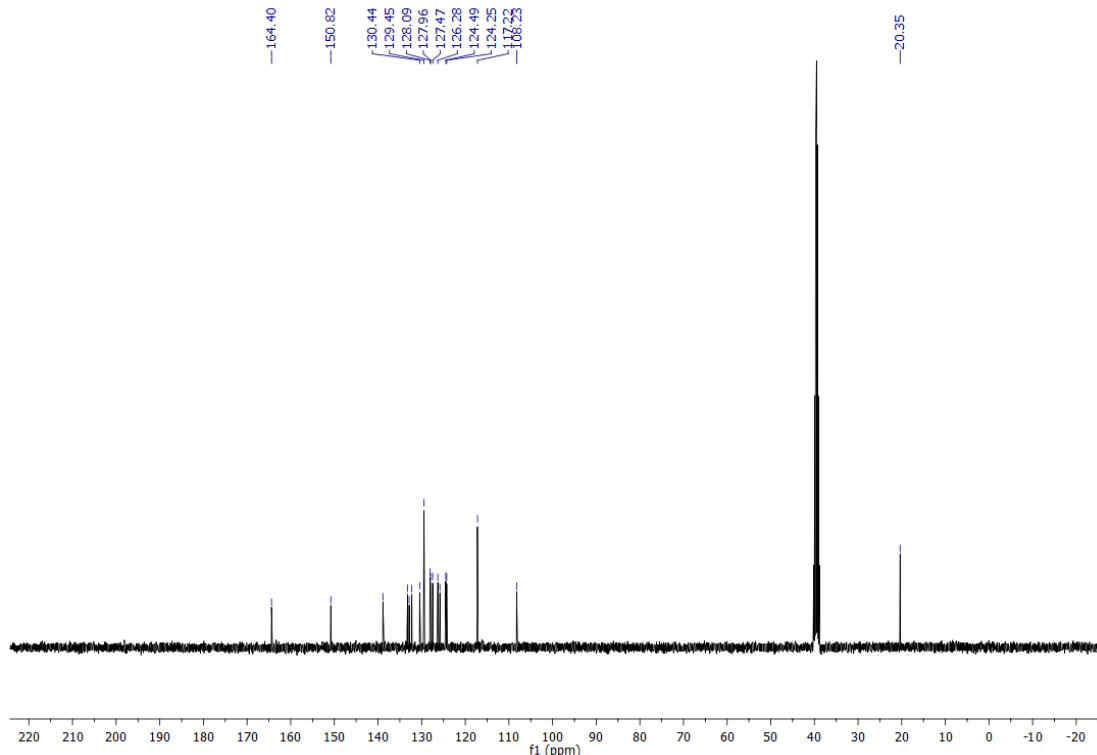


Figure S 46: ¹³C-NMR (101 MHz, DMSO- d_6) of compound 15

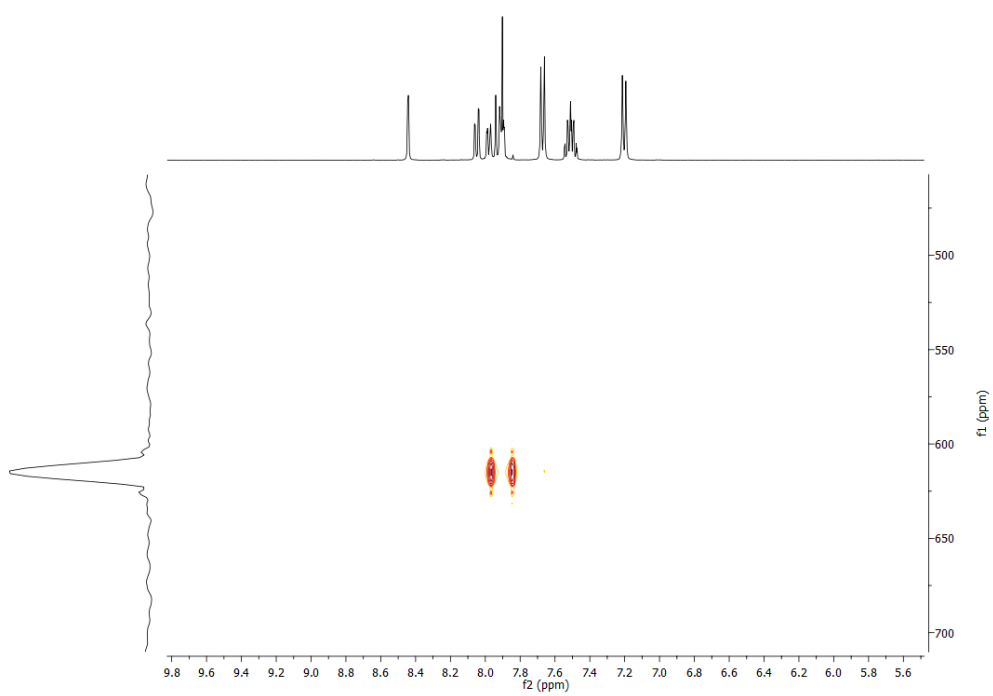


Figure S 47: ^1H - ^{77}Se -HMBC (400 MHz, 76 MHz, $\text{DMSO}-d_6$) of compound 15

Compound 16

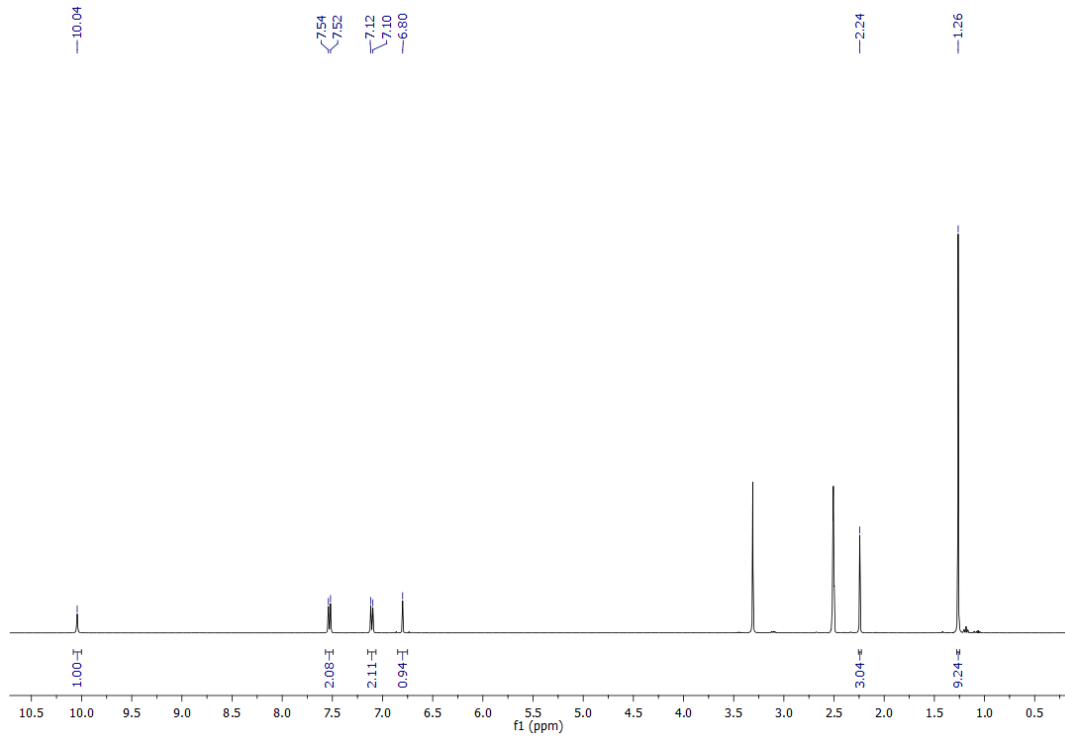


Figure S 48: ^1H -NMR (400 MHz, $\text{DMSO}-d_6$) of compound 16

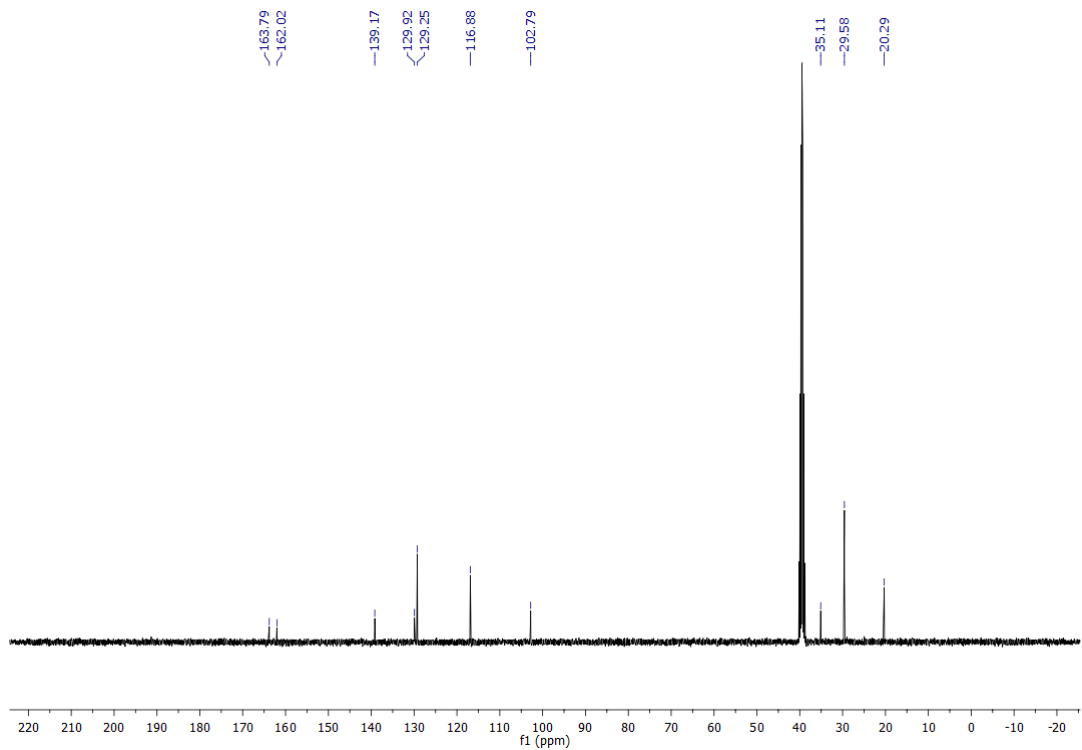


Figure S 49: ^{13}C -NMR (101 MHz, $\text{DMSO}-d_6$) of compound 16

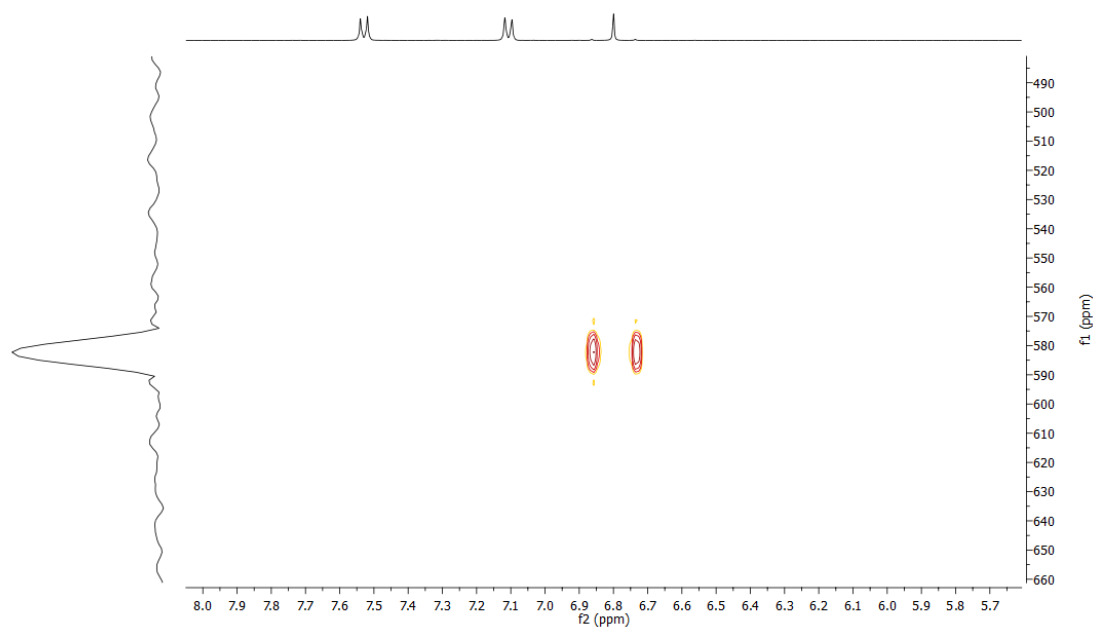


Figure S 50: ^1H - ^{77}Se -HMBC (400 MHz, 76 MHz, $\text{DMSO}-d_6$) of compound 16

Compound 17

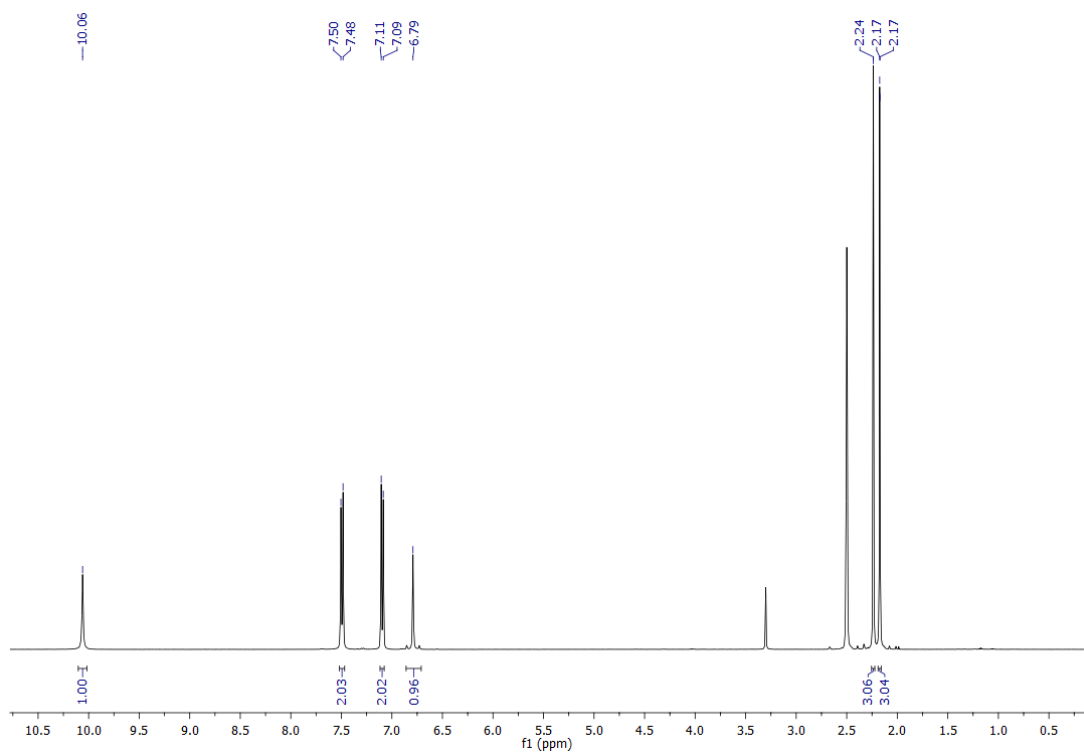


Figure S 51: ¹H-NMR (400 MHz, DMSO- d_6) of compound 17

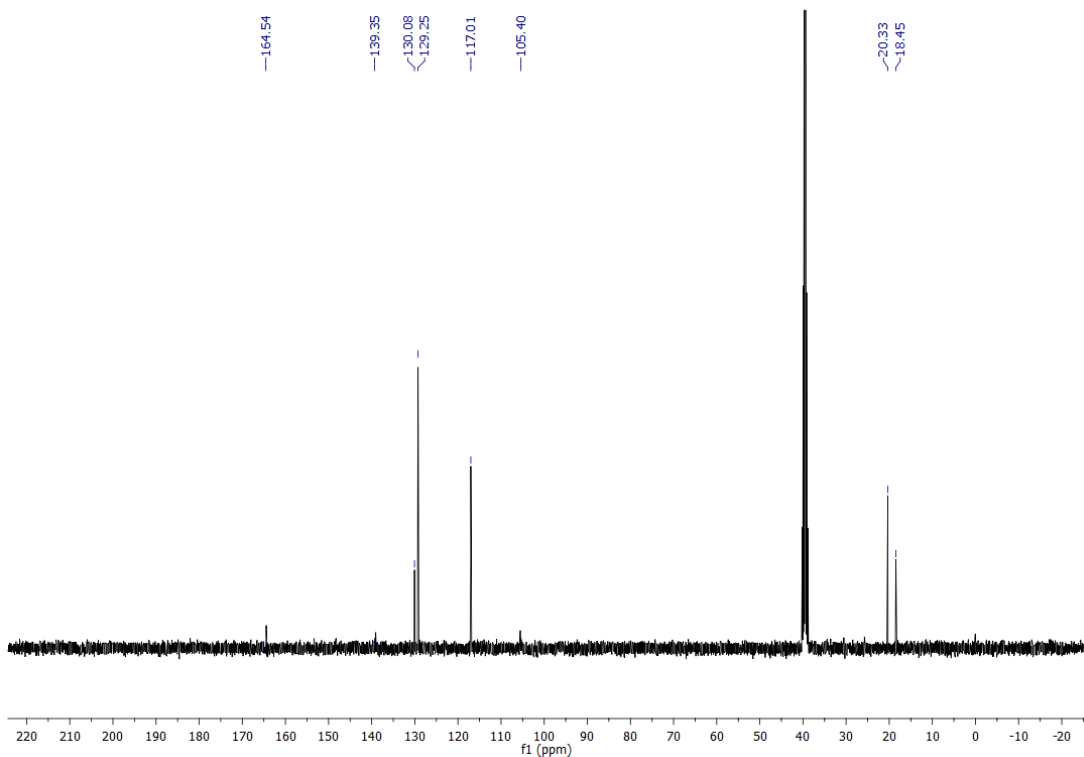


Figure S 52: ¹³C-NMR (101 MHz, DMSO- d_6) of compound 17

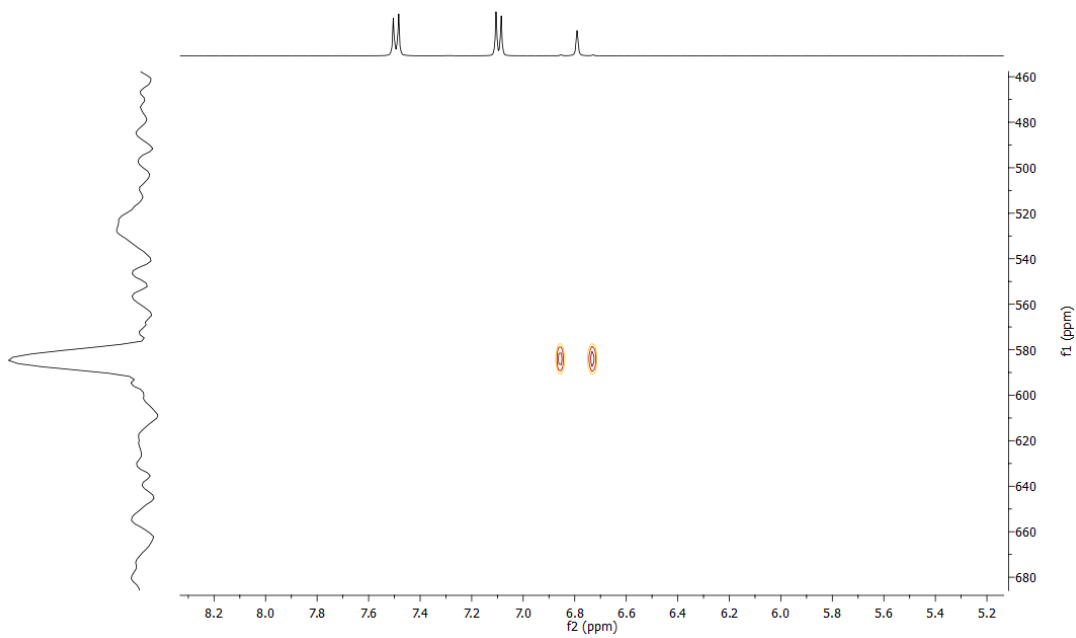


Figure S 53: ^1H - ^{77}Se -HMBC (400 MHz, 76 MHz, $\text{DMSO}-d_6$) of compound 17

Compound 18

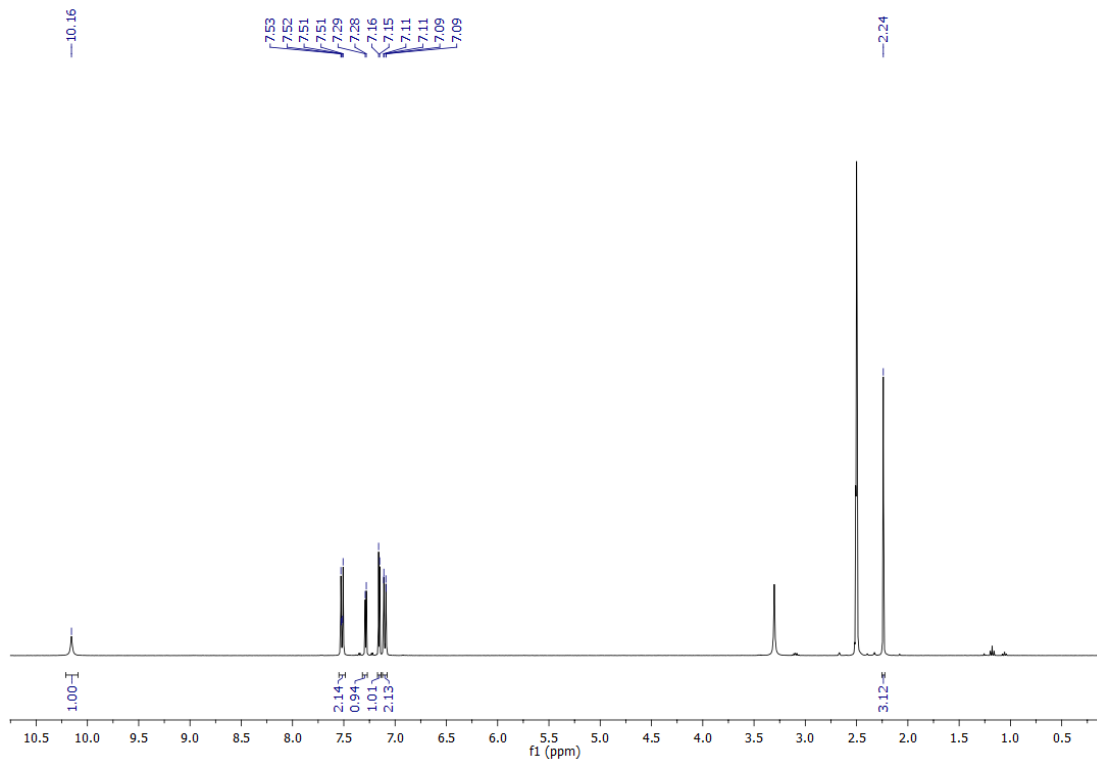


Figure S 54: ^1H -NMR (400 MHz, $\text{DMSO}-d_6$) of compound 18

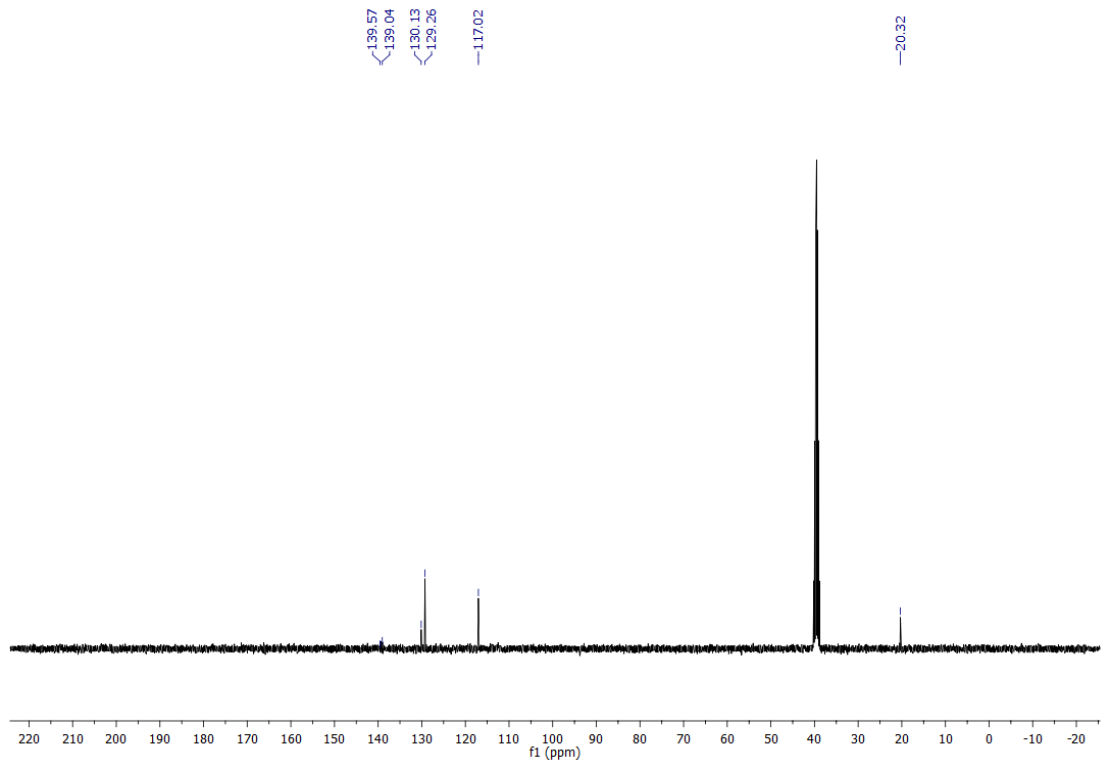


Figure S 55: ^{13}C -NMR (101 MHz, $\text{DMSO}-d_6$) of compound 18

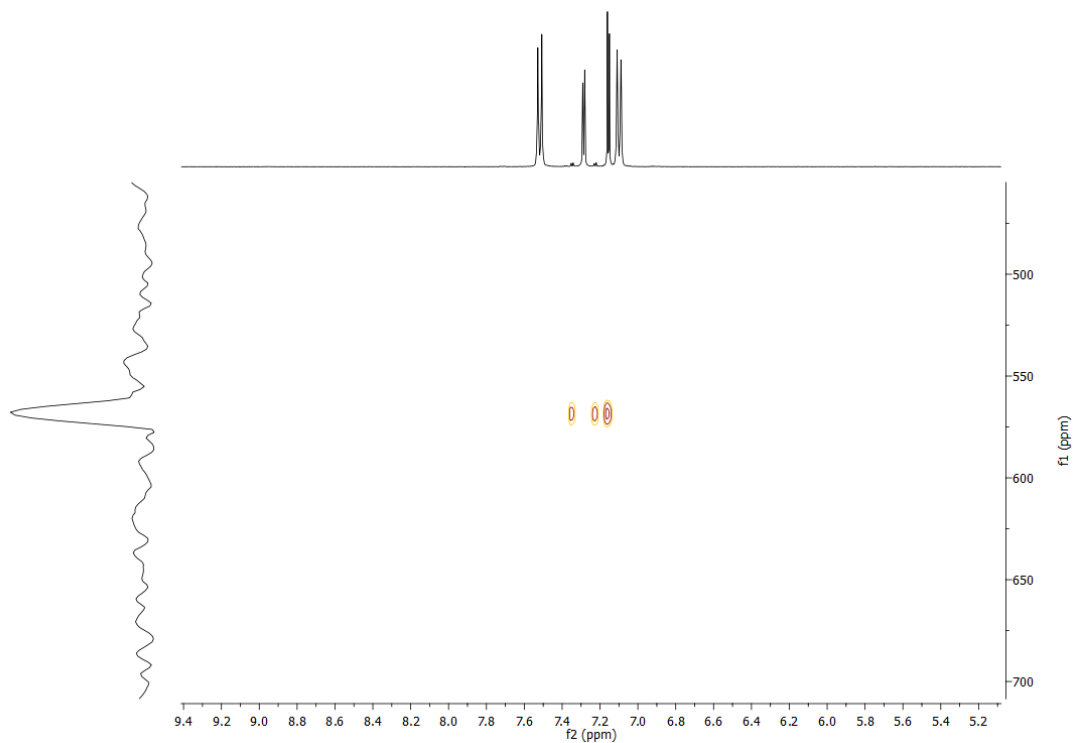


Figure S 56: ^1H - ^{77}Se -HMBC (400 MHz, 76 MHz, $\text{DMSO}-d_6$) of compound 18

Compound 19

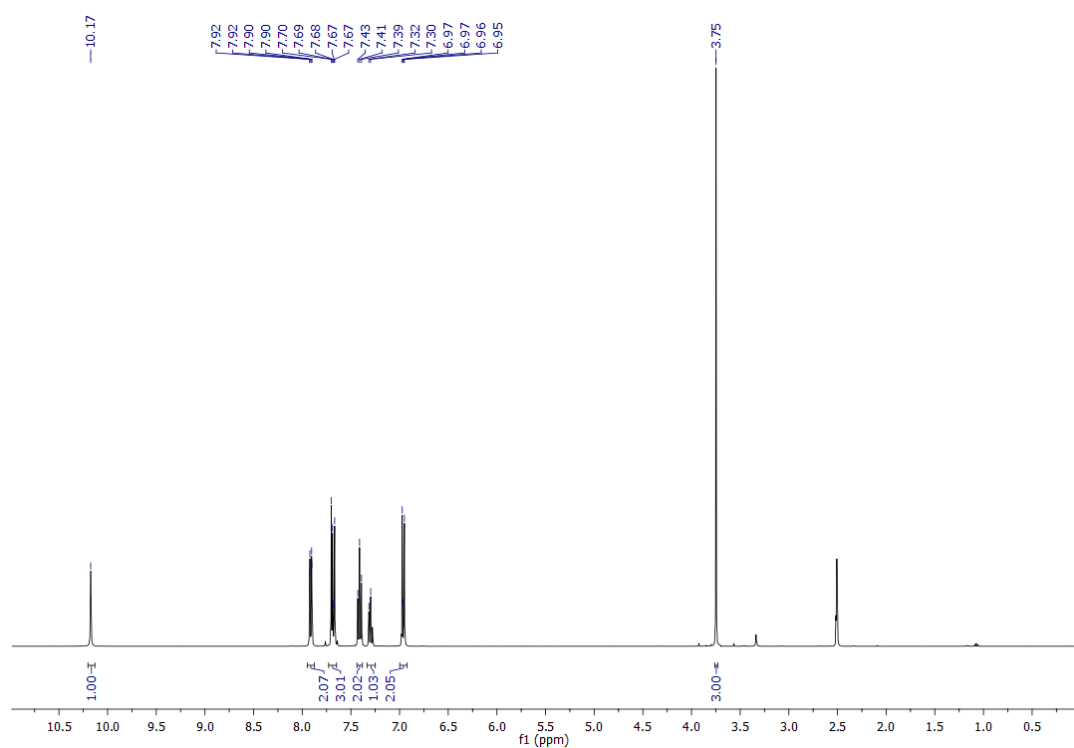


Figure S 57: ¹H-NMR (400 MHz, DMSO- d_6) of compound 19

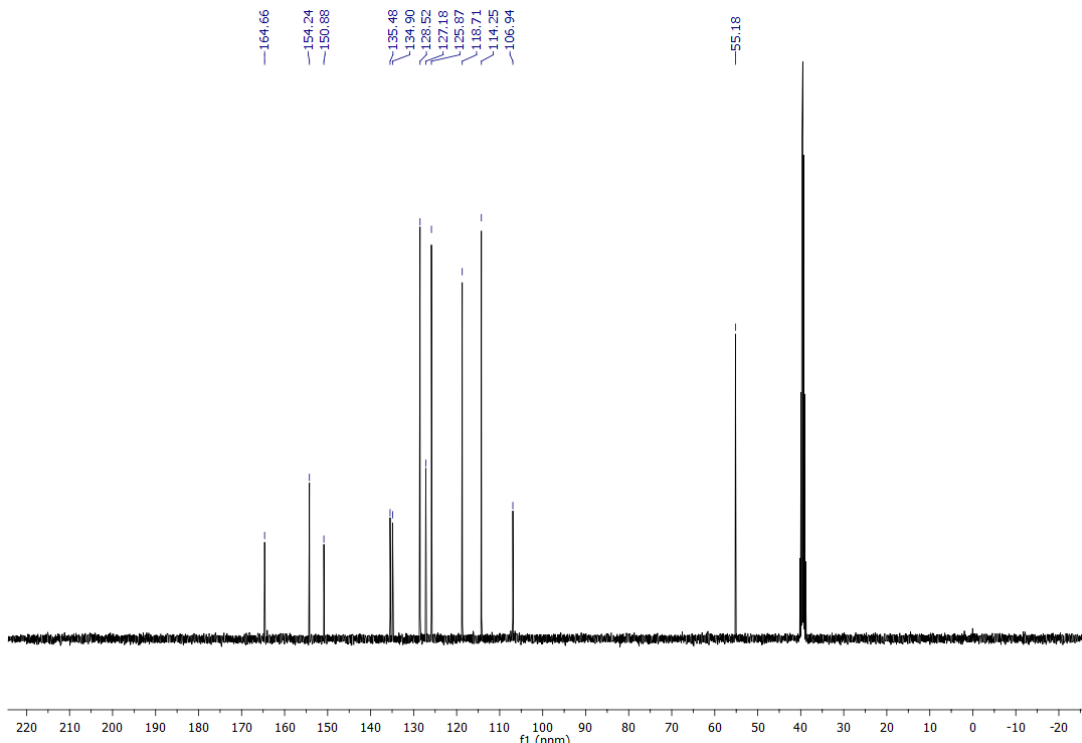


Figure S 58: ¹³C-NMR (101 MHz, DMSO- d_6) of compound 19

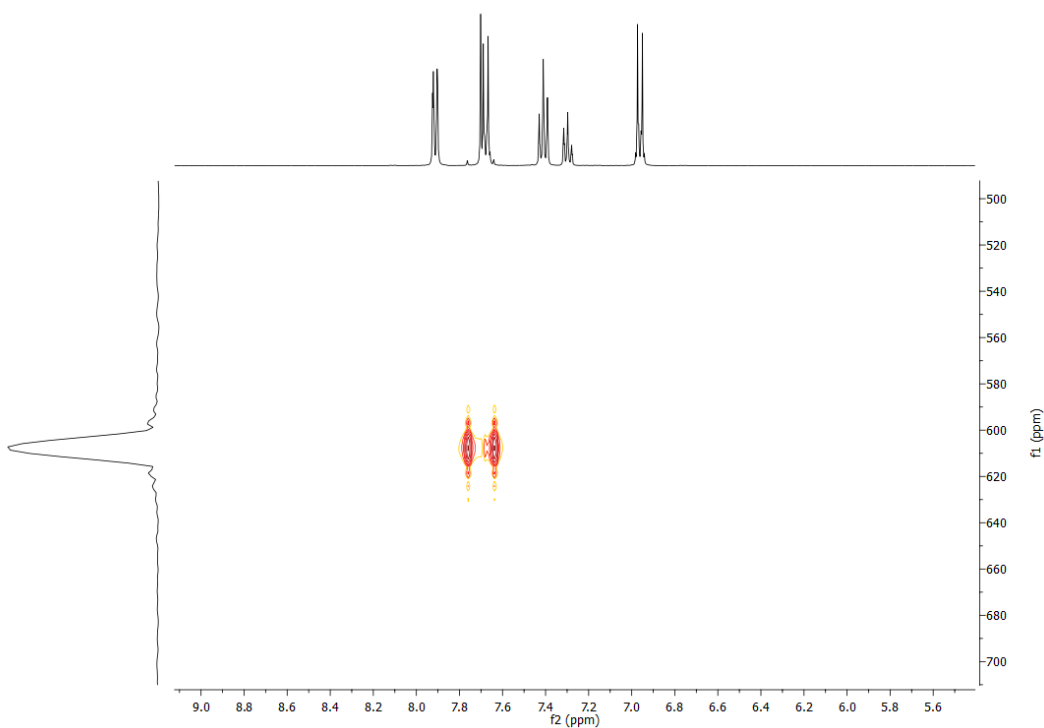


Figure S 59: ^1H - ^{77}Se -HMBC (400 MHz, 76 MHz, $\text{DMSO}-d_6$) of compound 19

Compound 20

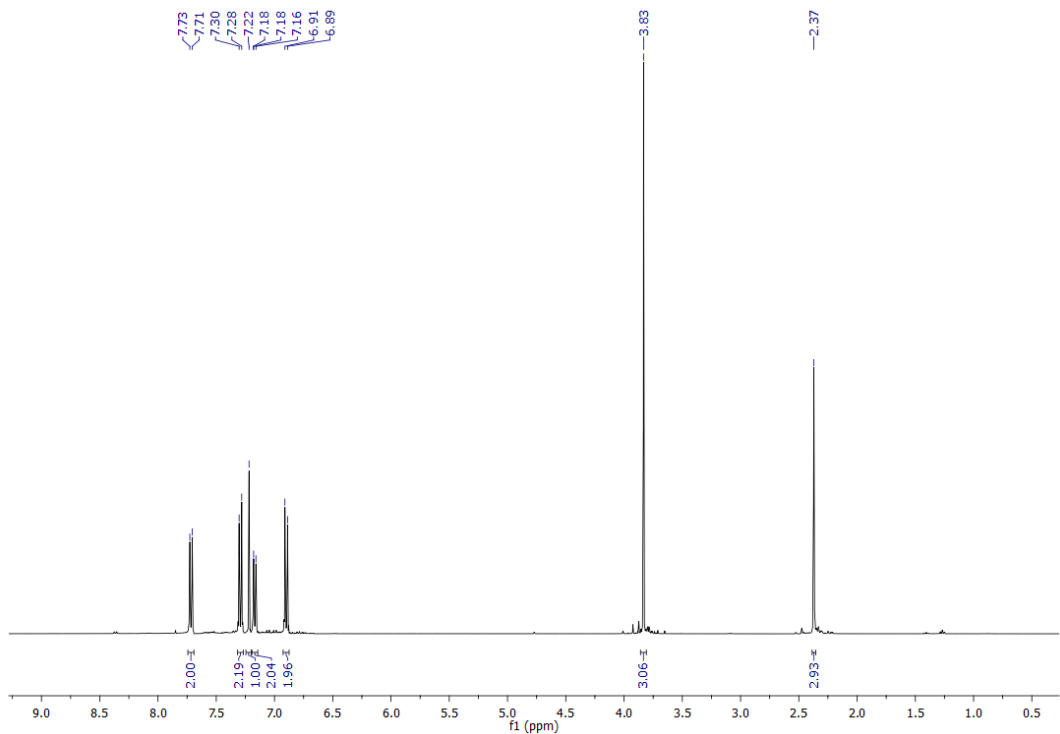


Figure S 60: ^1H -NMR (400 MHz, $\text{DMSO}-d_6$) of compound 20

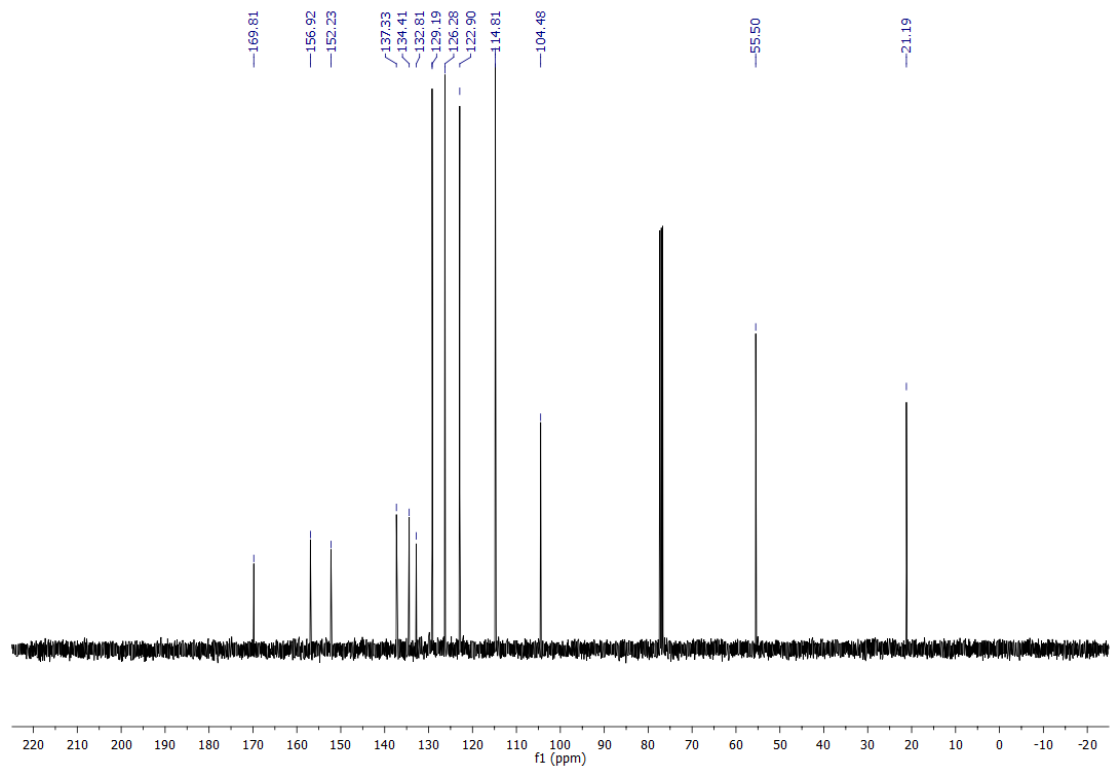


Figure S 61: ^{13}C -NMR (101 MHz, $\text{DMSO}-d_6$) of compound 20

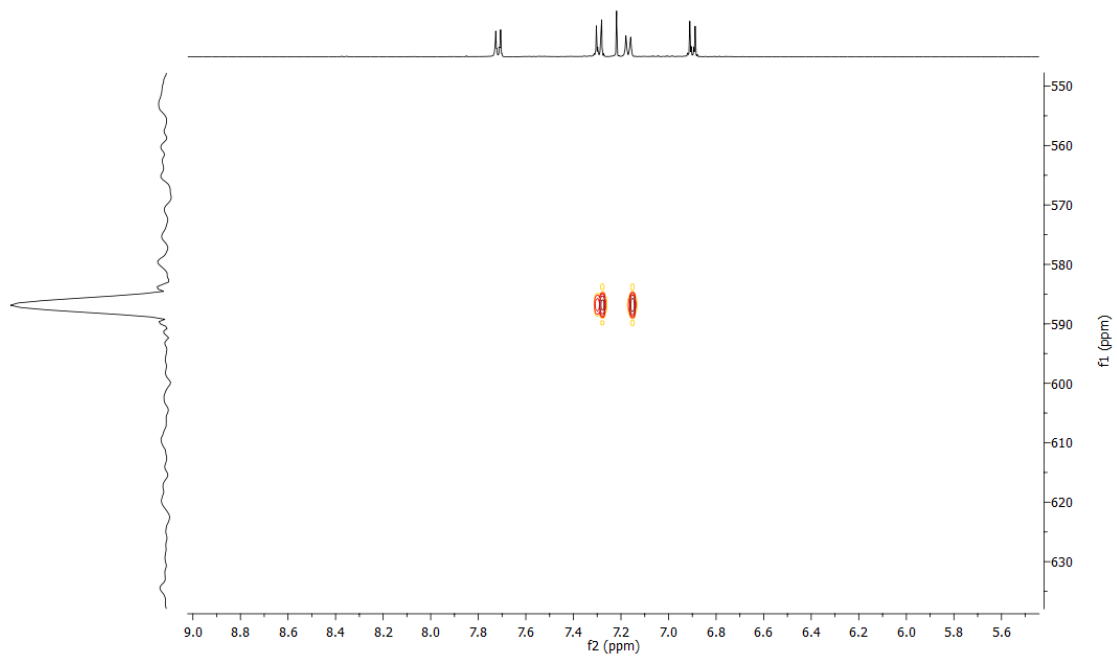


Figure S 62: $^1\text{H}-^{77}\text{Se}$ -HMBC (400 MHz, 76 MHz, $\text{DMSO}-d_6$) of compound 20

Compound 21

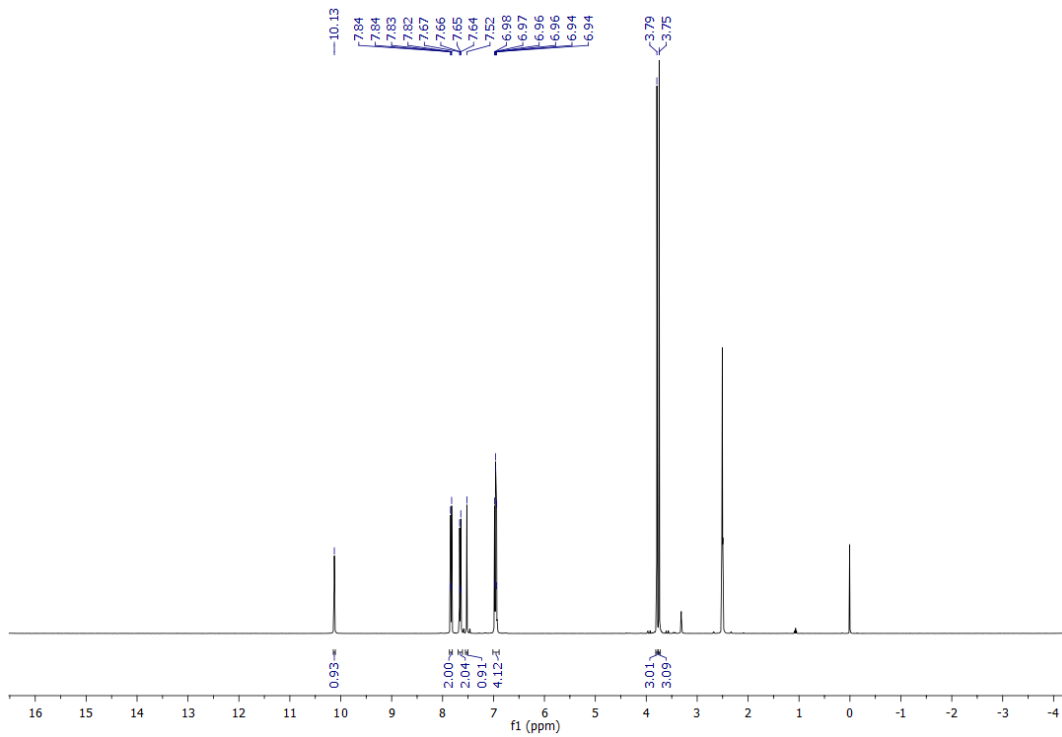


Figure S 63: ^1H -NMR (400 MHz, $\text{DMSO}-d_6$) of compound 21

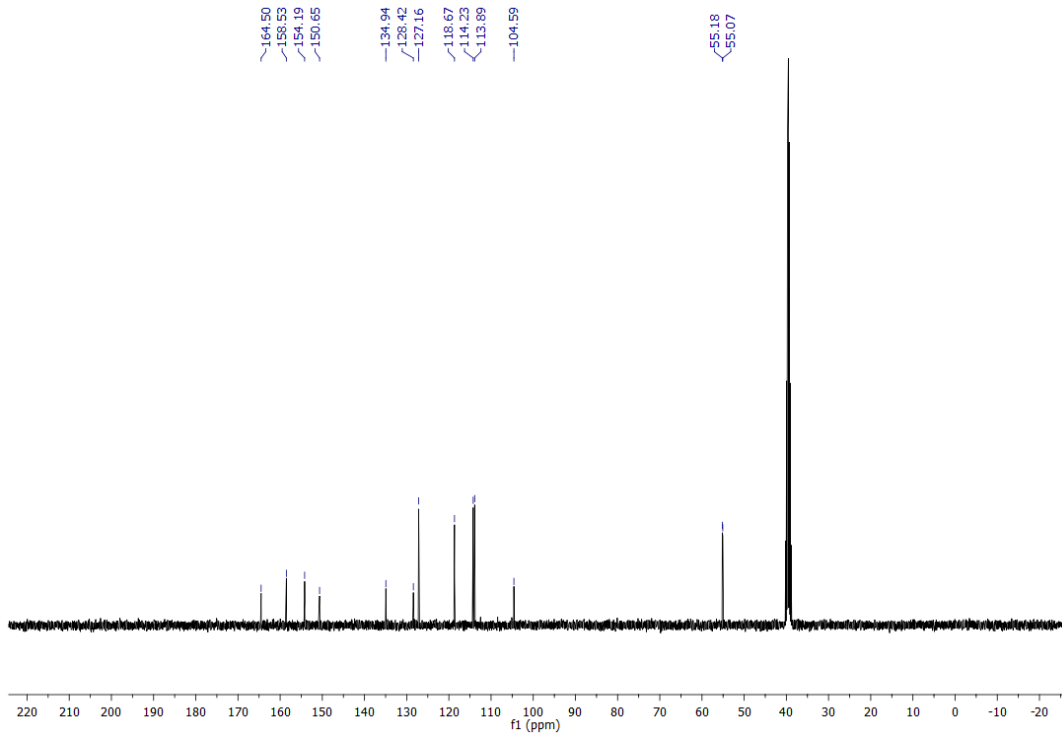


Figure S 64: ^{13}C -NMR (101 MHz, $\text{DMSO}-d_6$) of compound 21

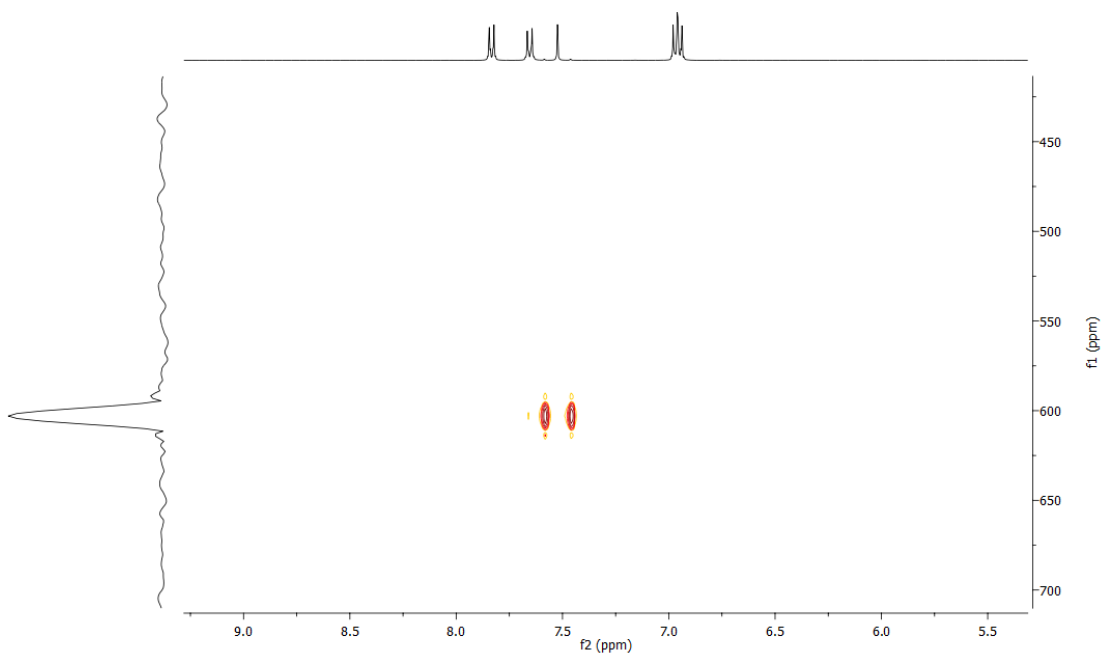


Figure S 65: ^1H - ^{77}Se -HMBC (400 MHz, 76 MHz, $\text{DMSO}-d_6$) of compound 21

Compound 22

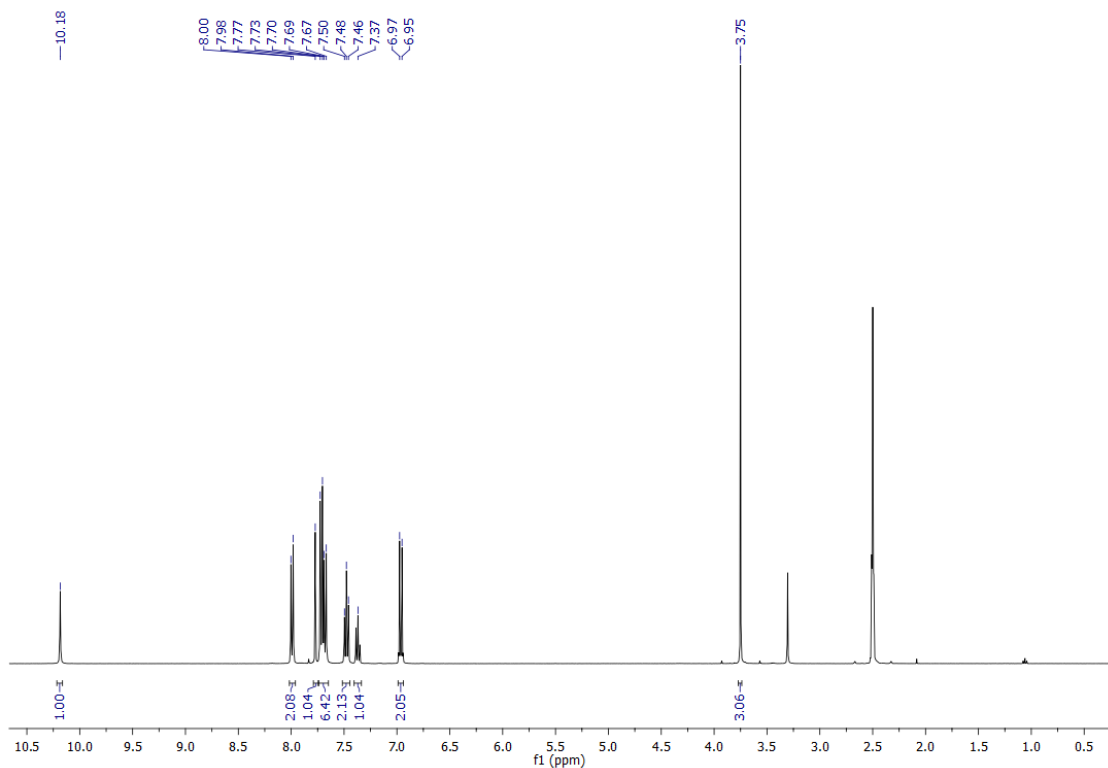


Figure S 66: ^1H -NMR (400 MHz, $\text{DMSO}-d_6$) of compound 22

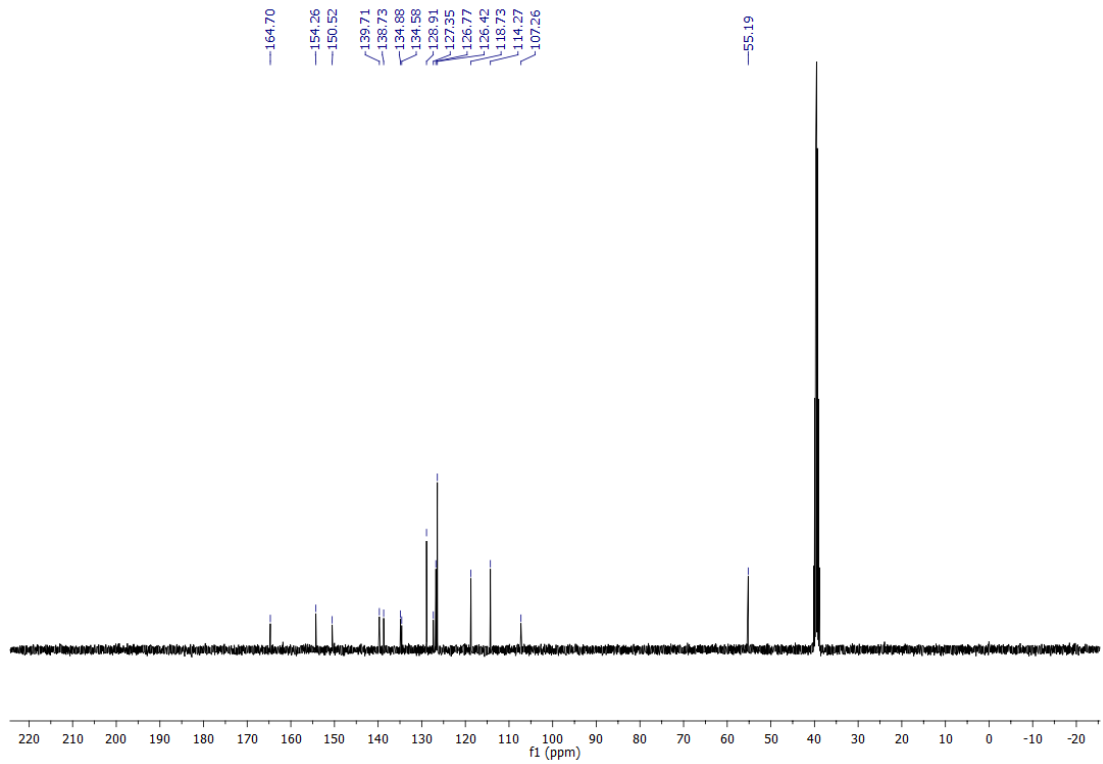


Figure S 67: ^{13}C -NMR (101 MHz, $\text{DMSO}-d_6$) of compound 22

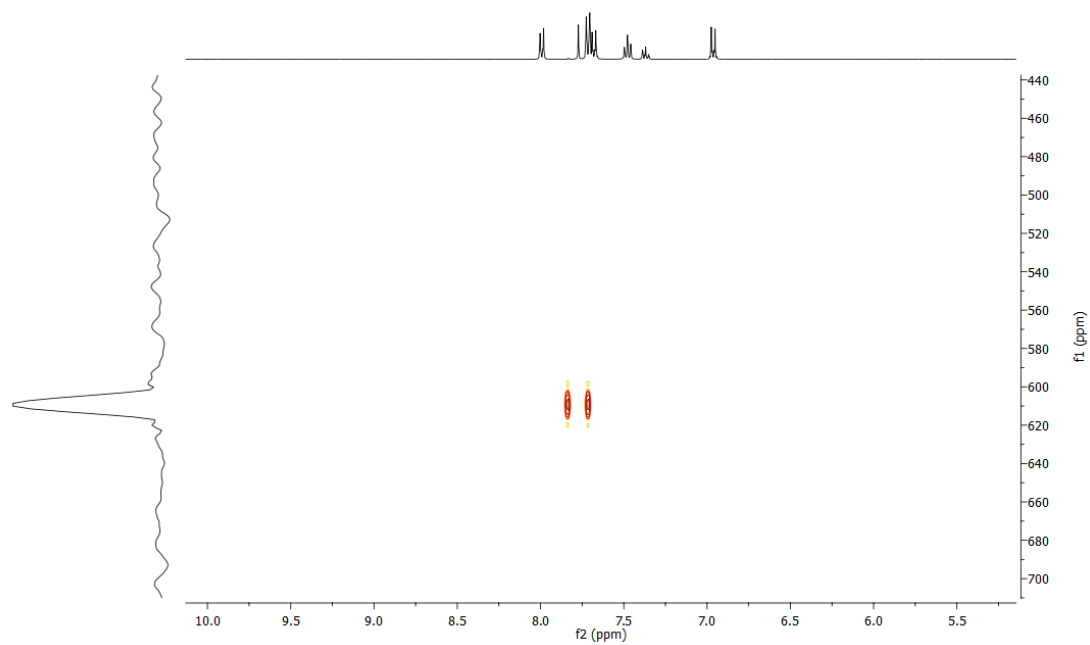


Figure S 68: ^1H - ^{77}Se -HMBC (400 MHz, 76 MHz, $\text{DMSO}-d_6$) of compound 22

Compound 23

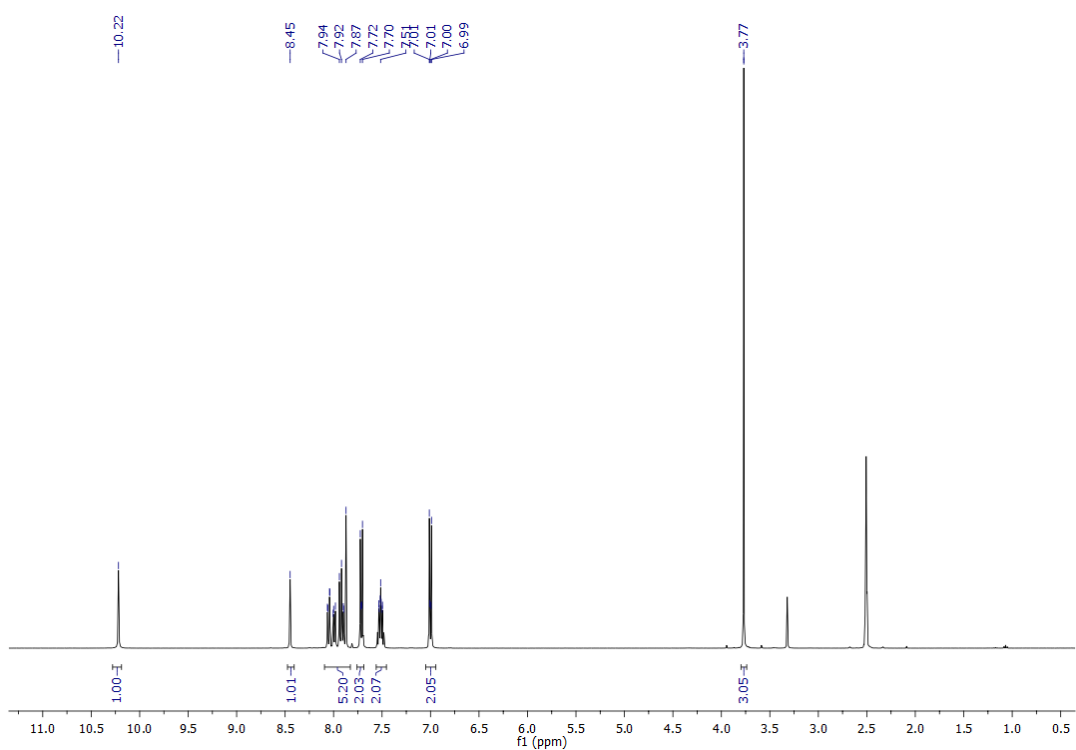


Figure S 69: ^1H -NMR (400 MHz, $\text{DMSO}-d_6$) of compound 23

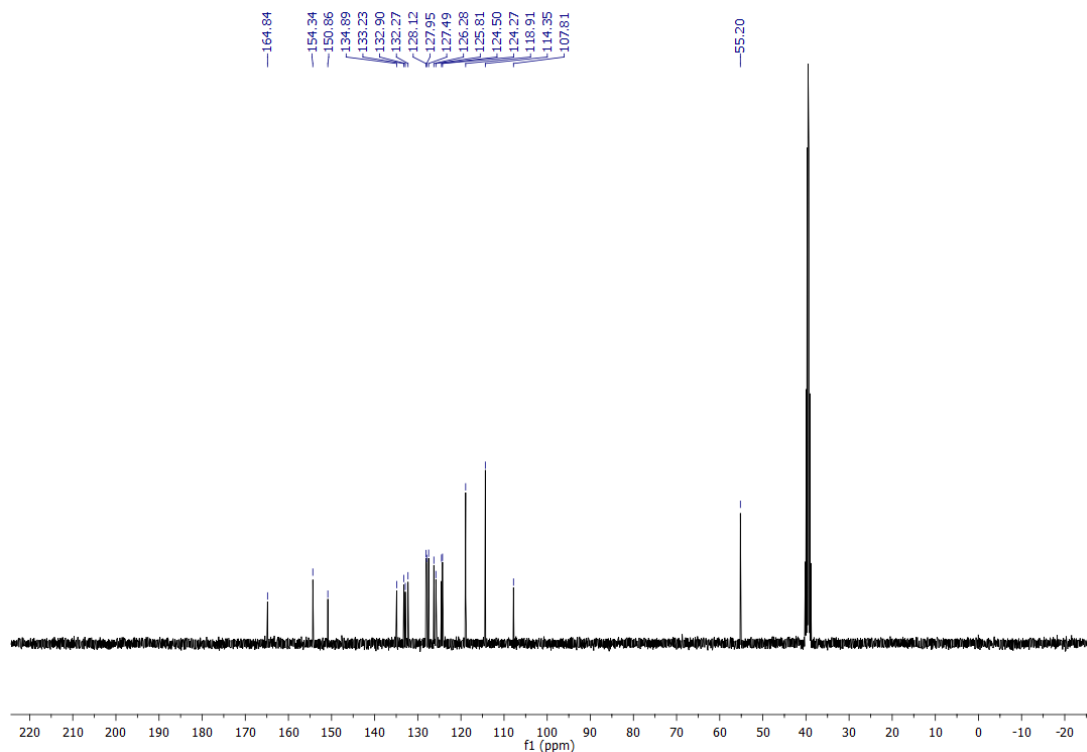


Figure S 70: ^{13}C -NMR (101 MHz, $\text{DMSO}-d_6$) of compound 23

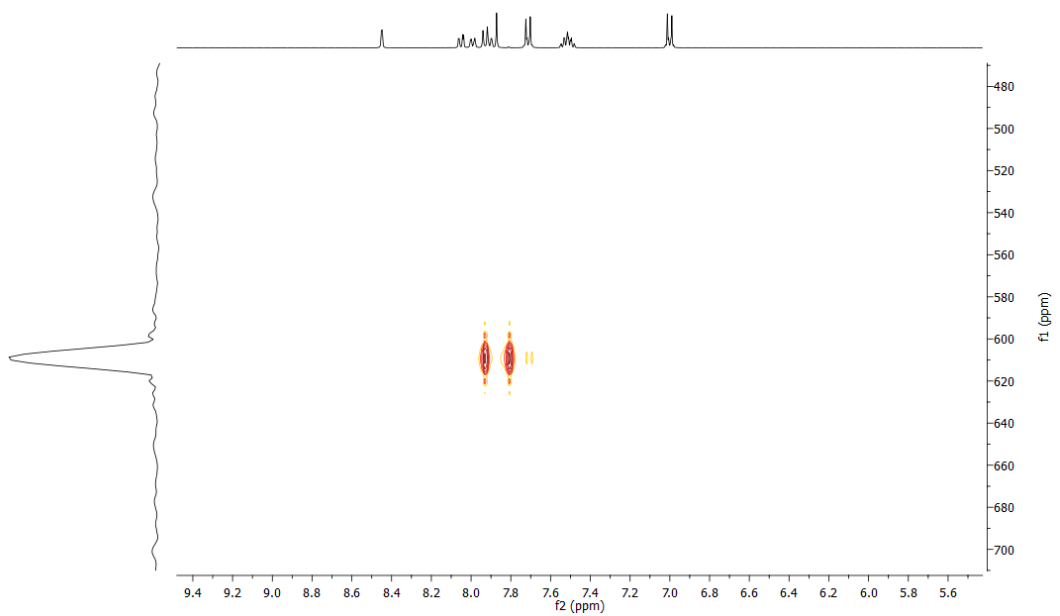


Figure S 71: ^1H - ^{77}Se -HMBC (400 MHz, 76 MHz, $\text{DMSO}-d_6$) of compound 23

Compound 24

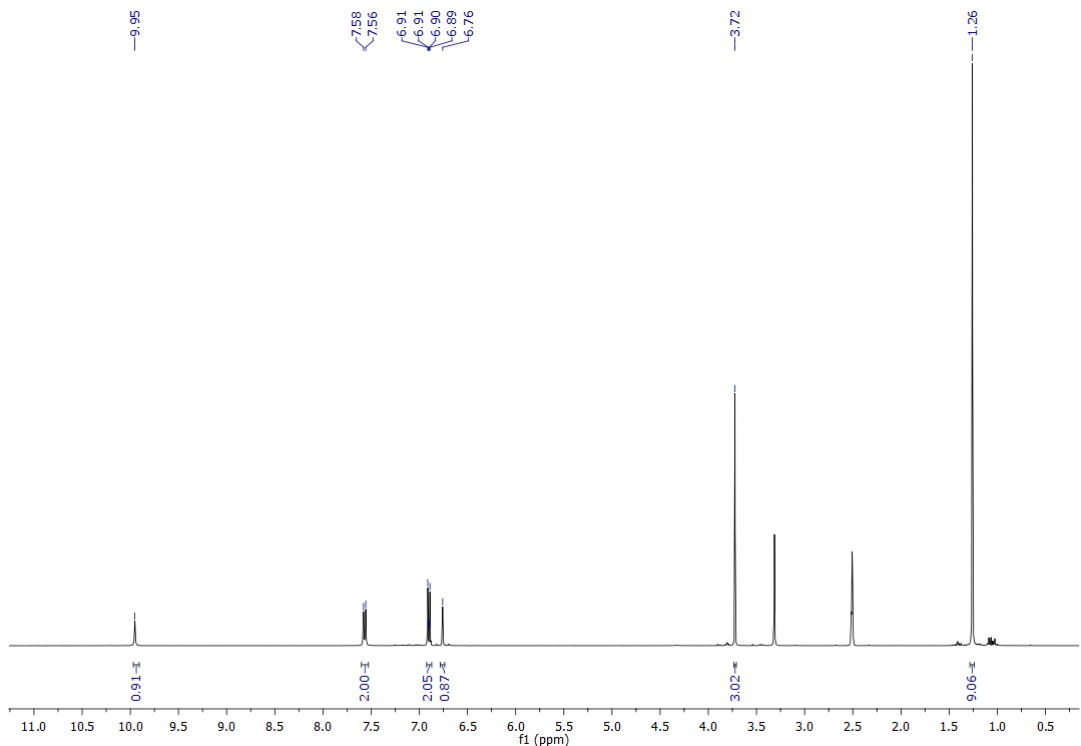


Figure S 72: ^1H -NMR (400 MHz, $\text{DMSO}-d_6$) of compound 24

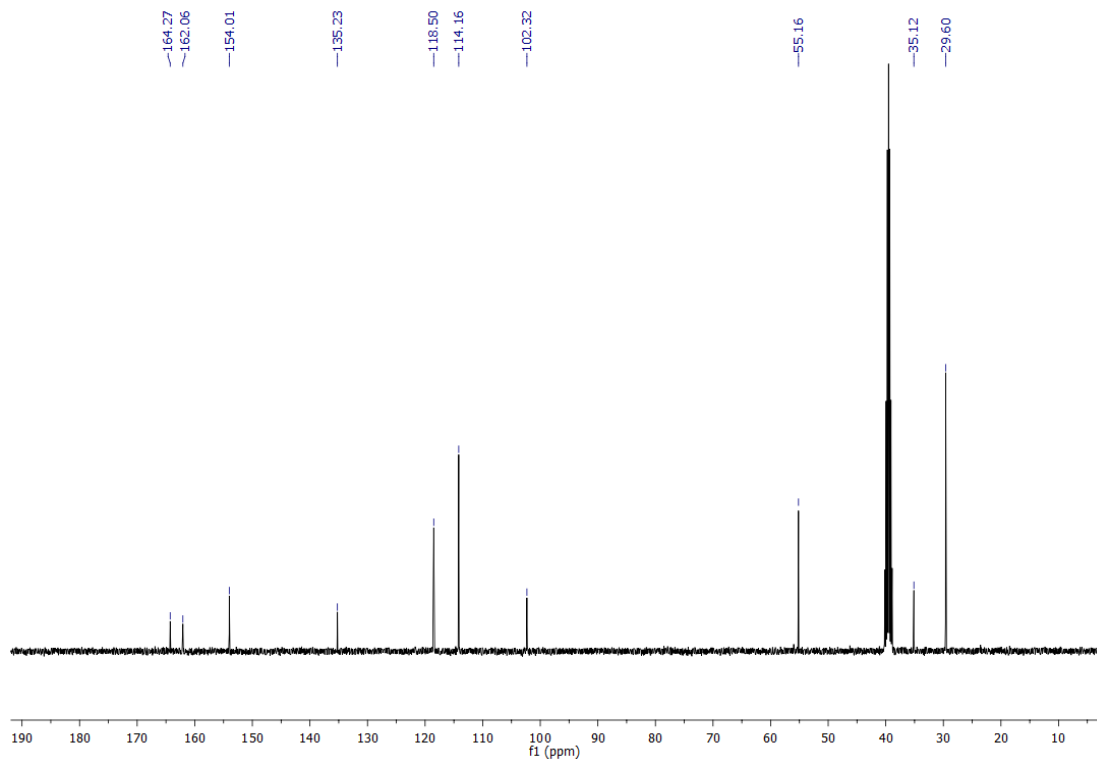


Figure S 73: ^{13}C -NMR (101 MHz, $\text{DMSO}-d_6$) of compound 24

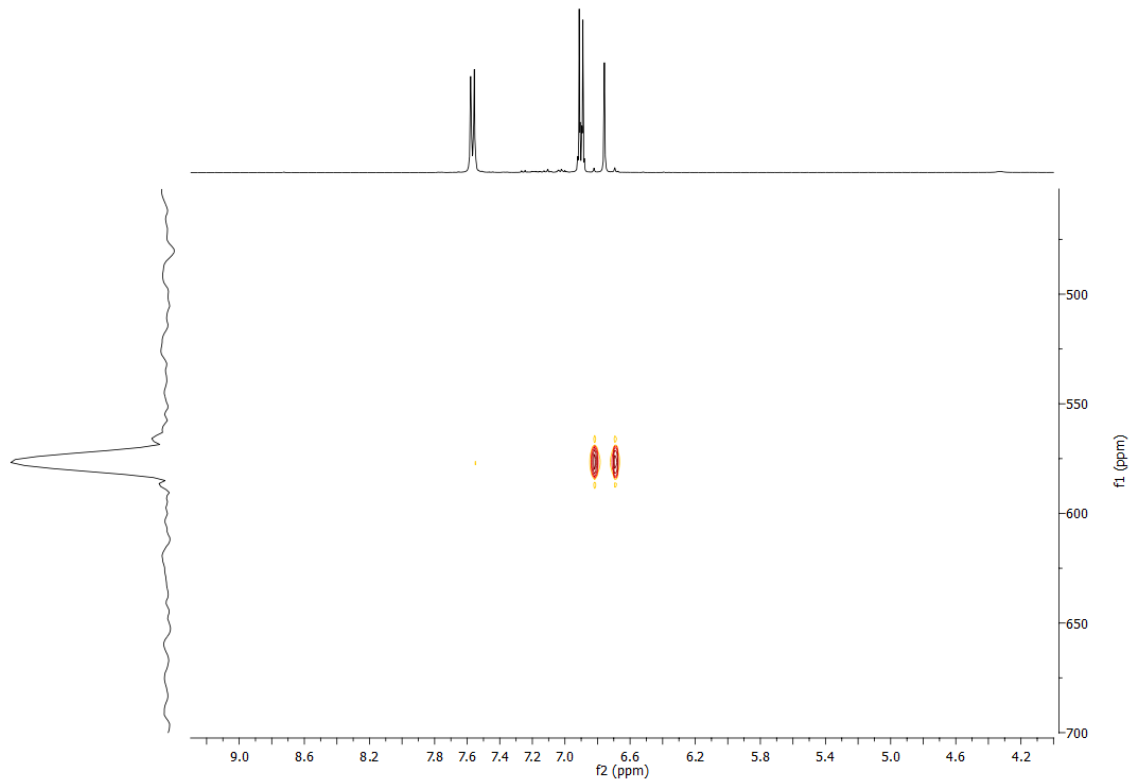


Figure S 74: ^1H - ^{77}Se -HMBC (400 MHz, 76 MHz, $\text{DMSO}-d_6$) of compound 24

Compound 25

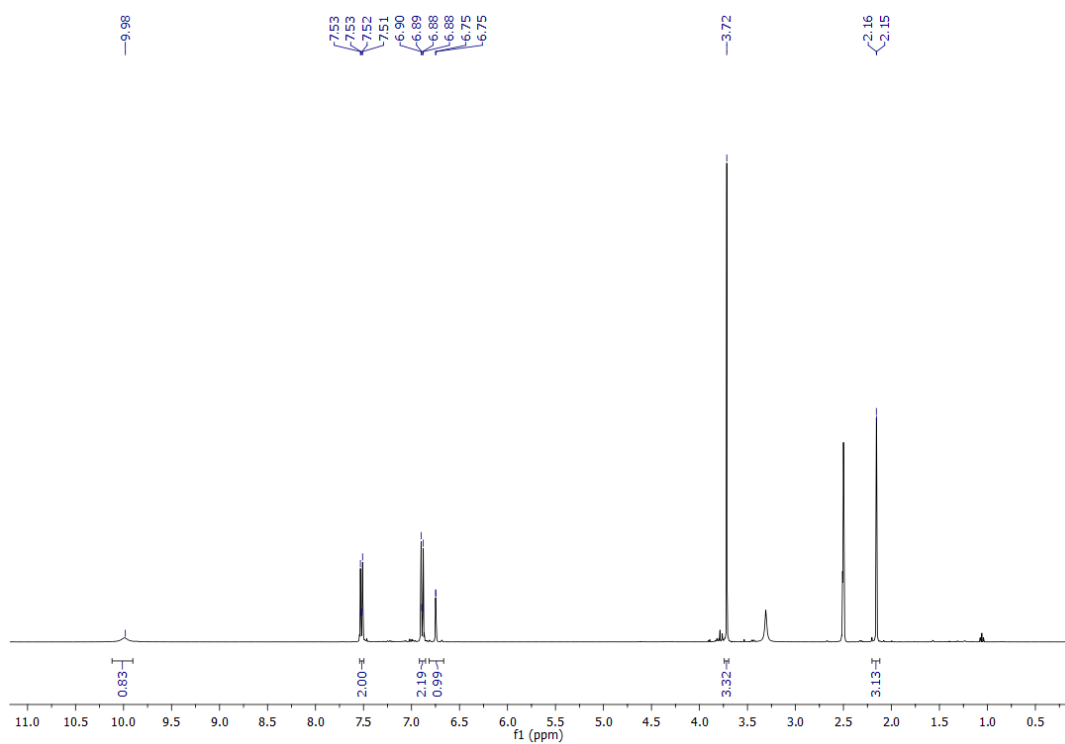


Figure S 75: ¹H-NMR (400 MHz, DMSO- d_6) of compound 25

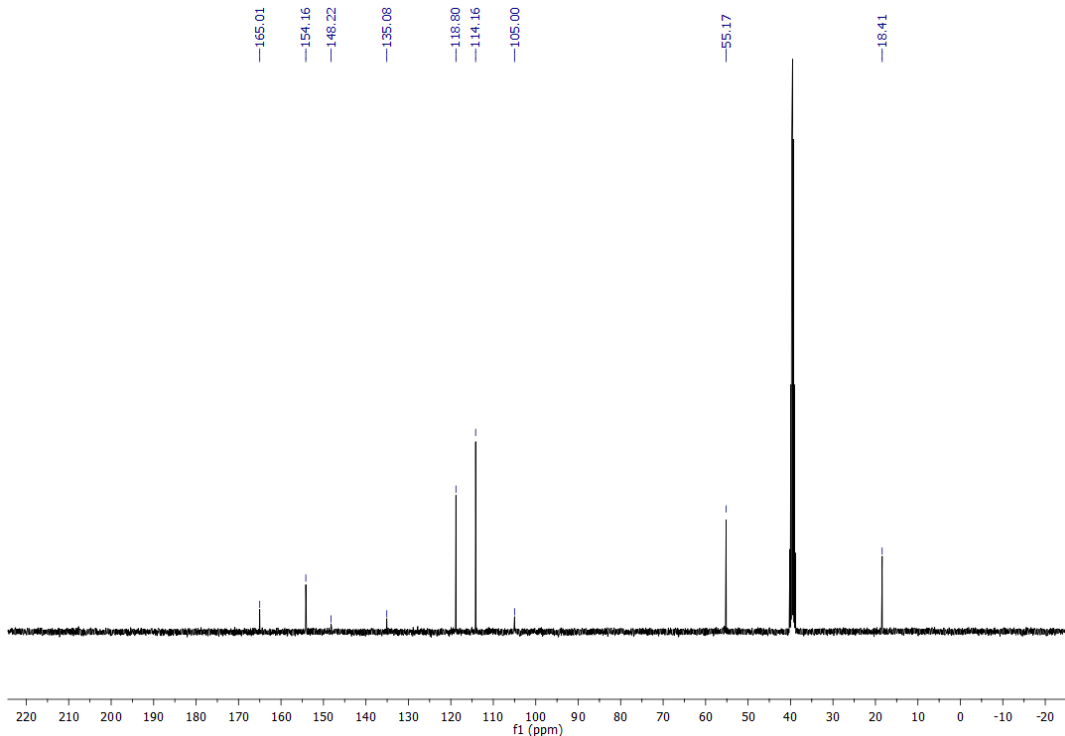


Figure S 76 : ¹³C-NMR (101 MHz, DMSO- d_6) of compound 25

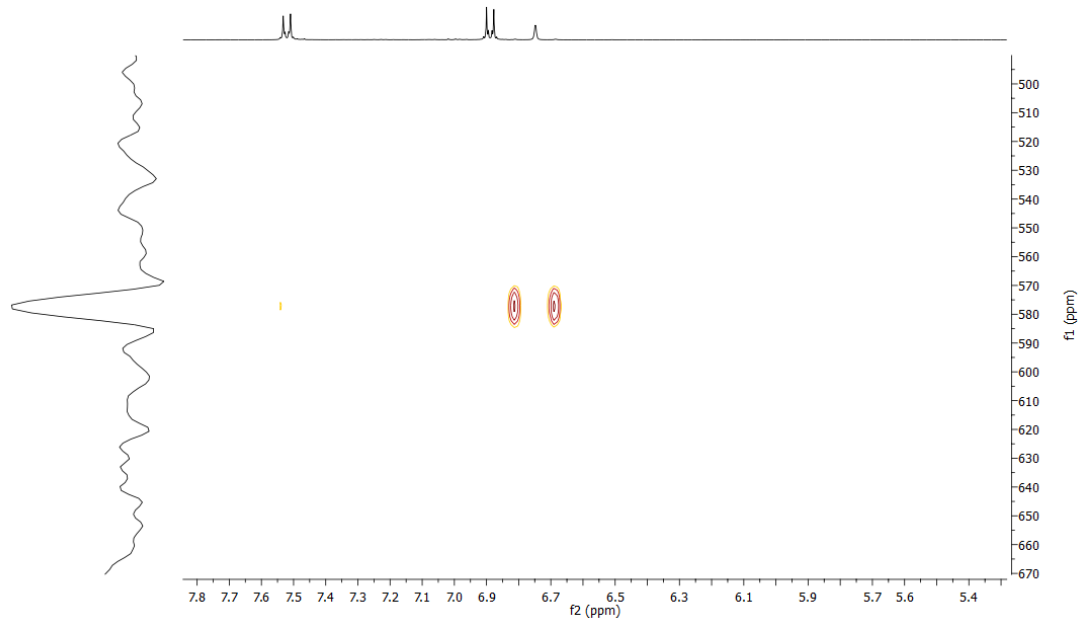


Figure S 77: ^1H - ^{77}Se -HMBC (400 MHz, 76 MHz, $\text{DMSO}-d_6$) of compound 25

Compound 26

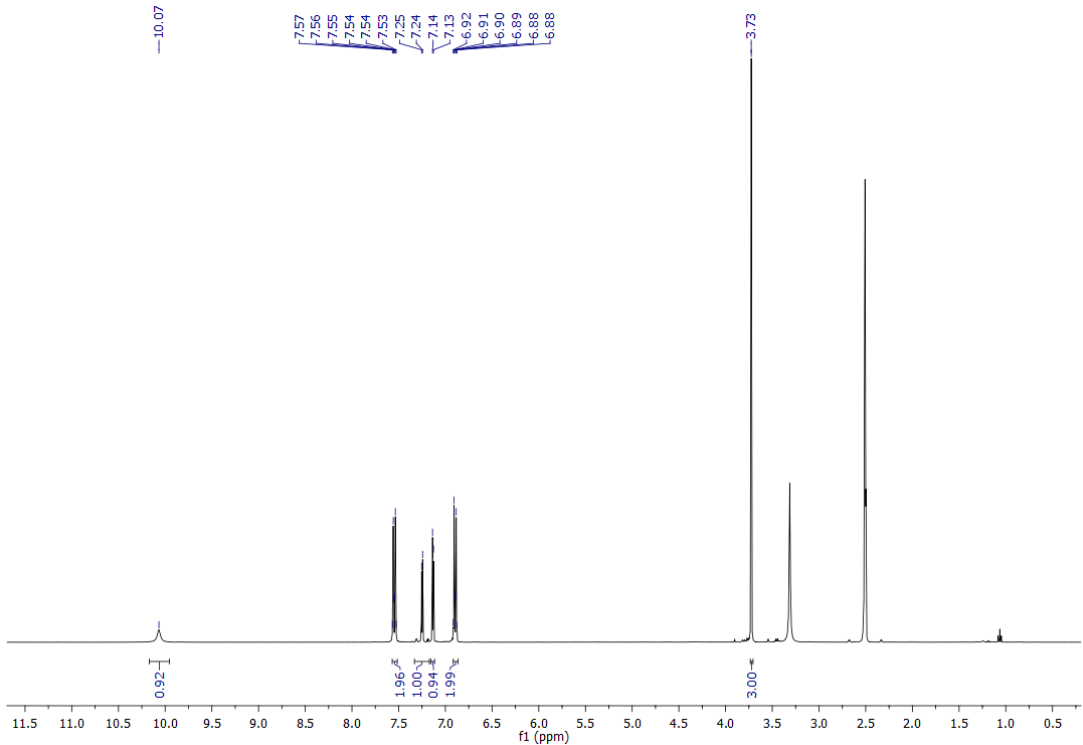


Figure S 78: ^1H -NMR (400 MHz, $\text{DMSO}-d_6$) of compound 26

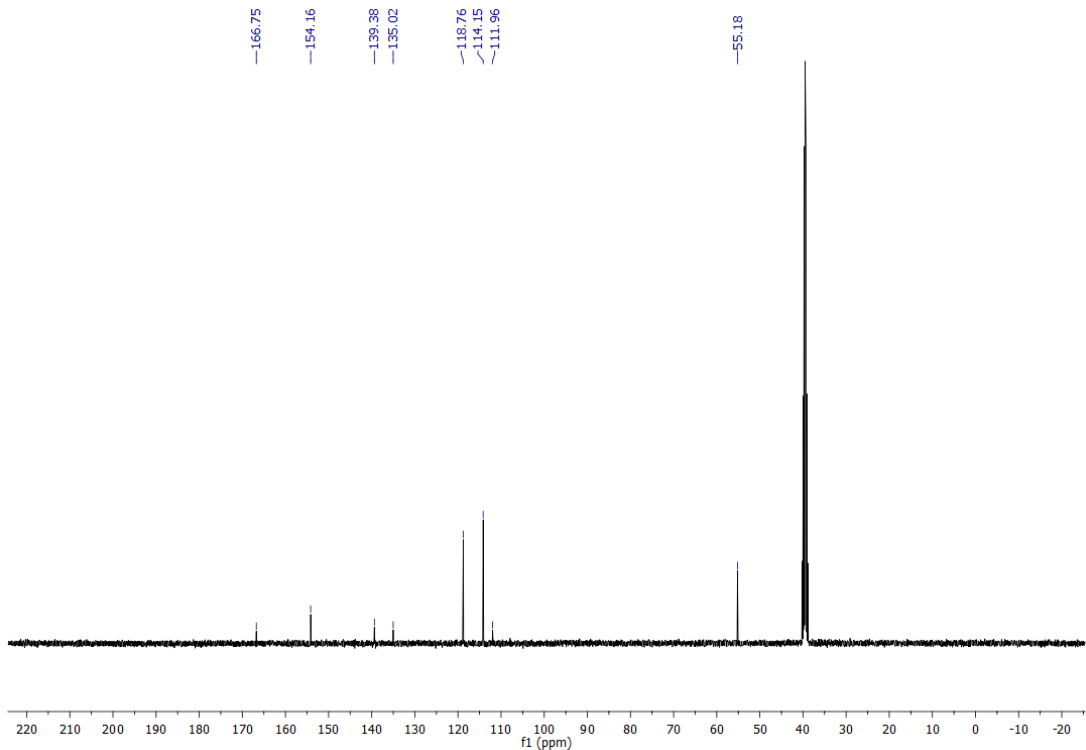


Figure S 79: ^{13}C -NMR (101 MHz, DMSO-d_6) of compound 26

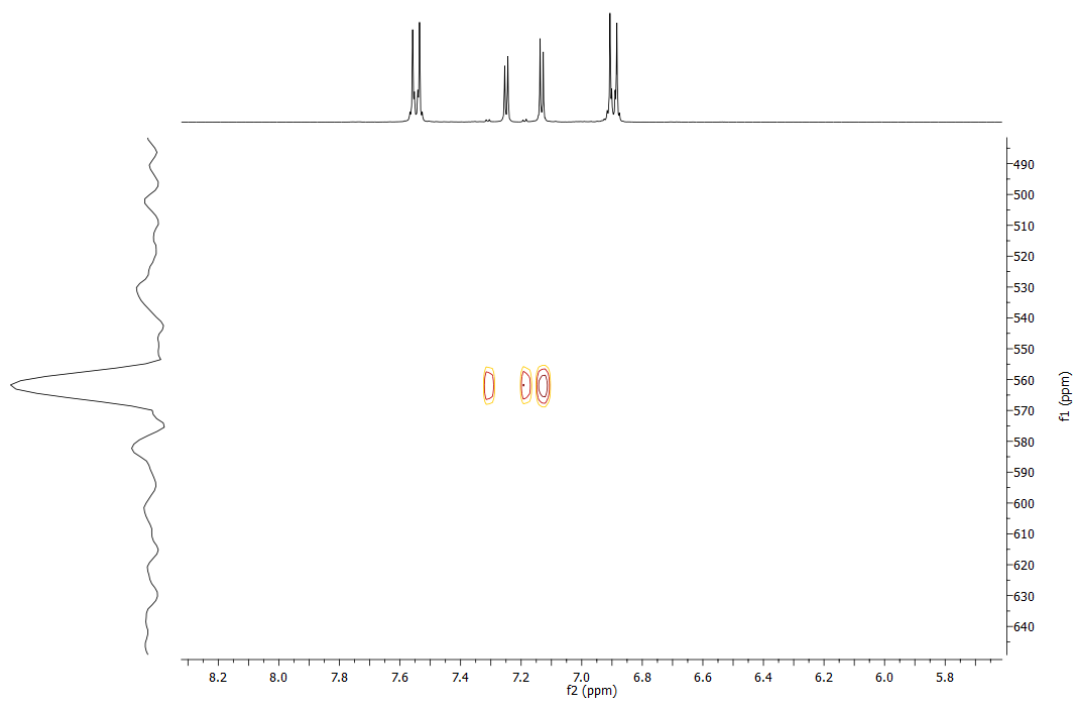
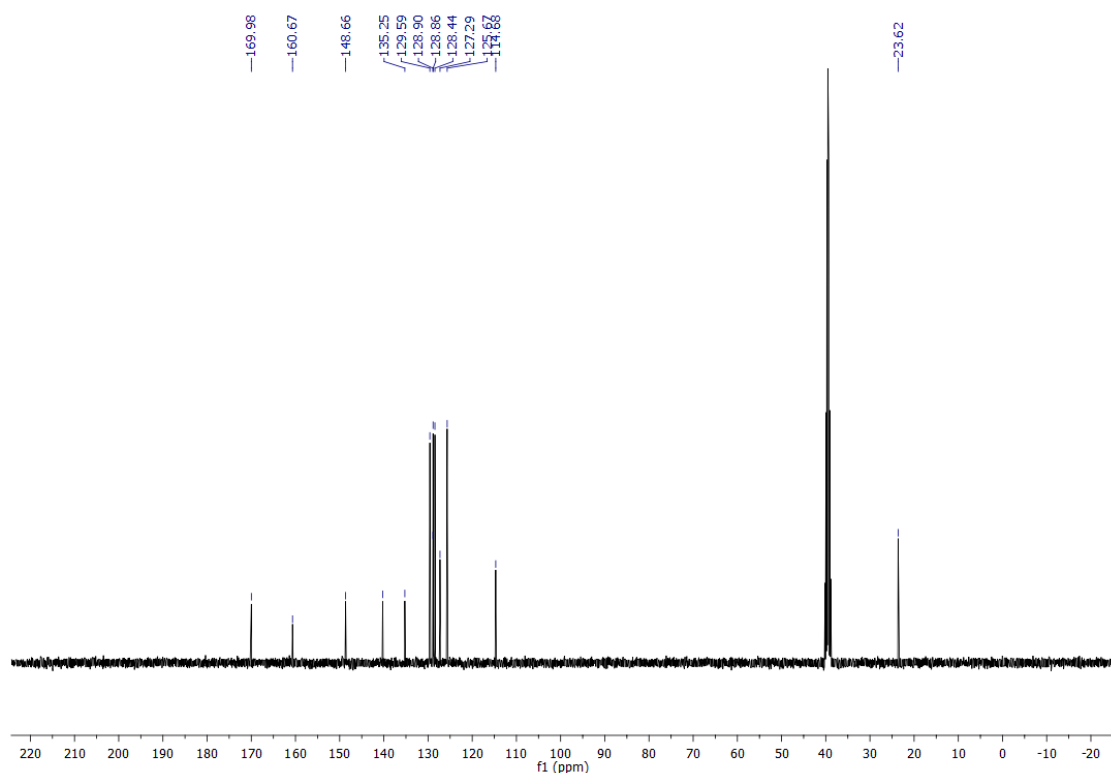
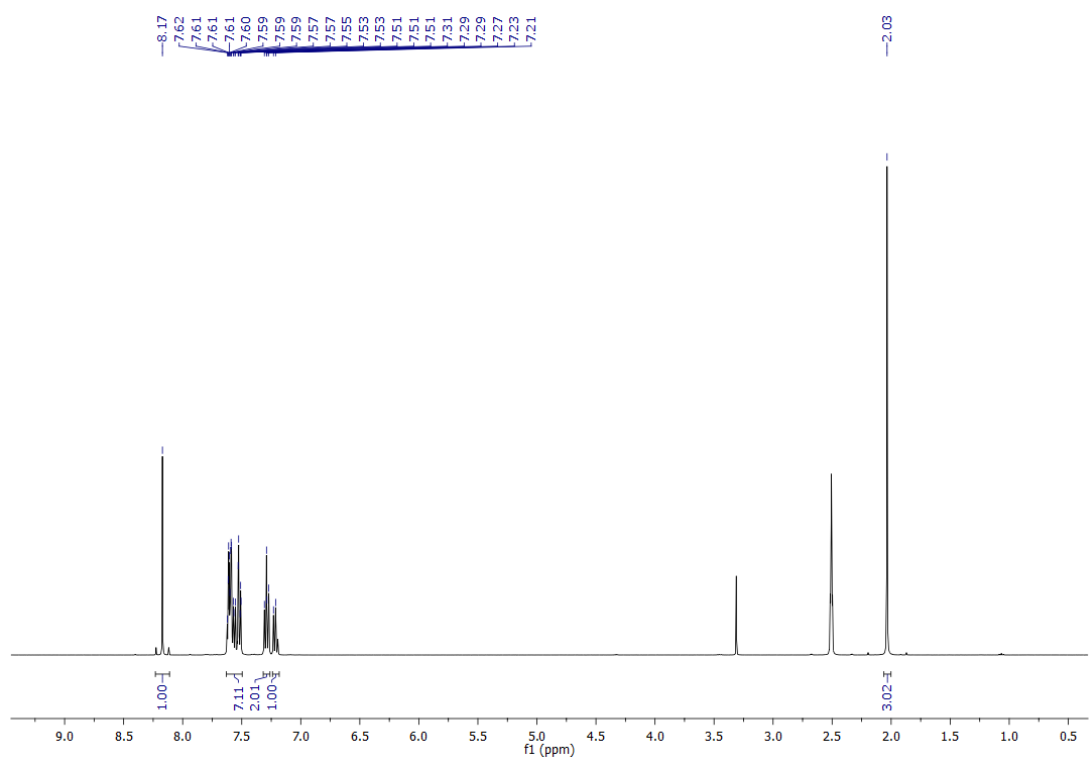


Figure S 80: $^1\text{H}-^{77}\text{Se}$ -HMBC (400 MHz, 76 MHz, DMSO-d_6) of compound 26

Compound 27



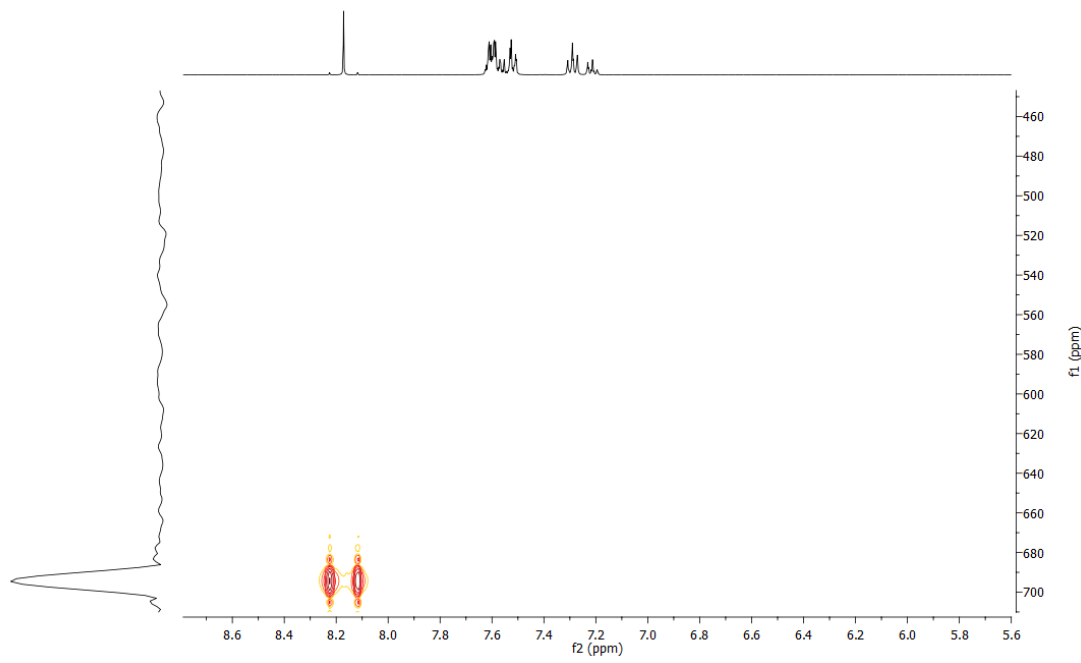


Figure S 83: ^1H - ^{77}Se -HMBC (400 MHz, 76 MHz, $\text{DMSO}-d_6$) of compound 27

Compound 28

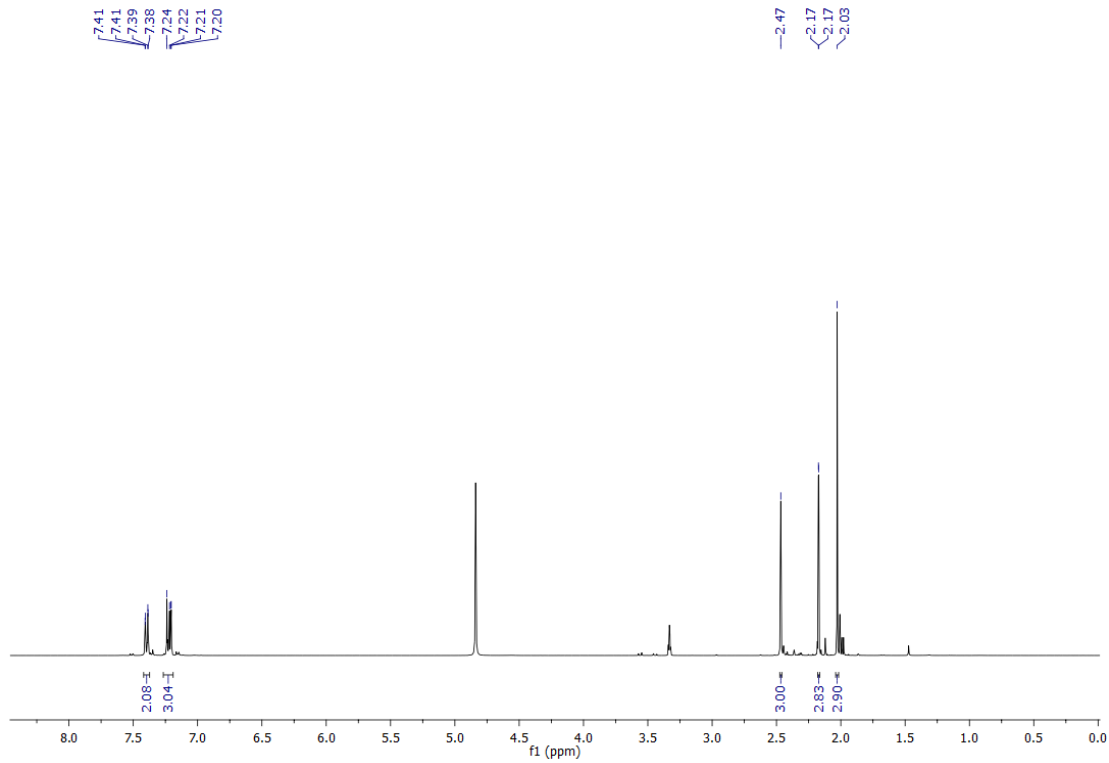


Figure S 84: ^1H -NMR (400 MHz, MeOD) of compound 28

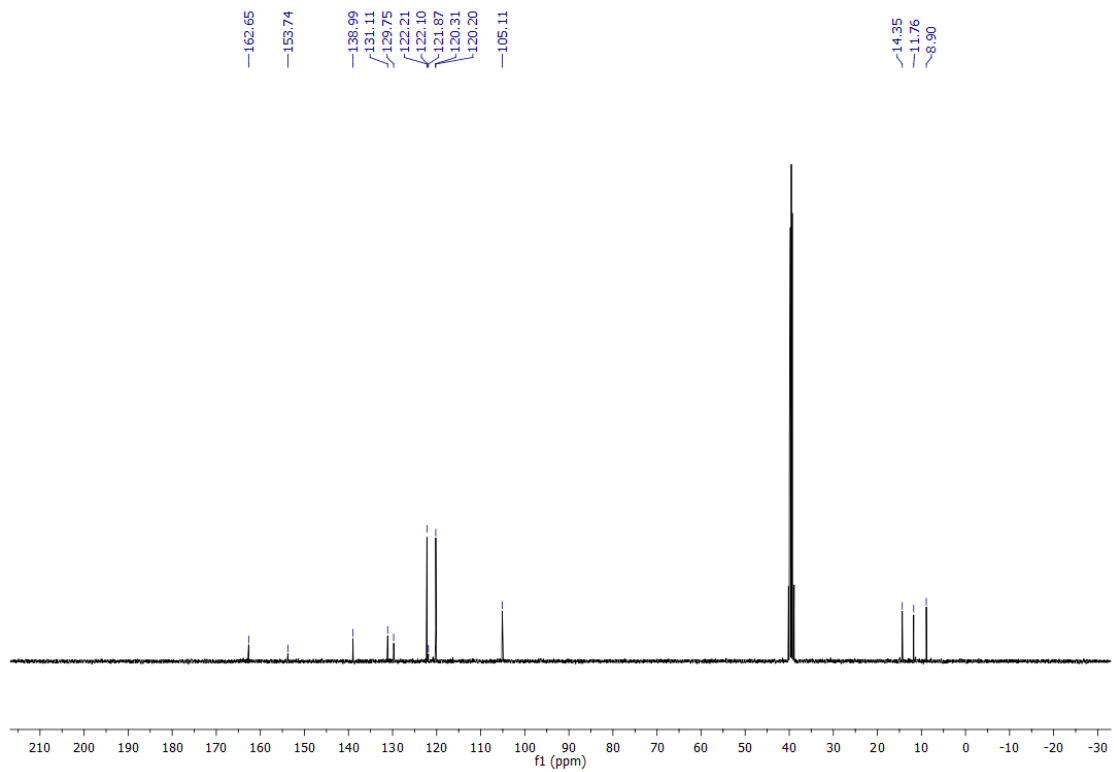


Figure S 85: ^{13}C -NMR (101 MHz, MeOD) of compound 28

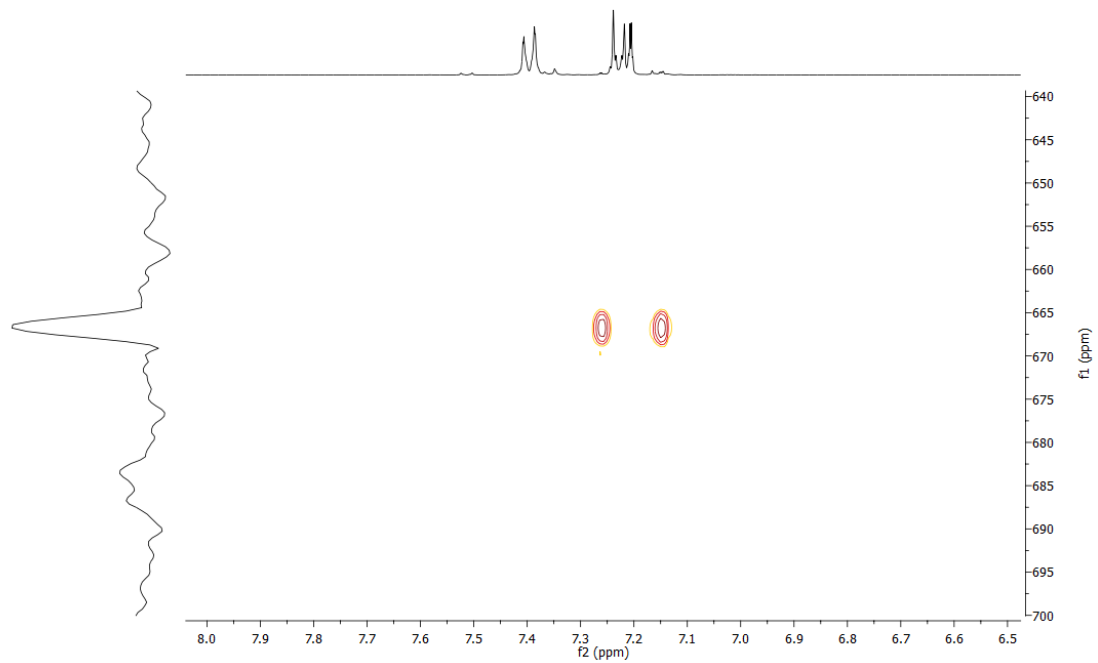


Figure S 86: ^1H - ^{77}Se -HMBC (400 MHz, 76 MHz, MeOD) of compound 28

Compound 29

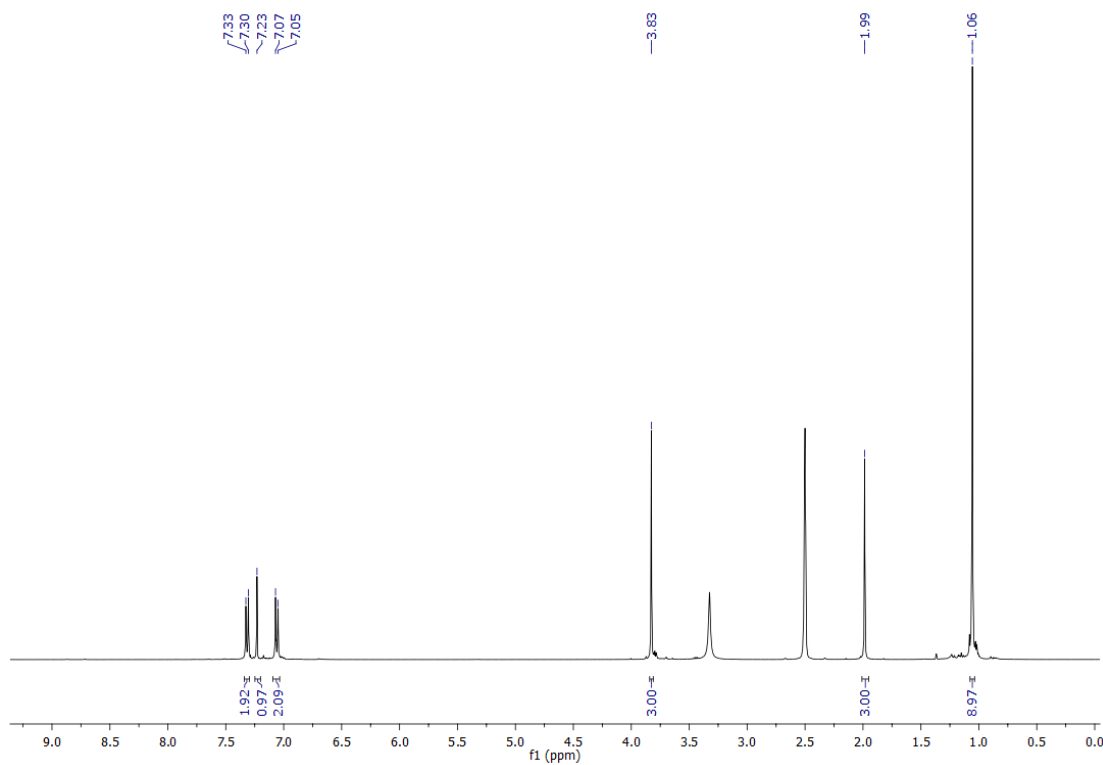


Figure S 87: ¹H-NMR (400 MHz, DMSO-*d*₆) of compound 29

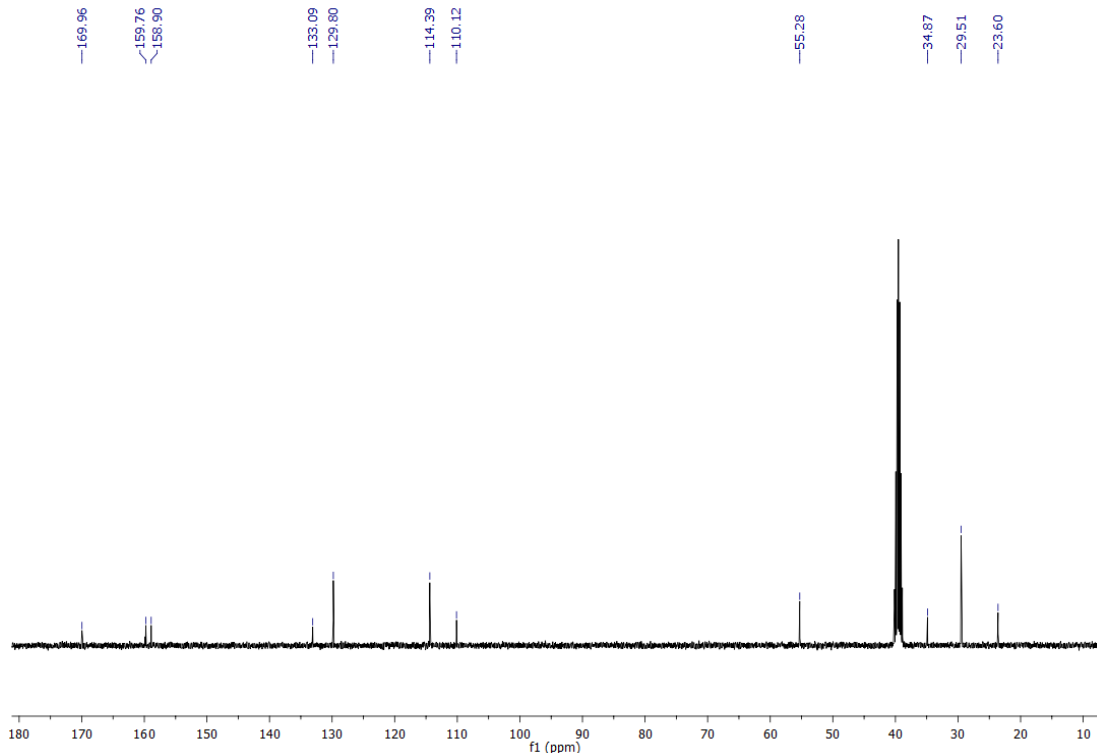


Figure S 88: ¹³C-NMR (101 MHz, DMSO-*d*₆) of compound 29

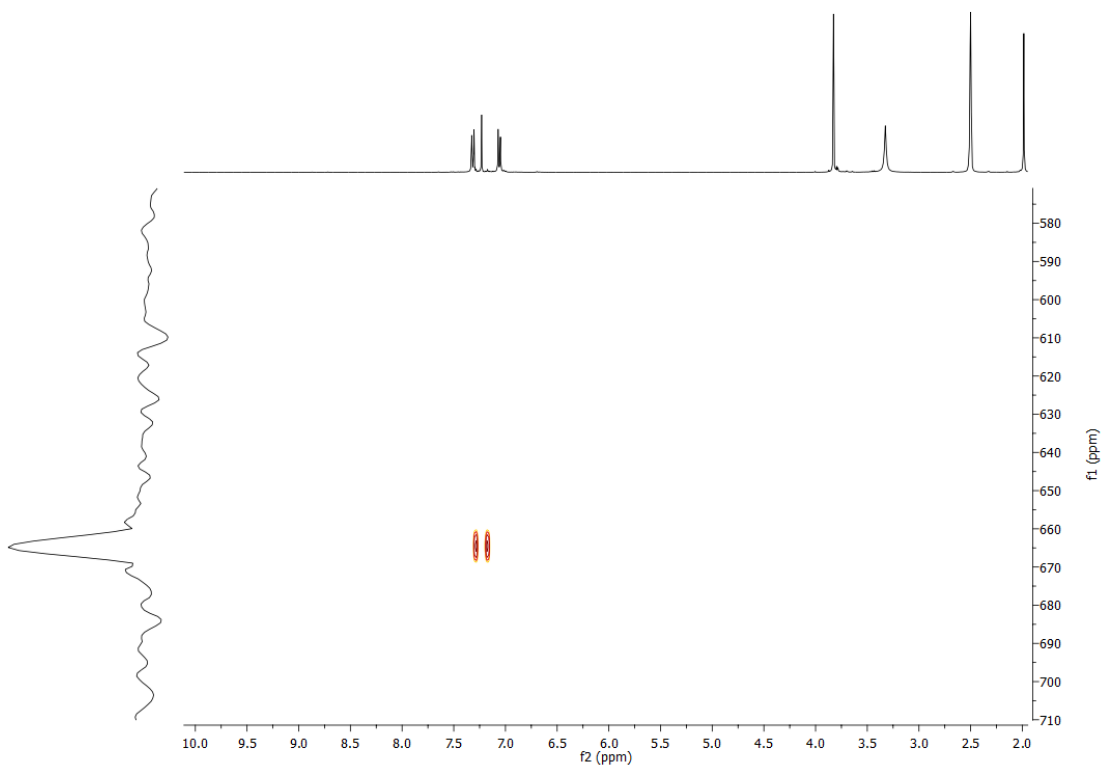


Figure S 89: ^1H - ^{77}Se -HMBC (400 MHz, 76 MHz, DMSO- d_6) of compound 29

Compound 30

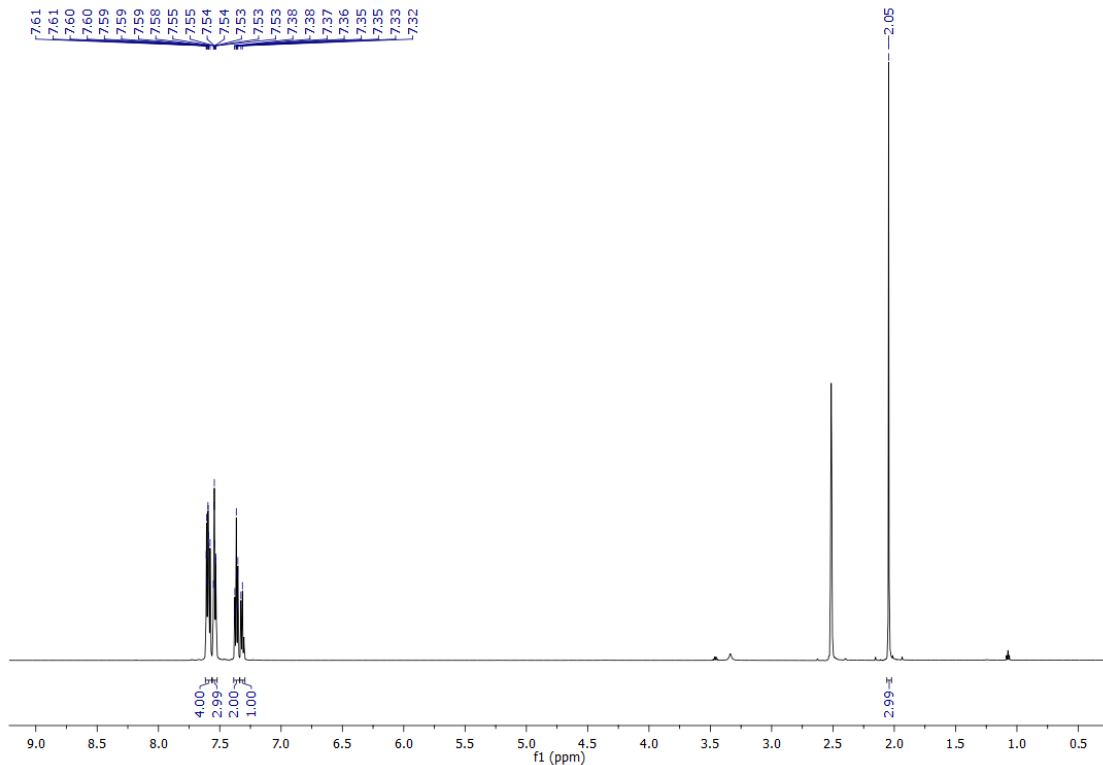


Figure S 90: ^1H -NMR (600 MHz, DMSO- d_6) of compound 30

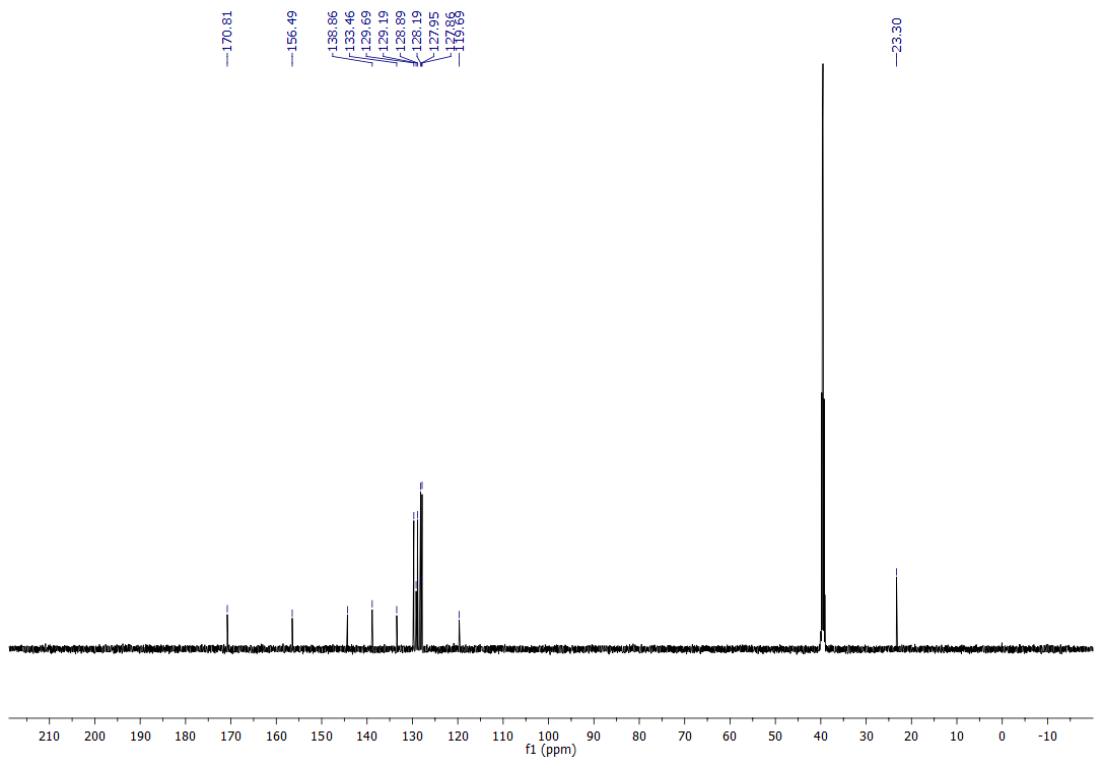


Figure S 91: ^{13}C -NMR (151 MHz, $\text{DMSO}-d_6$) of compound 30

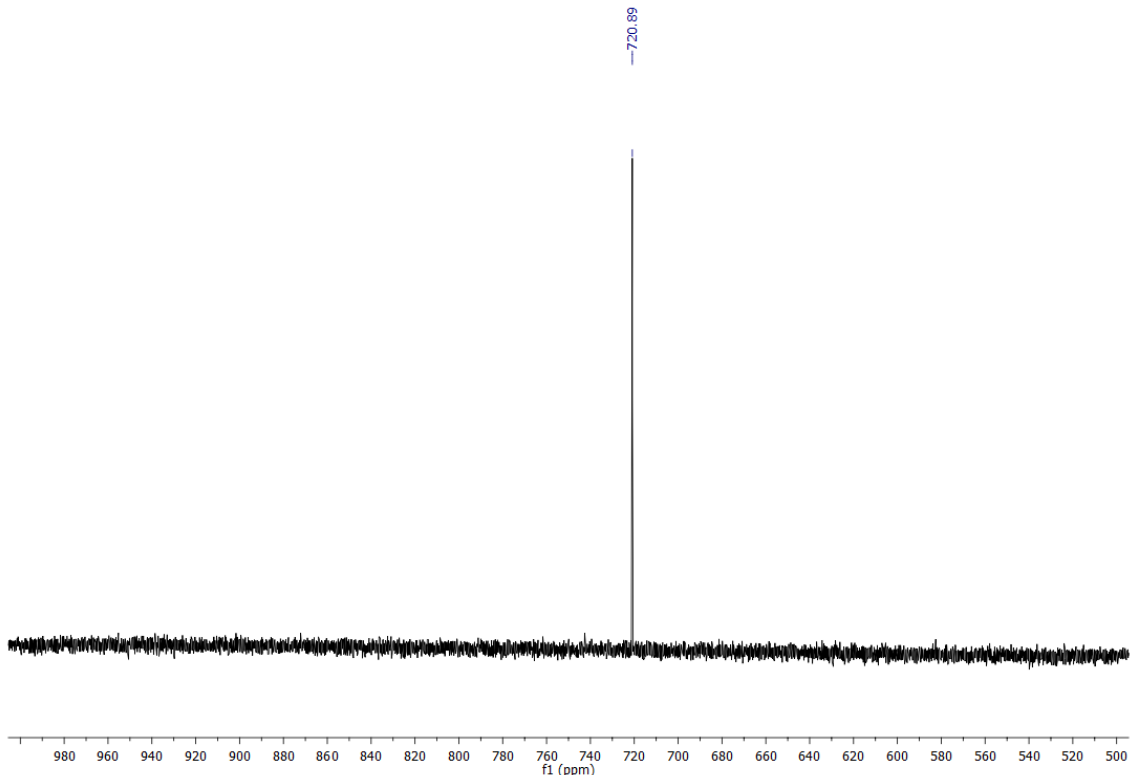


Figure S 92: ^{77}Se -NMR (114 MHz, $\text{DMSO}-d_6$) of compound 30

Compound 31

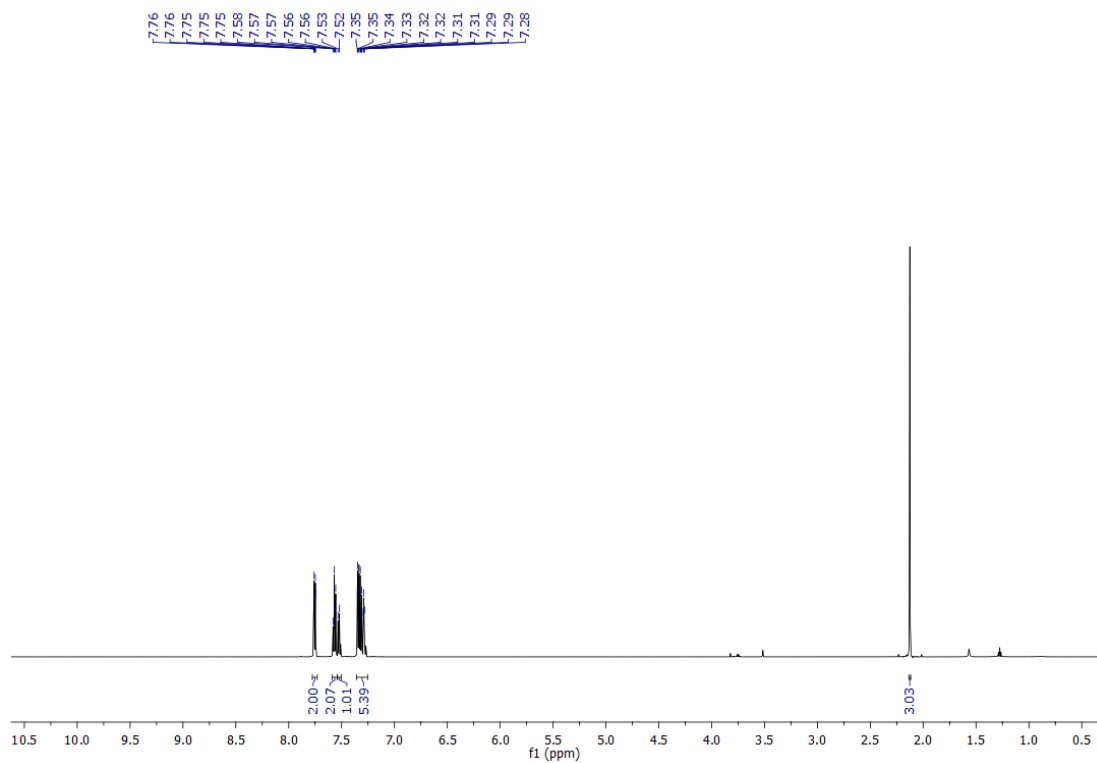


Figure S 93: ¹H-NMR (600 MHz, DMSO-*d*₆) of compound 31

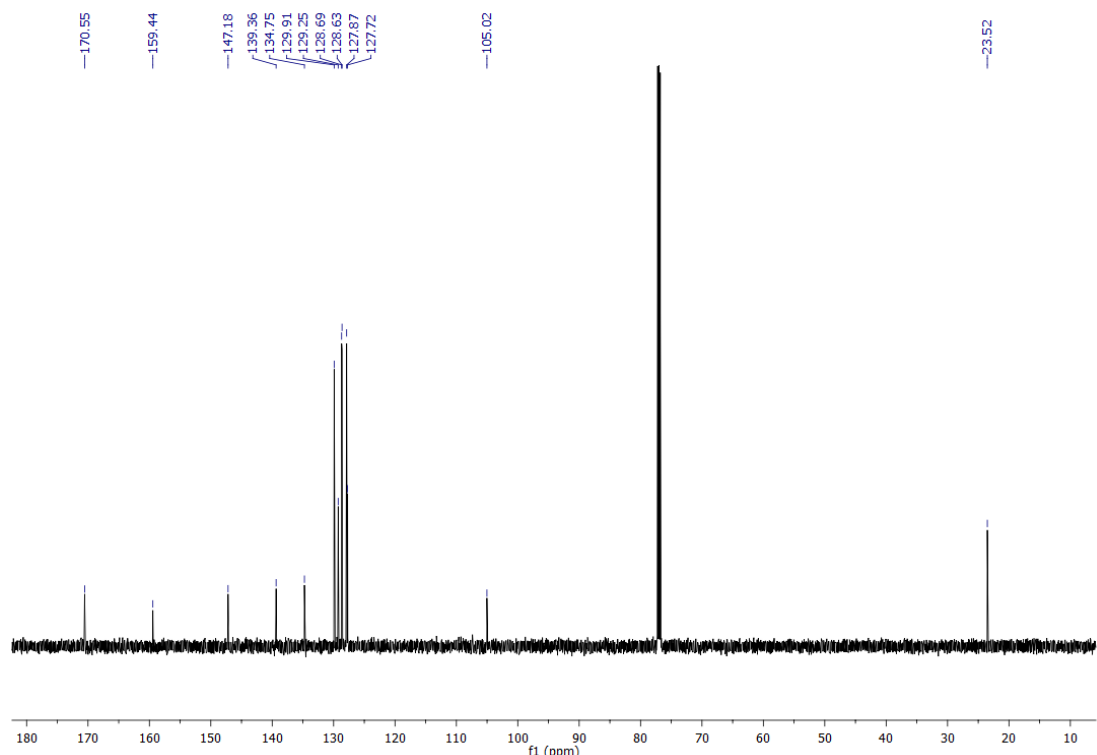


Figure S 94: ¹³C-NMR (151 MHz, DMSO-*d*₆) of compound 31

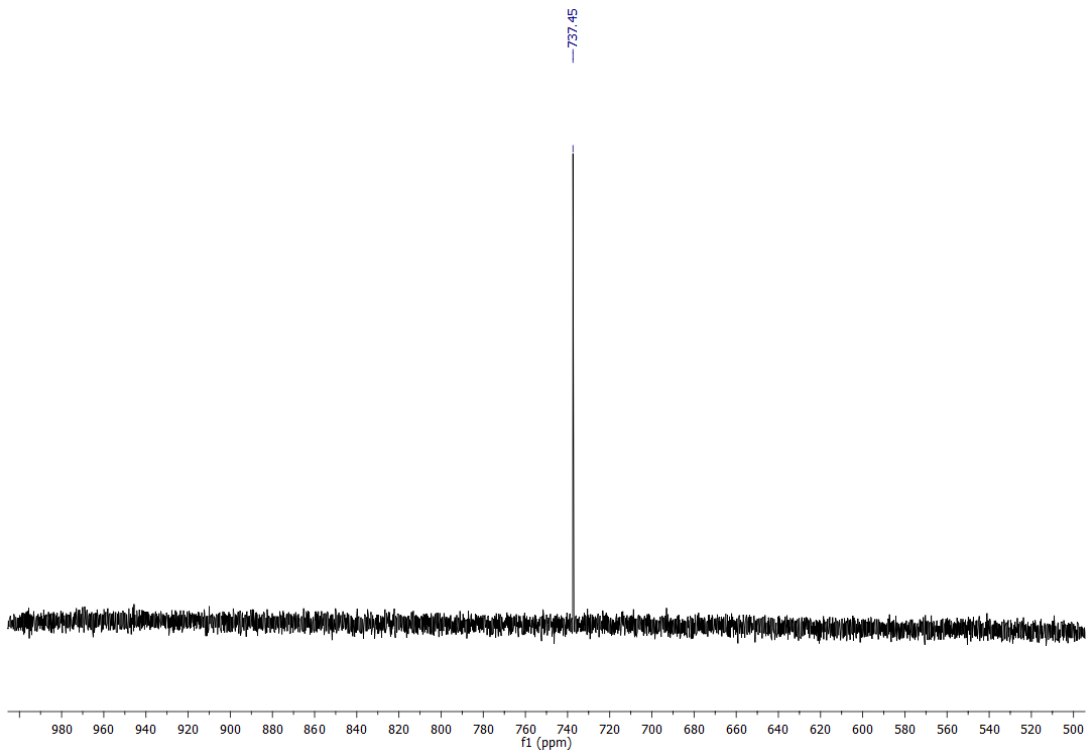


Figure S 95: ^{77}Se -NMR (114 MHz, $\text{DMSO}-d_6$) of compound 31

Compound 32

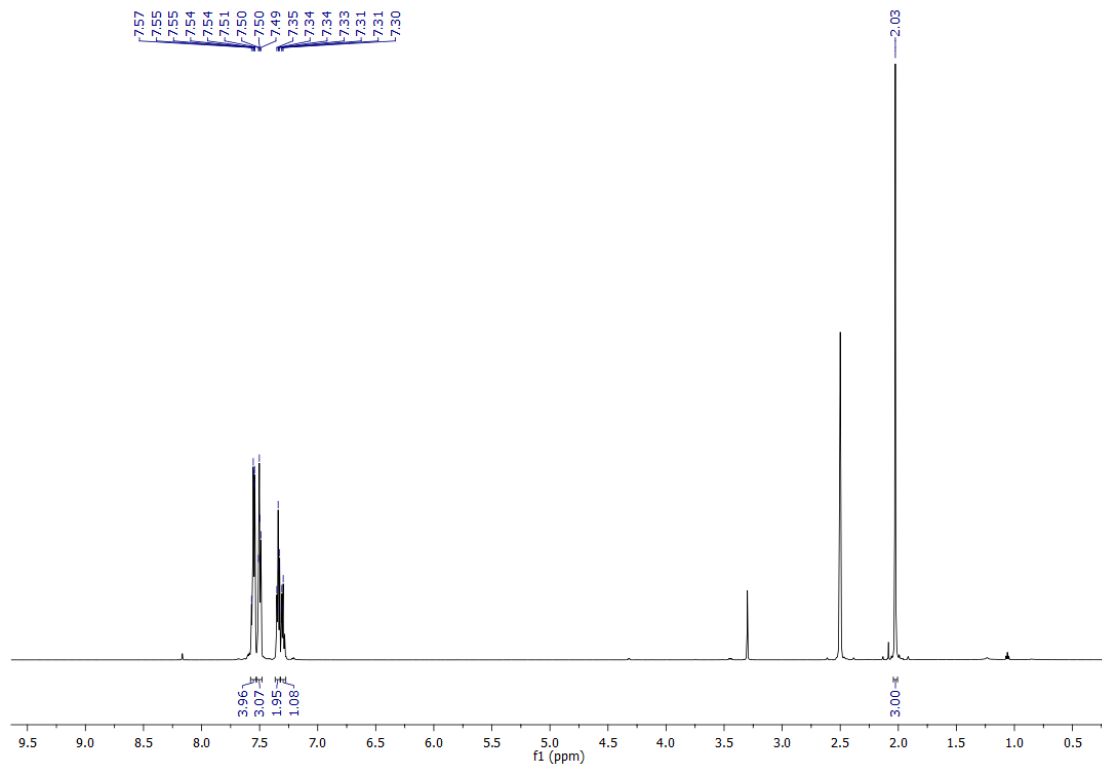


Figure S 96: ^1H -NMR (600 MHz, $\text{DMSO}-d_6$) of compound 32

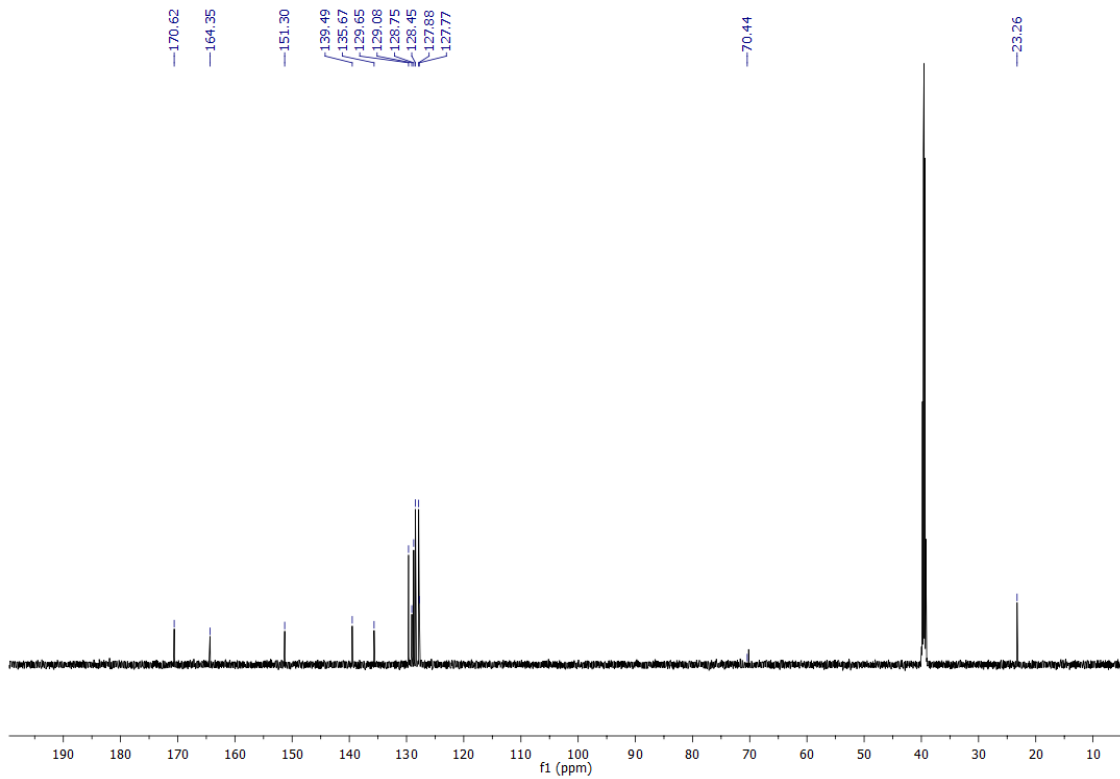


Figure S 97: ^{13}C -NMR (151 MHz, $\text{DMSO}-d_6$) of compound 32

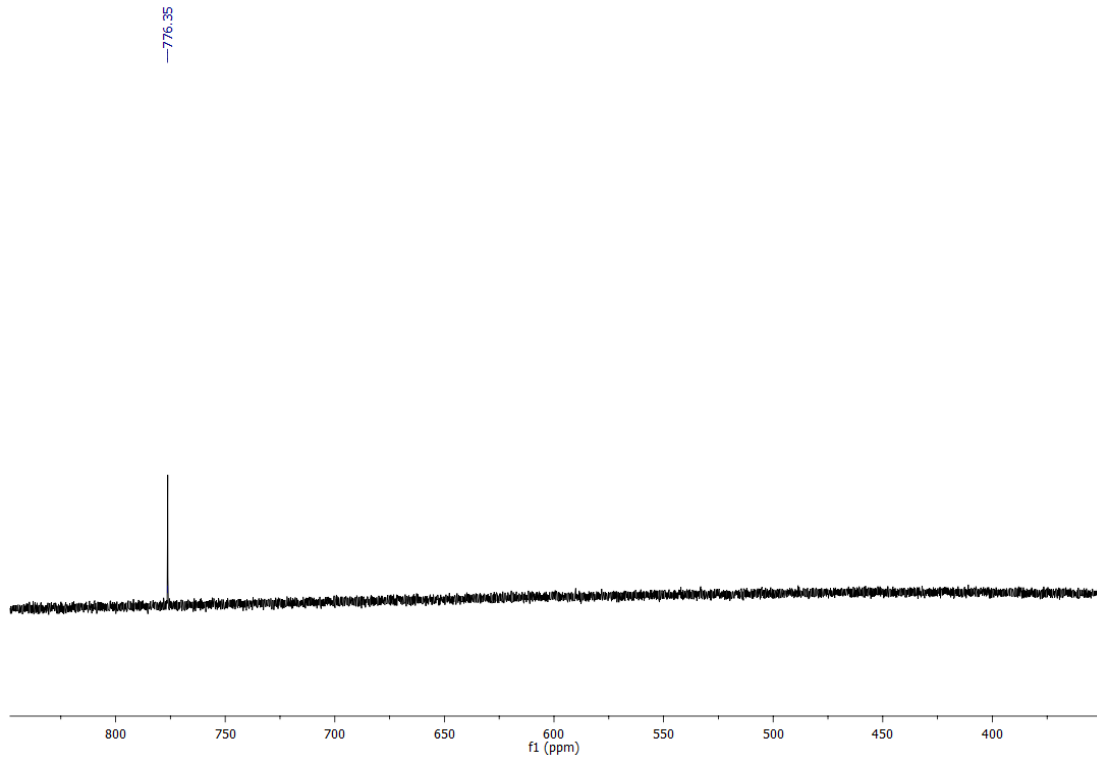


Figure S 98: ^{77}Se -NMR (114 MHz, $\text{DMSO}-d_6$) of compound 32

Compound 33

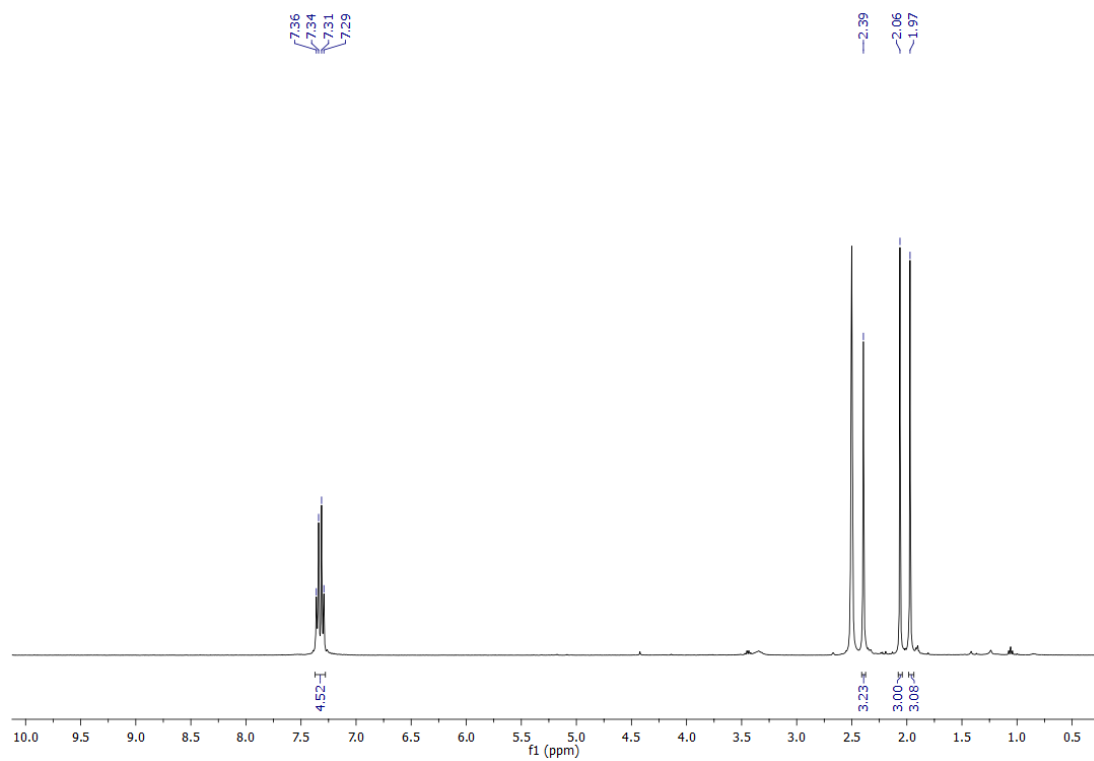


Figure S 99: ¹H-NMR (400 MHz, DMSO-d₆) of compound 33

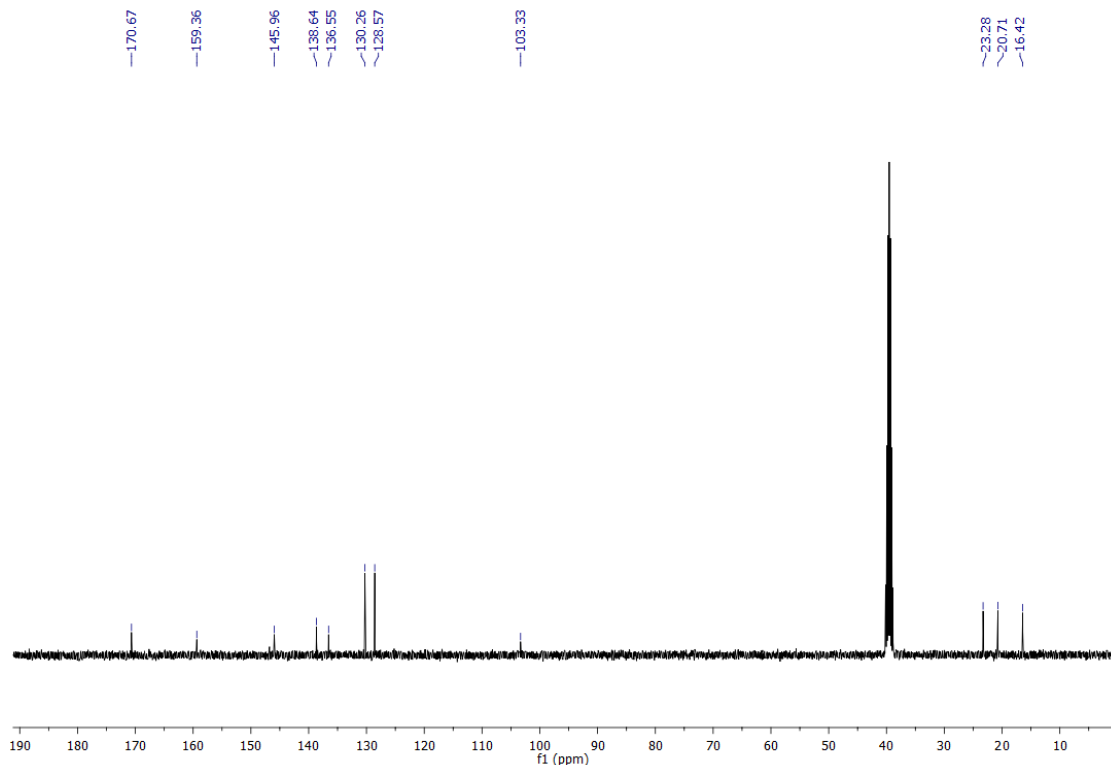


Figure S 100: ¹³C-NMR (101 MHz, DMSO-d₆) of compound 33

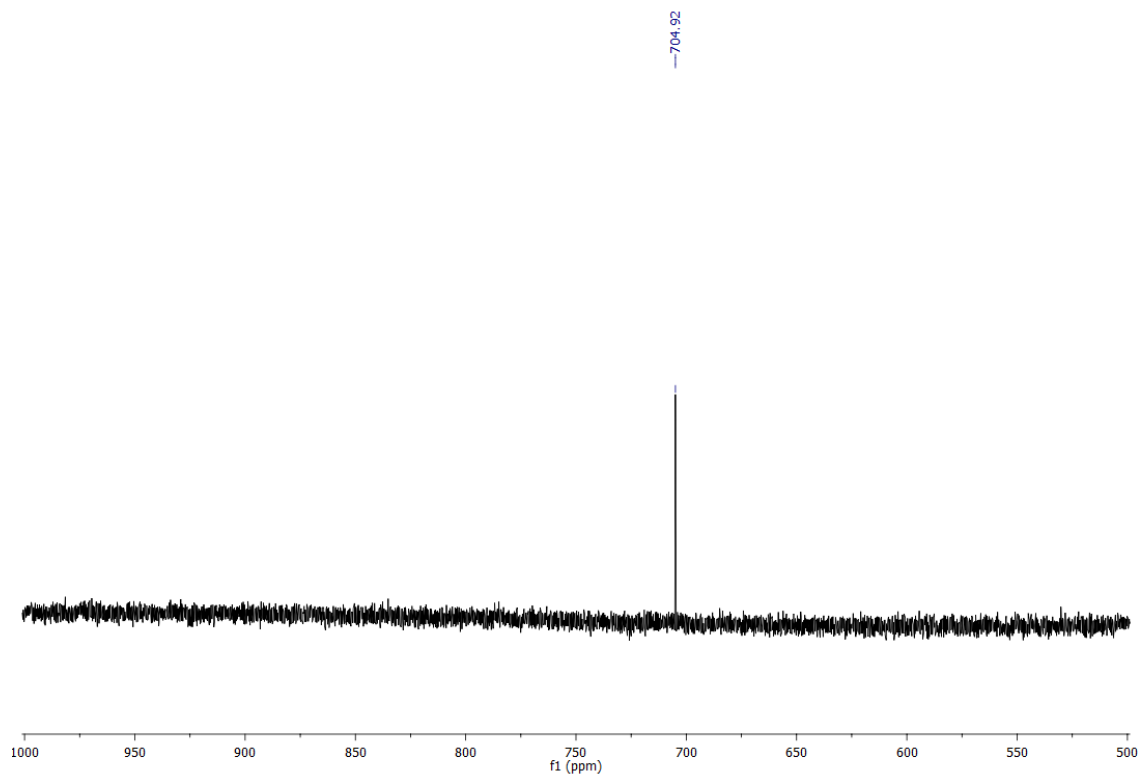


Figure S 101: ^{77}Se -NMR (76 MHz, $\text{DMSO}-d_6$) of compound 33

Compound 34

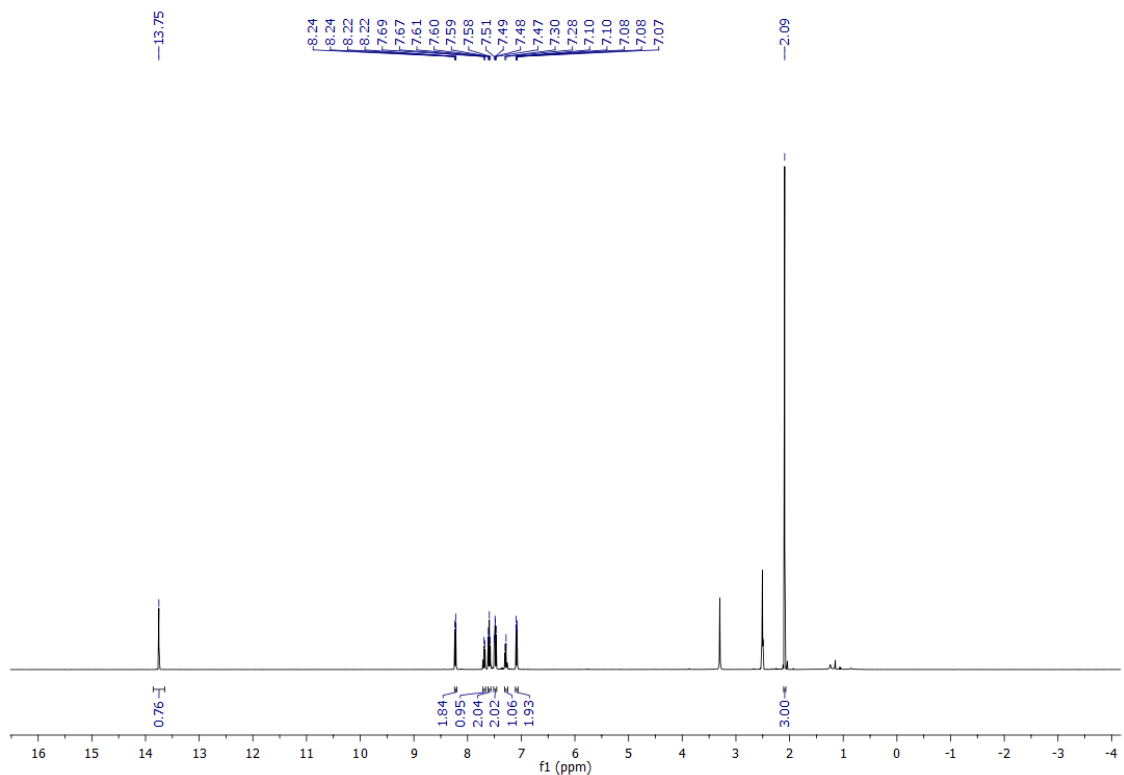


Figure S 102: ^1H -NMR (400 MHz, $\text{DMSO}-d_6$) of compound 34

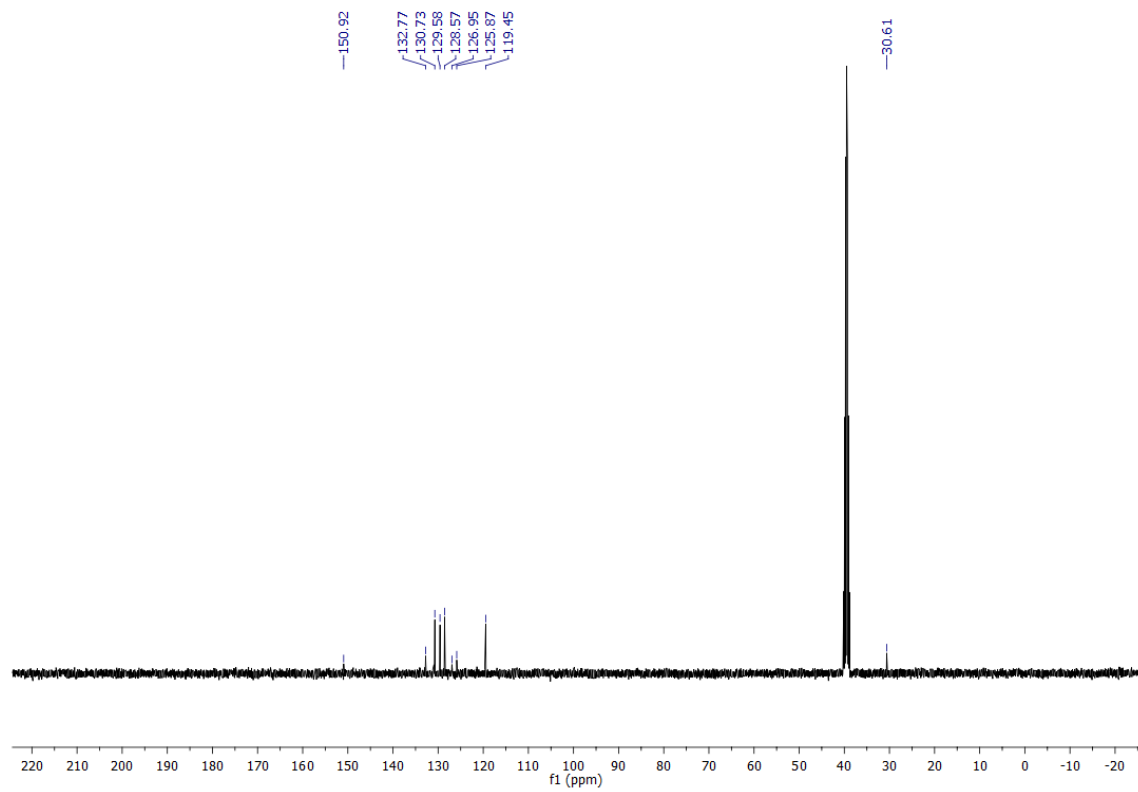


Figure S 103: ^{13}C -NMR (101 MHz, $\text{DMSO}-d_6$) of compound 34

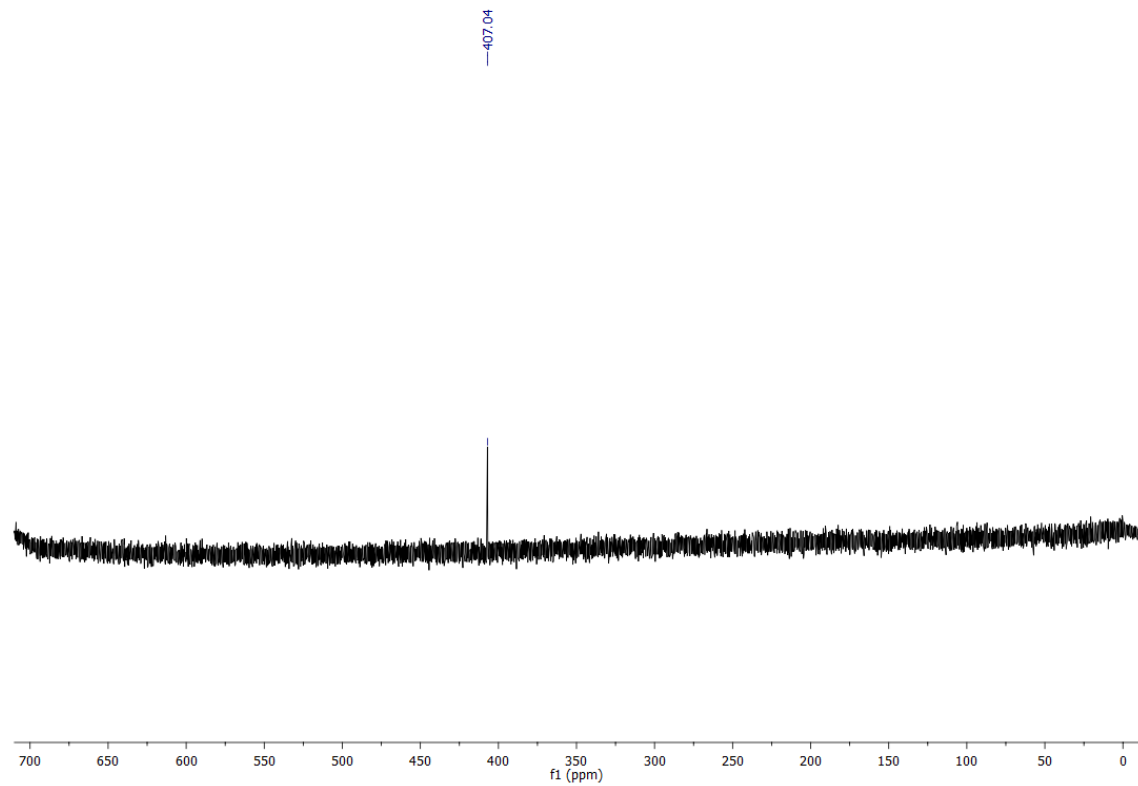


Figure S 104: ^{77}Se -NMR (76 MHz, $\text{DMSO}-d_6$) of compound 34

Compound 35

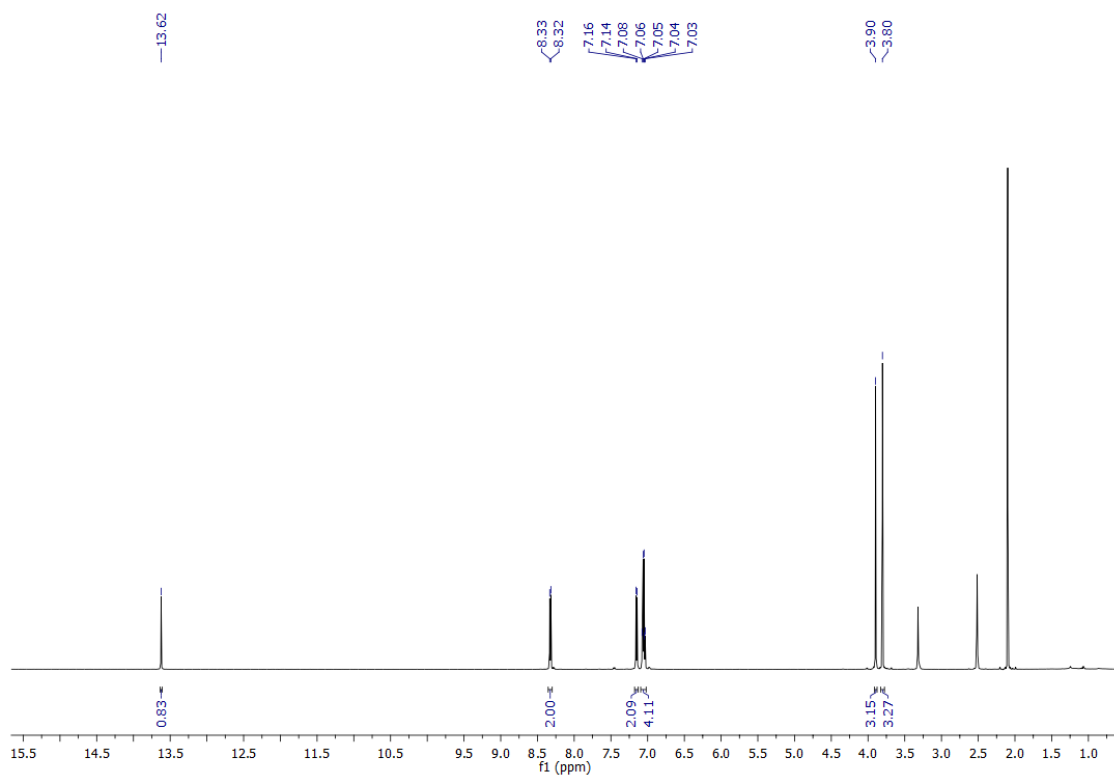


Figure S 105: ¹H-NMR (600 MHz, DMSO- d_6) of compound 35

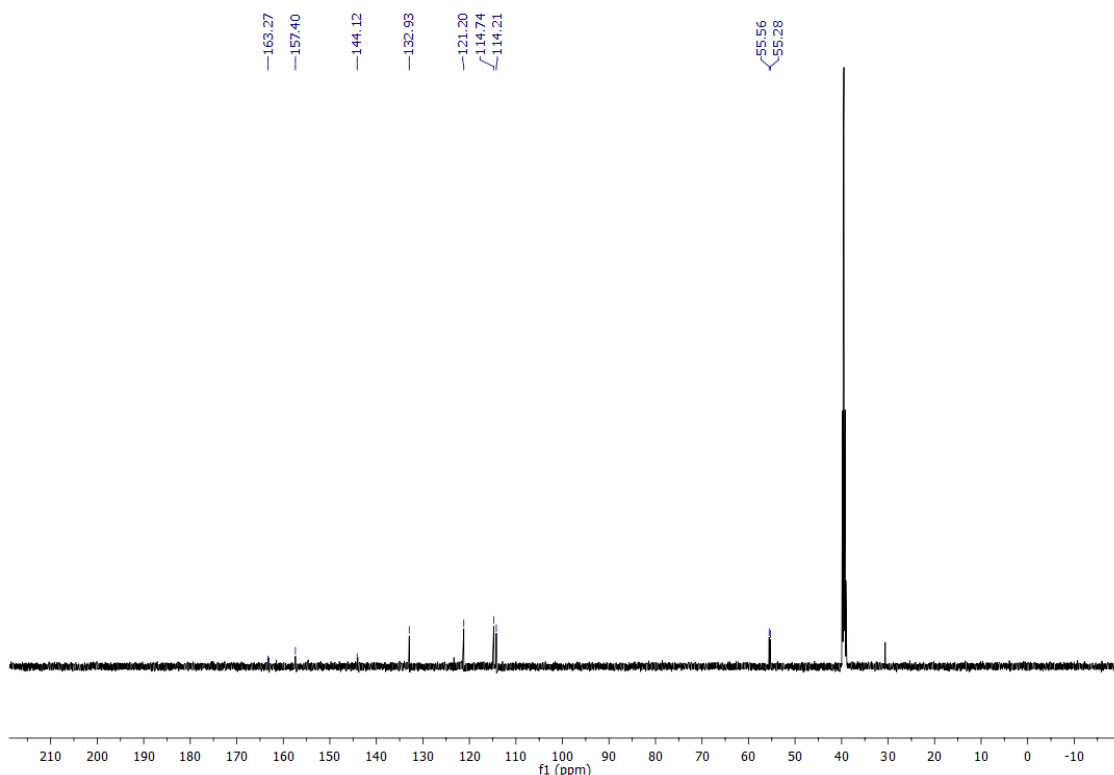


Figure S 106: ¹³C-NMR (151 MHz, DMSO- d_6) of compound 35

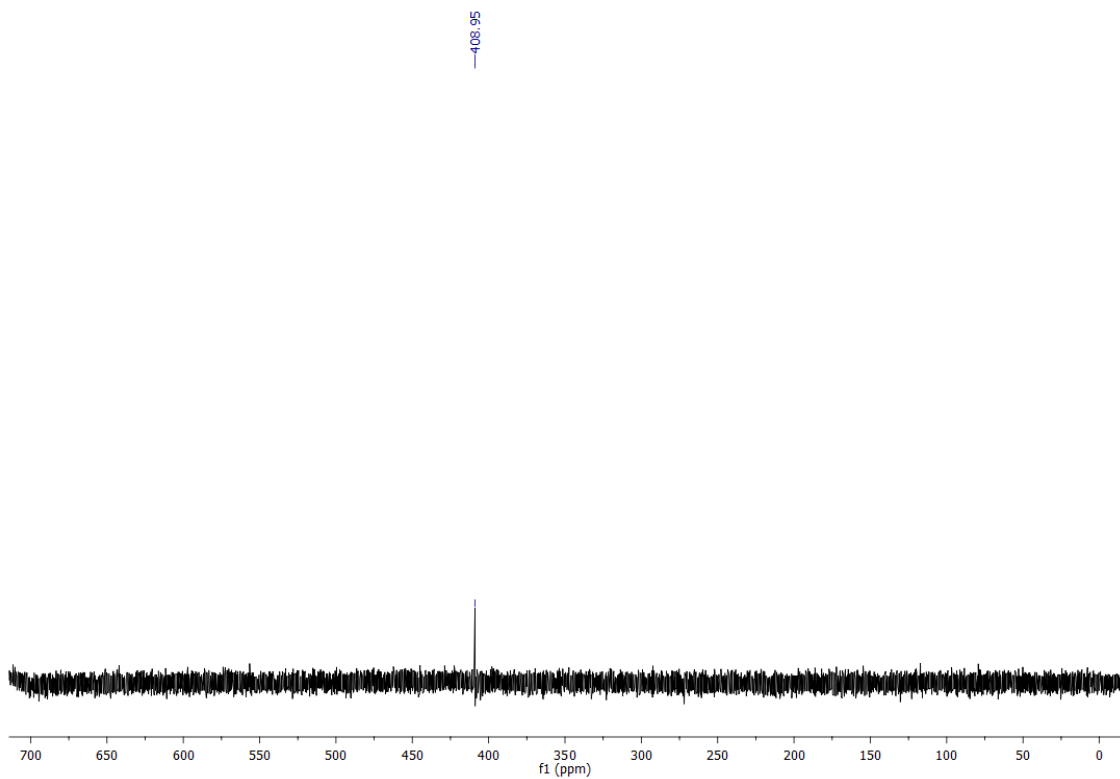


Figure S 107: ^{77}Se -NMR (114 MHz, $\text{DMSO}-d_6$) of compound 35

Compound 36

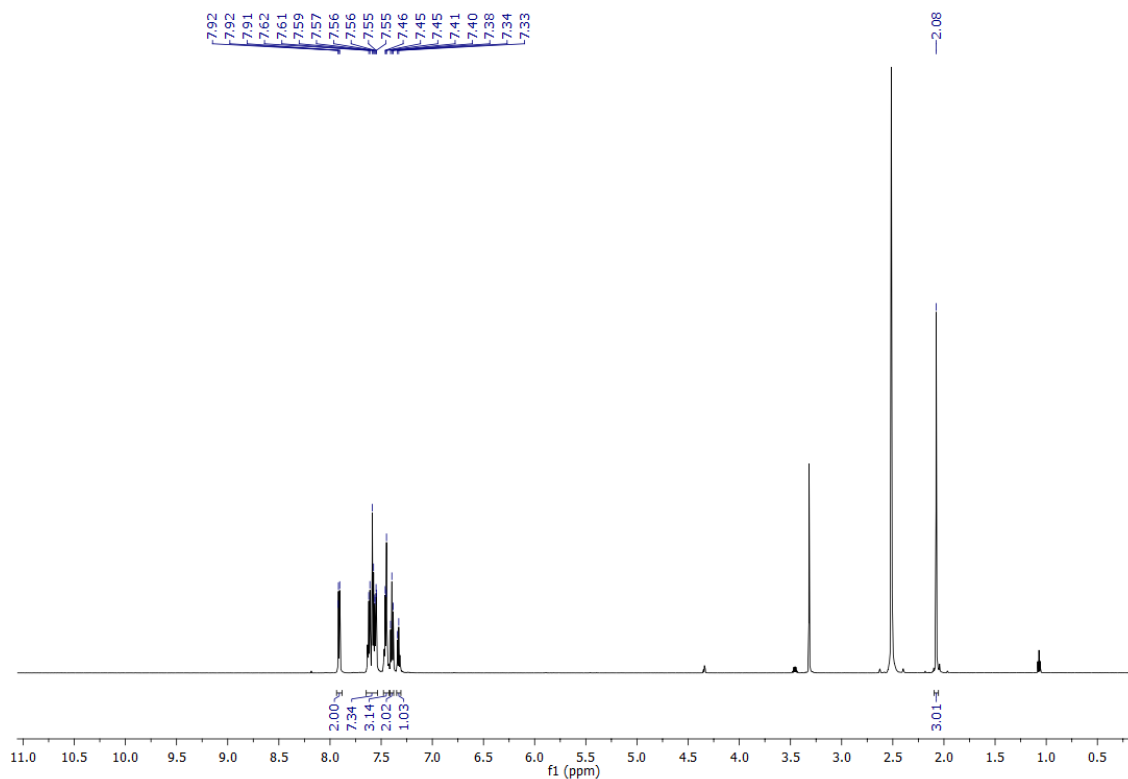


Figure S 108: ^1H -NMR (600 MHz, $\text{DMSO}-d_6$) of compound 36

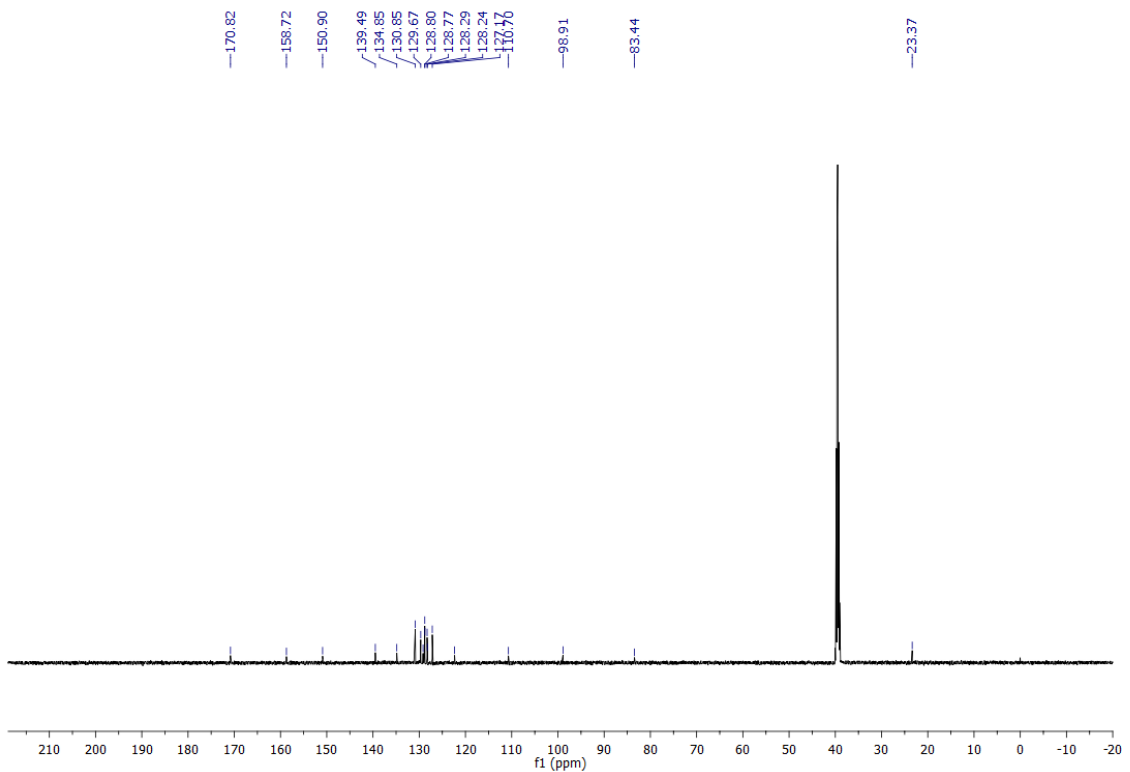


Figure S 109: ^{13}C -NMR (151 MHz, $\text{DMSO}-d_6$) of compound 36

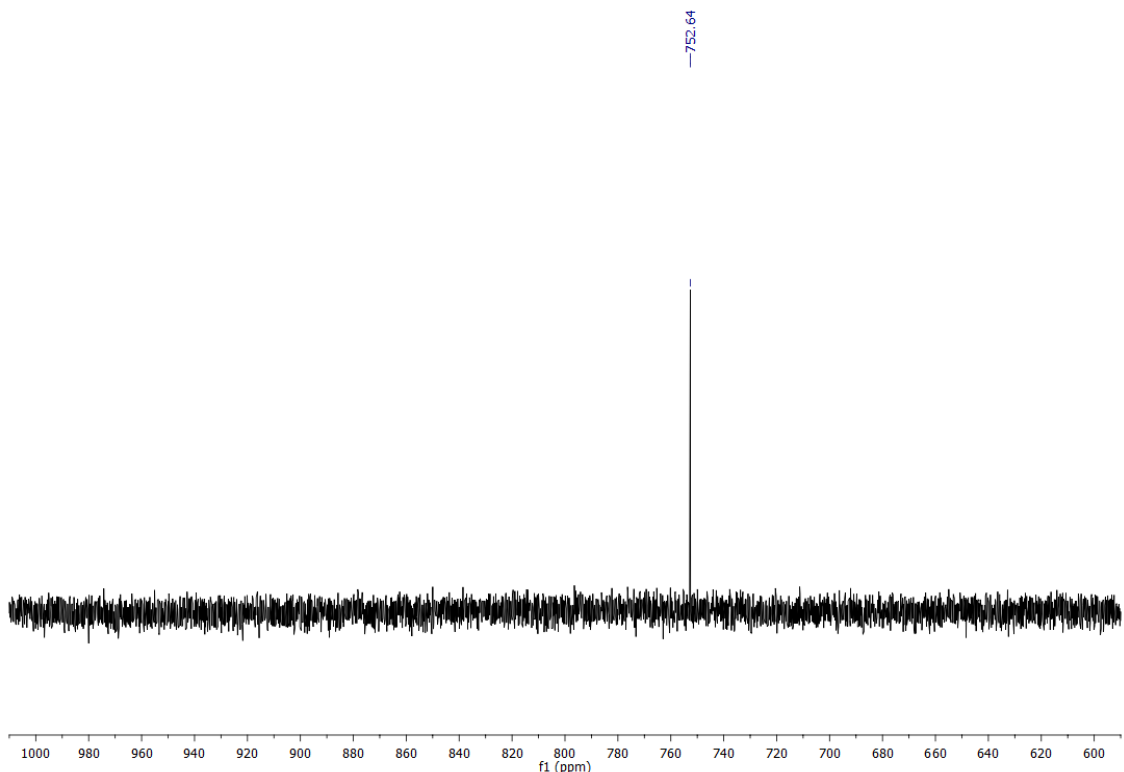


Figure S 110: ^{77}Se -NMR (76 MHz, $\text{DMSO}-d_6$) of compound 36

Compound 37

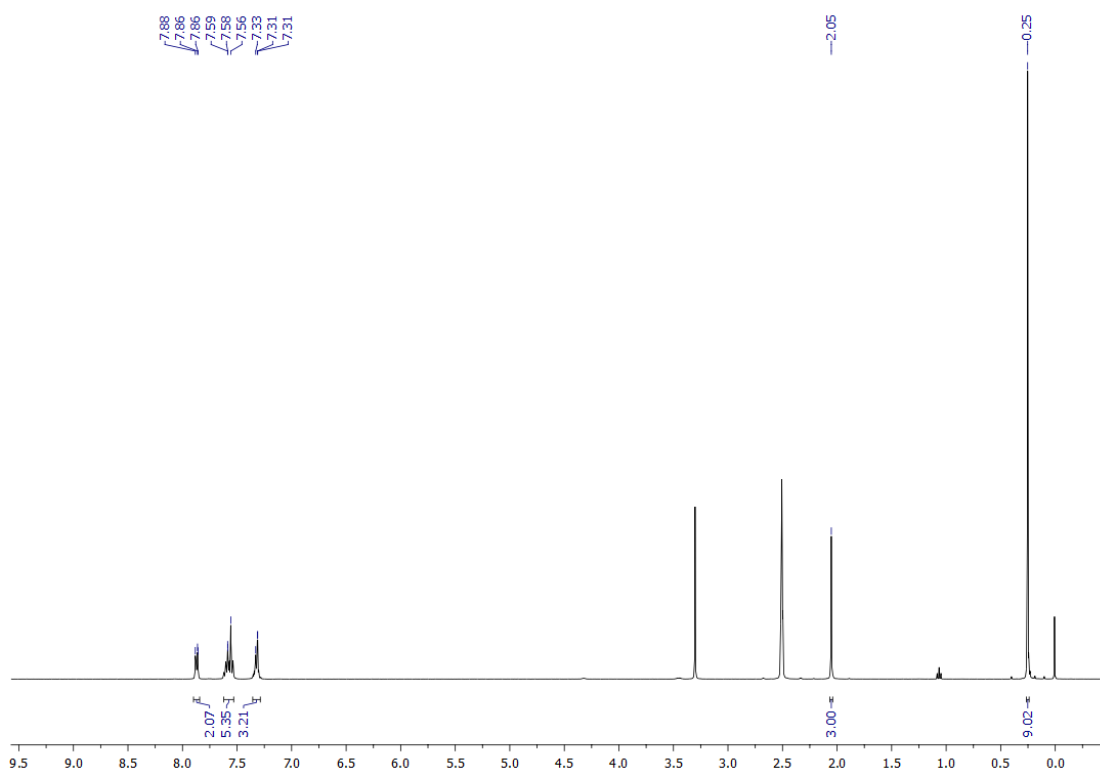


Figure S 111: ¹H-NMR (400 MHz, DMSO-*d*₆) of compound 37

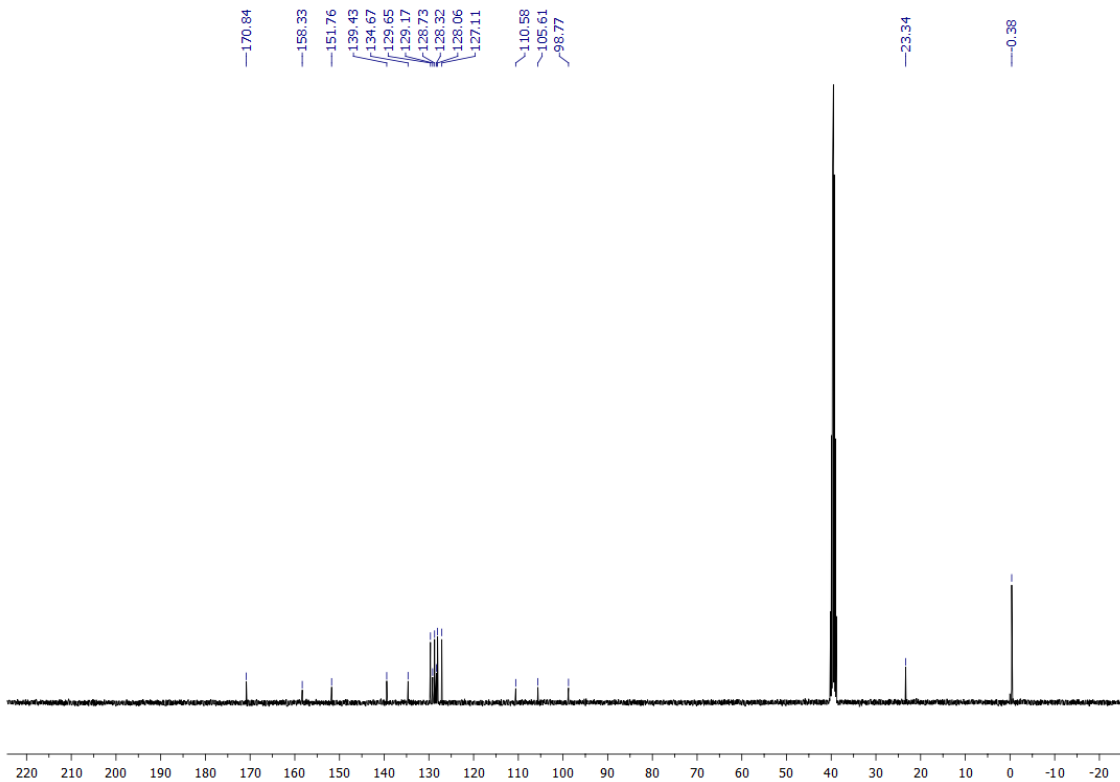


Figure S 112: ¹³C-NMR (101 MHz, DMSO-*d*₆) of compound 37

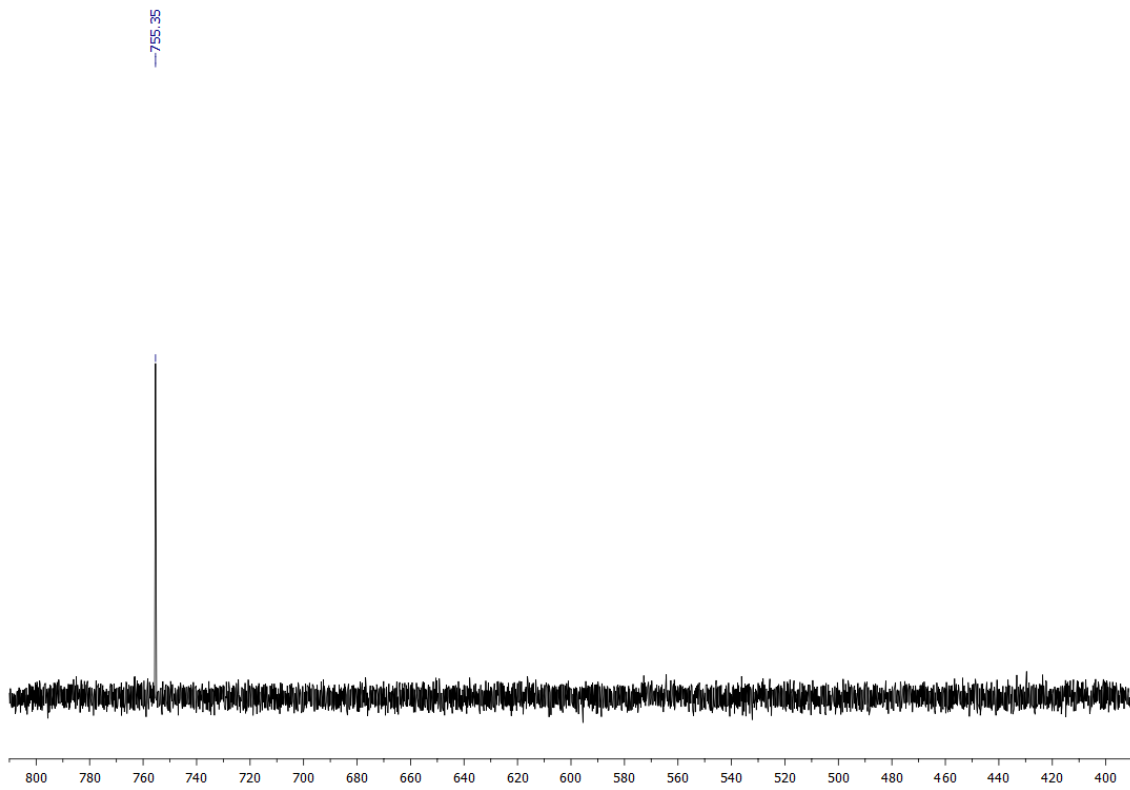


Figure S 113: ^{77}Se -NMR (76 MHz, DMSO) of compound 37

Compound 38

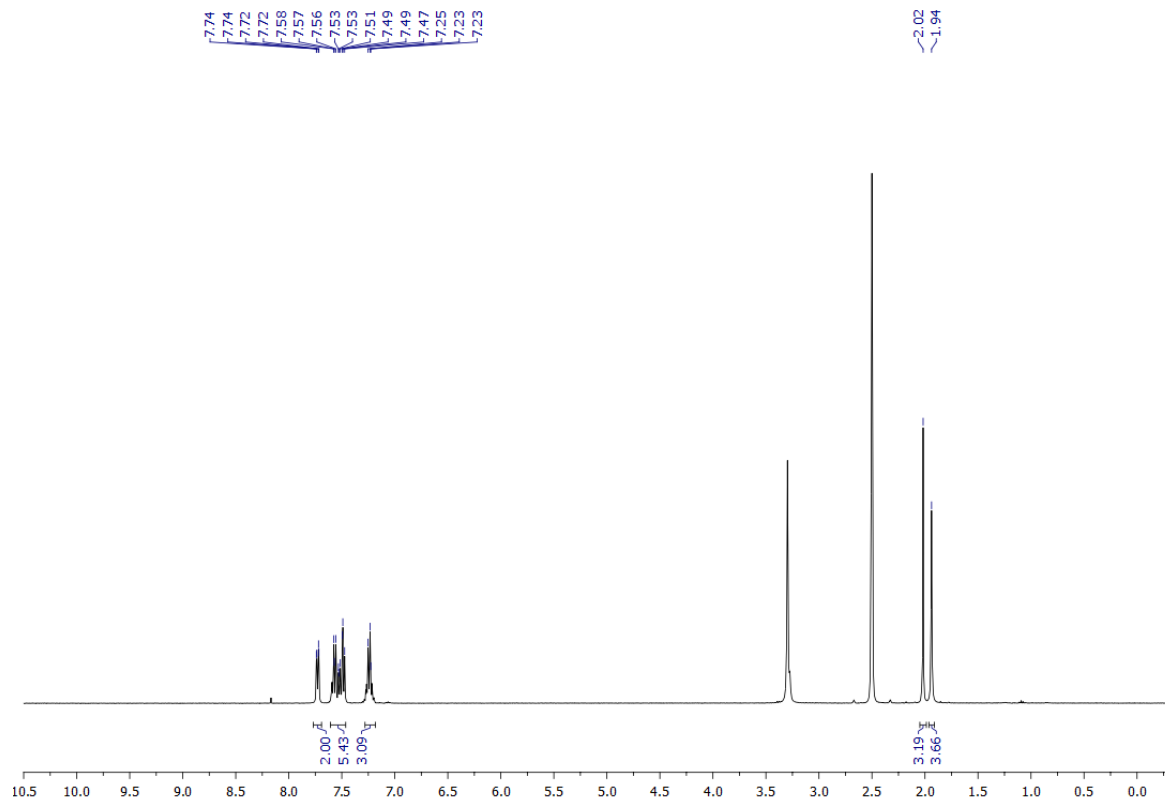


Figure S 114: ^1H -NMR (400 MHz, $\text{DMSO}-d_6$) of compound 38

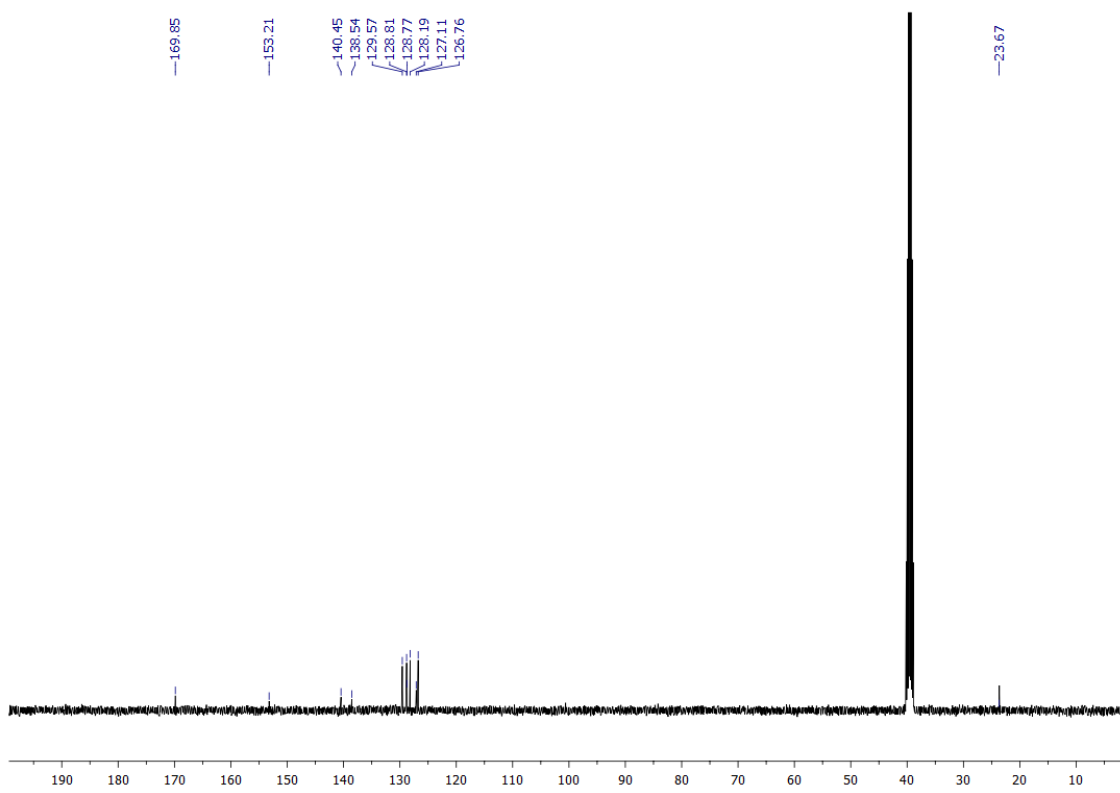


Figure S 115: ^{13}C -NMR (101 MHz, DMSO) of compound 38

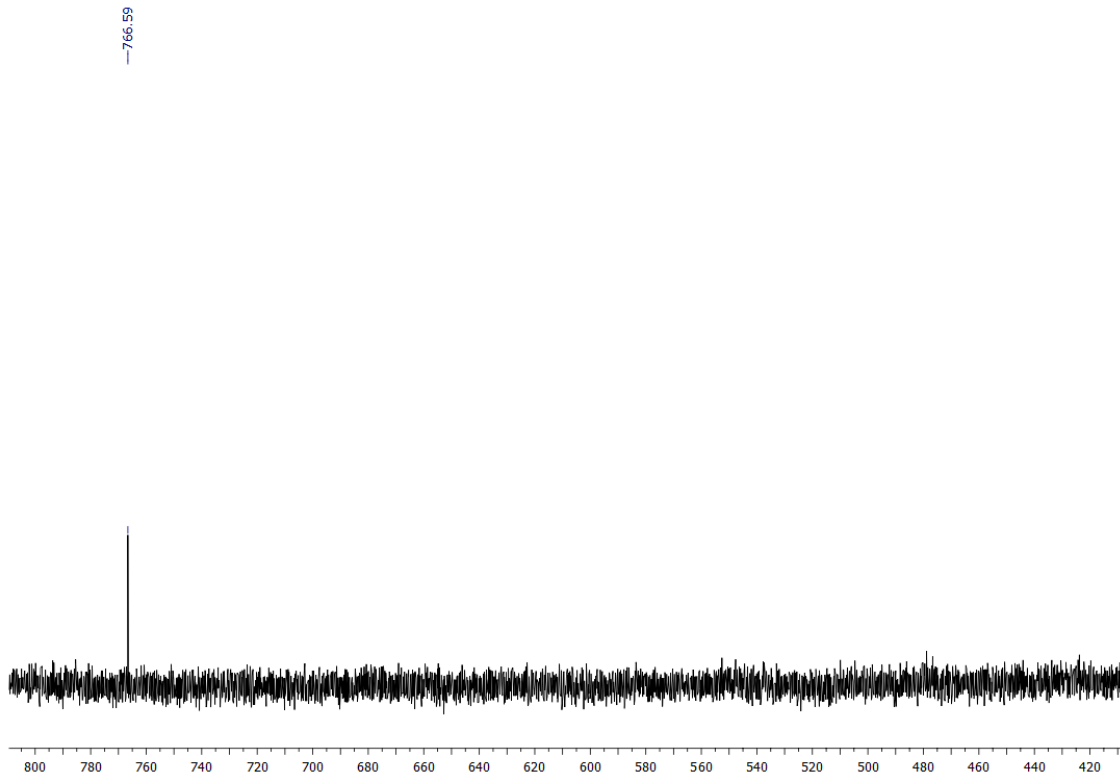


Figure S 116: ^{77}Se -NMR (76 MHz, DMSO) of compound 38

Compound 38S

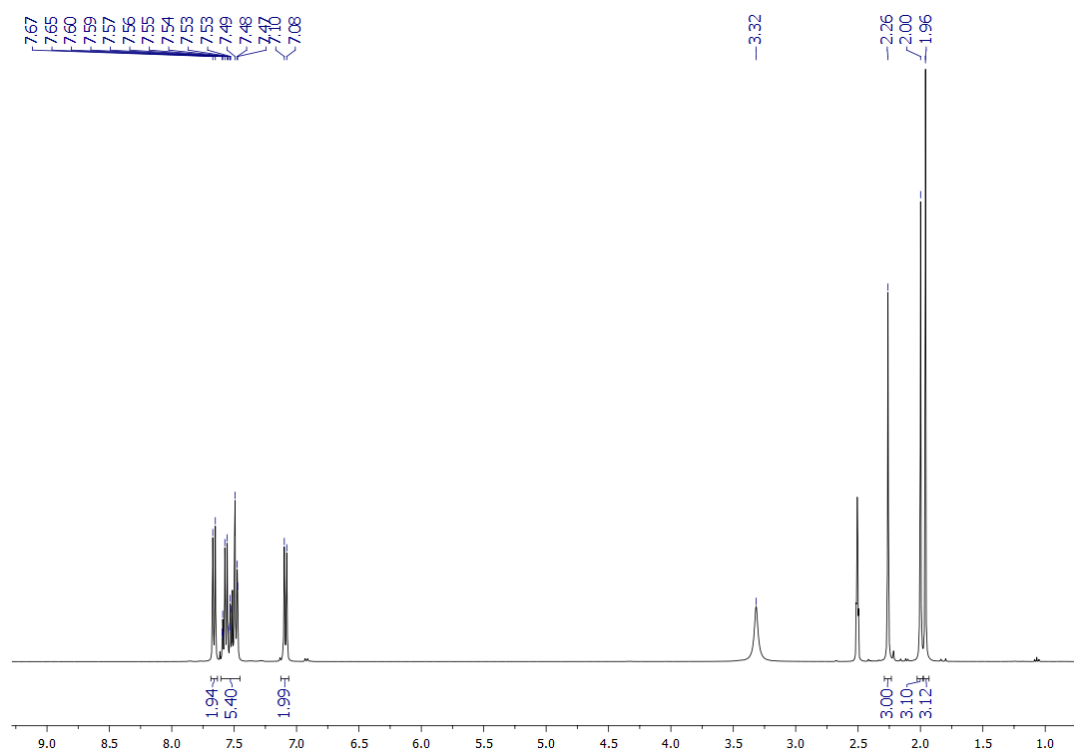


Figure S 117: ¹H-NMR (400 MHz, DMSO- d_6) of compound 38S

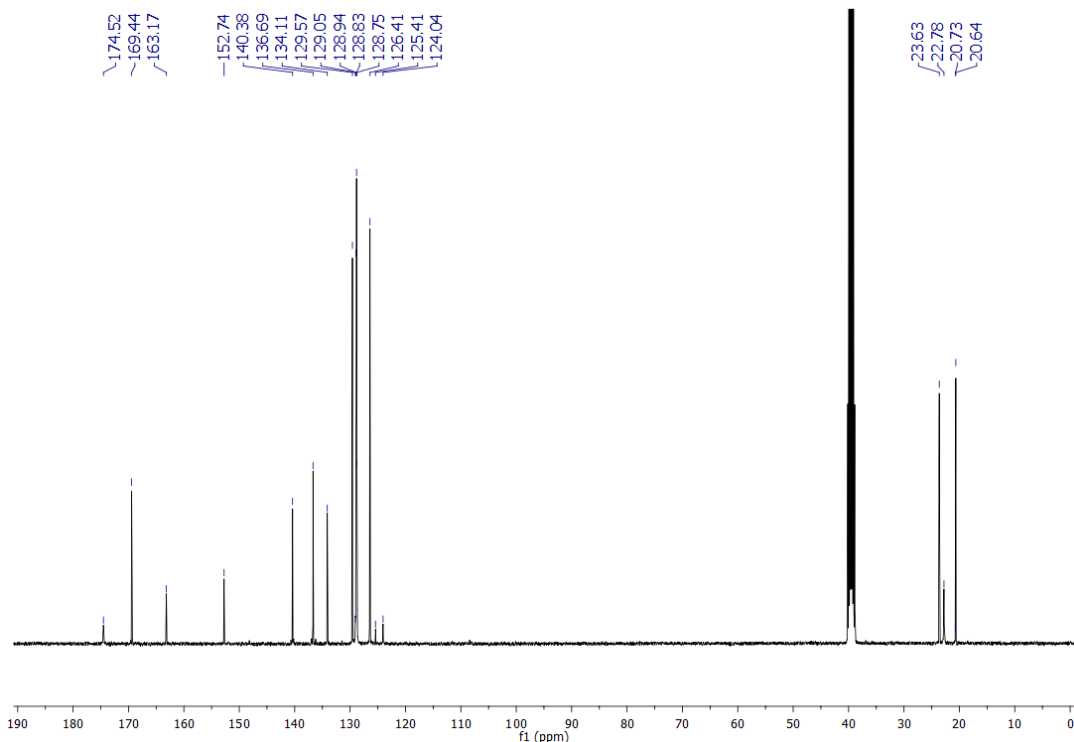


Figure S 118 ¹³C-NMR (101 MHz, DMSO) of compound 38S

Compound 39

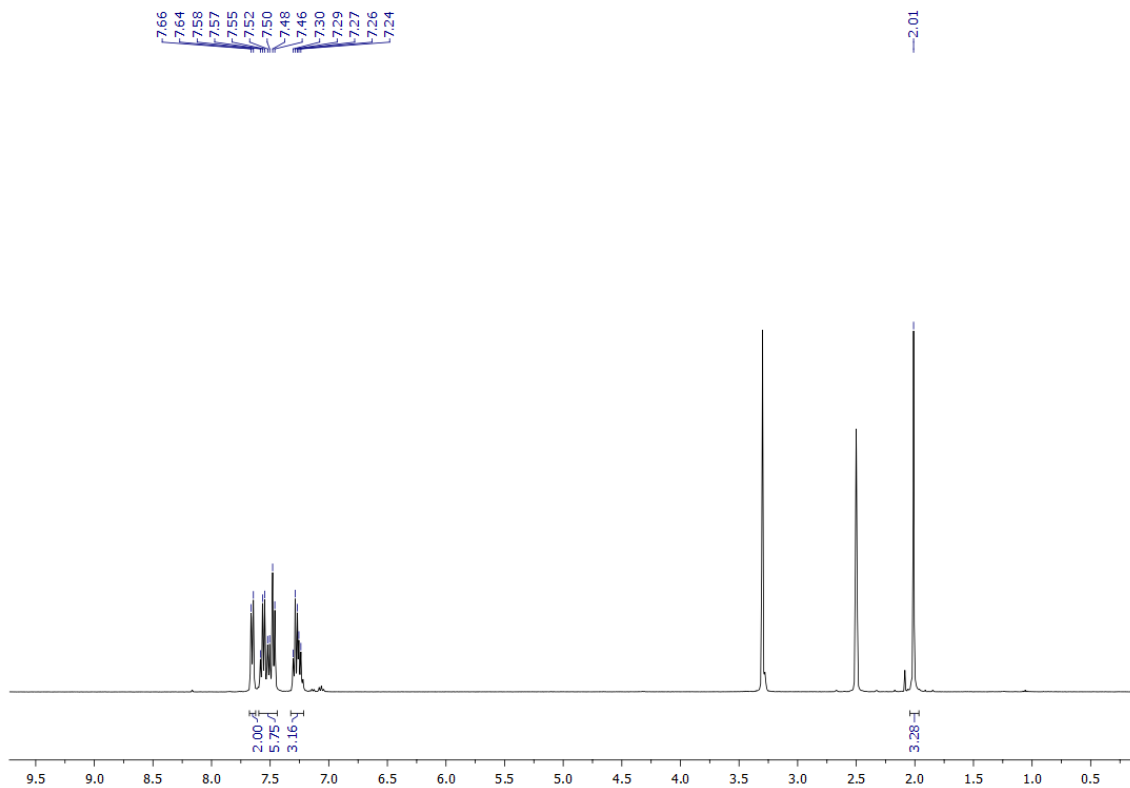


Figure S 119: ¹H-NMR (400 MHz, DMSO-*d*₆) of compound 39

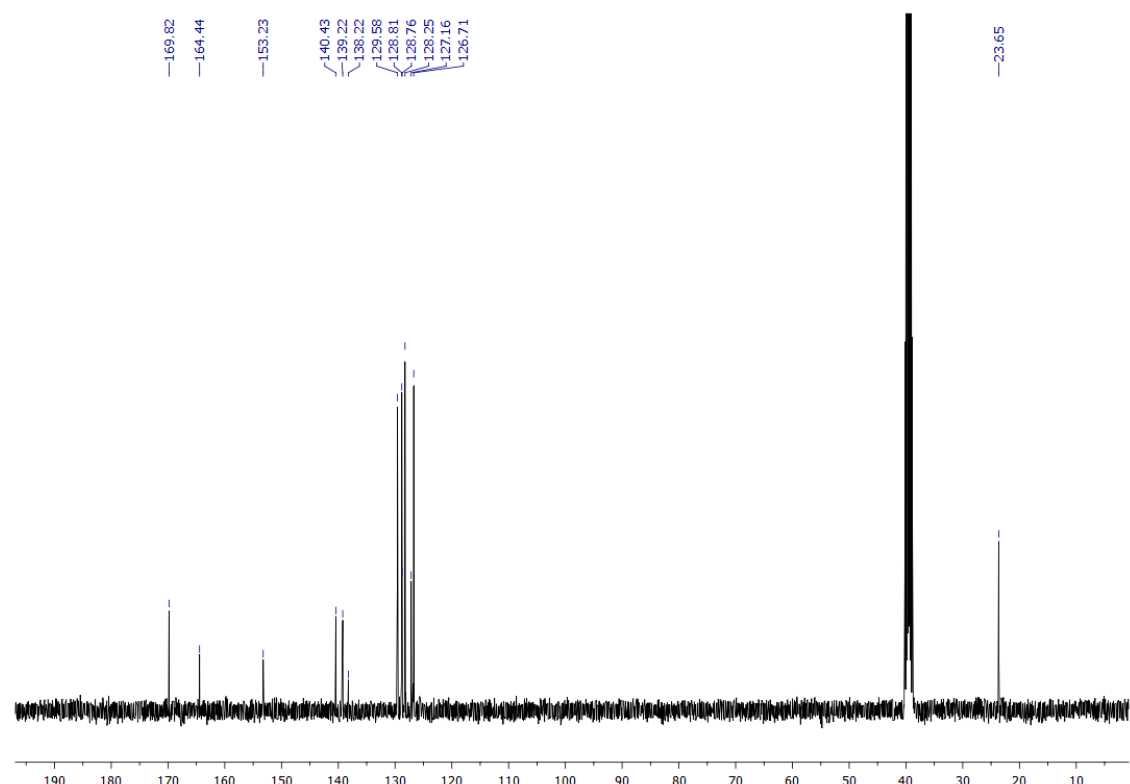


Figure S 120: ¹³C-NMR (101 MHz, DMSO) of compound 39

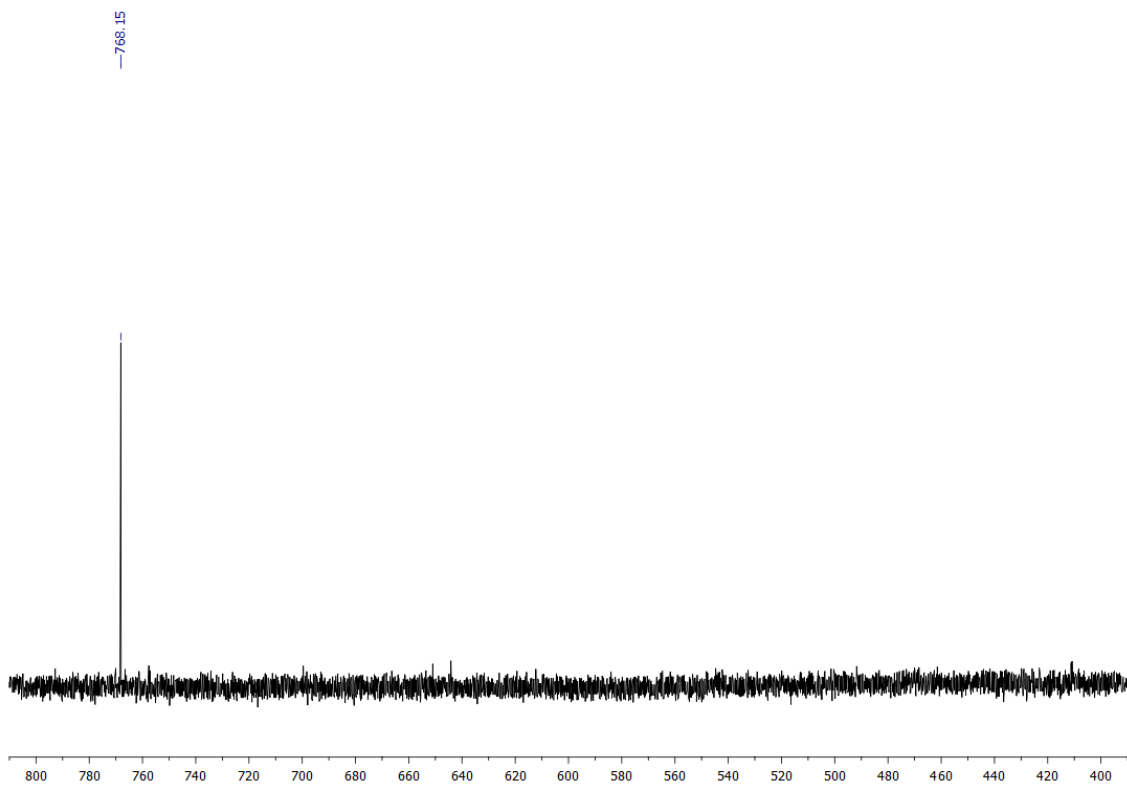


Figure S 121: ^{77}Se -NMR (76 MHz, DMSO) of compound 39

Compound 40

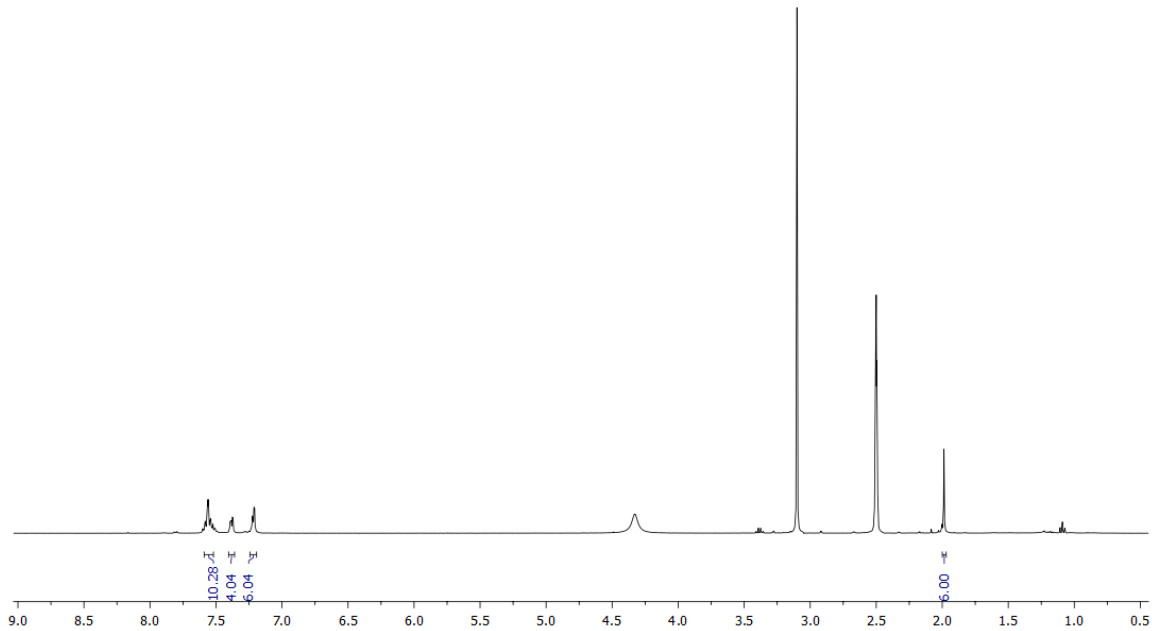


Figure S 122: ^1H -NMR (400 MHz, $\text{DMSO}-d_6$) of compound 40

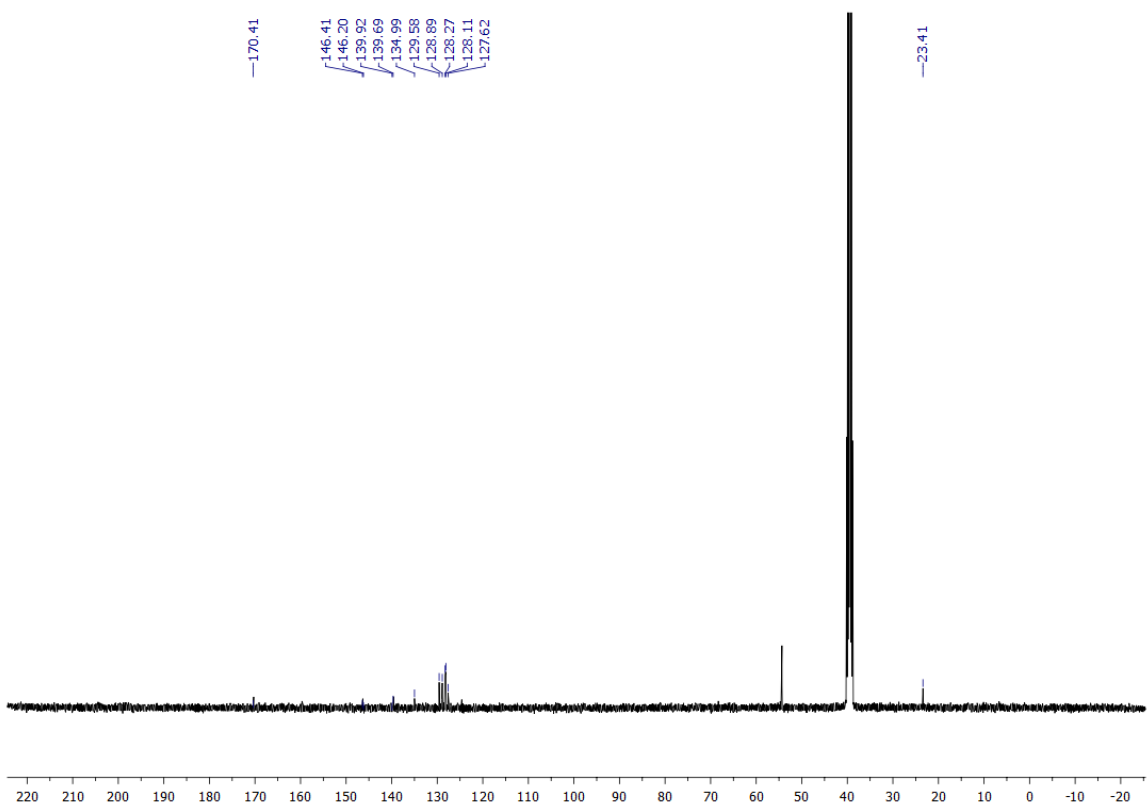


Figure S 123: ^{13}C -NMR (101 MHz, DMSO) of compound 40

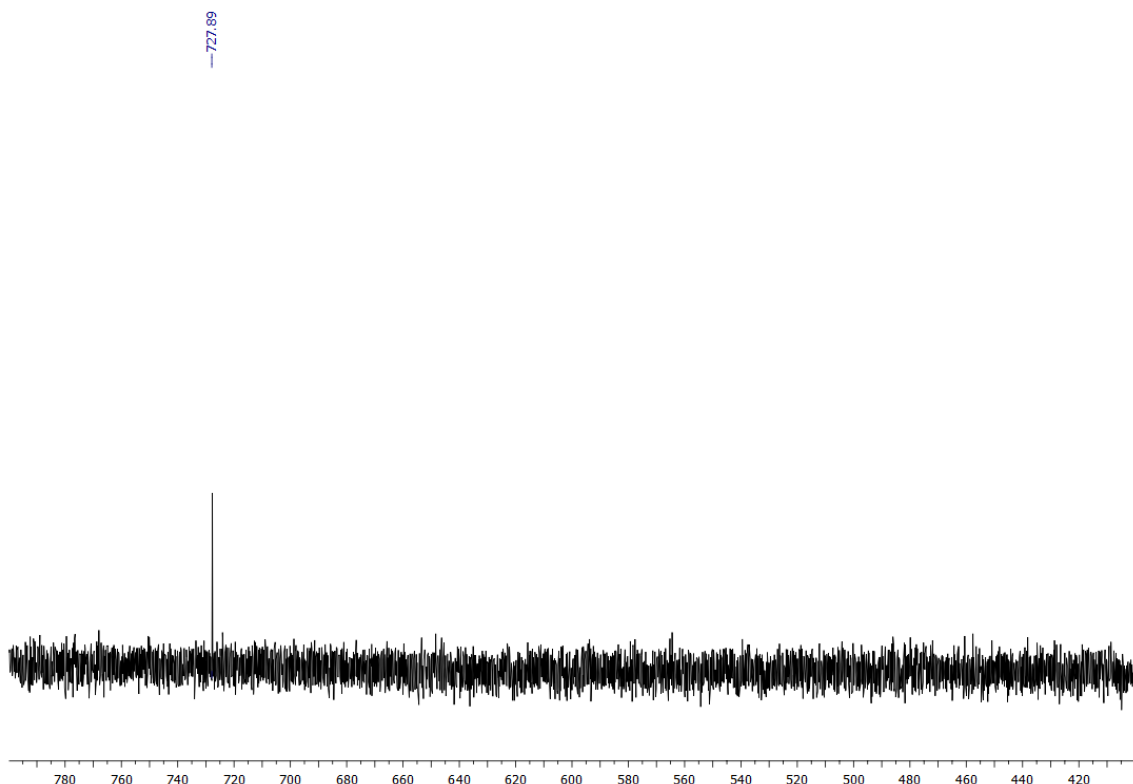


Figure S 124: ^{77}Se -NMR (76 MHz, DMSO) of compound 40

Table S 1: Crystallographic and refinement details

	1c	2a	2b	2c	3	5	6a	9
Identification code	2082322	2082323	2082320	2082340	2082337	2082329	2082333	2082310
Empirical formula	C ₈ H ₇ NOSe	C ₇ H ₈ N ₂ Se	C ₈ H ₁₀ N ₂ Se	C ₈ H ₁₀ N ₂ OSe	C ₁₅ H ₁₂ N ₂ Se	C ₁₆ H ₁₄ N ₂ OSe	C ₄₂ H ₃₄ I ₄ N ₄ Se ₂	C ₁₀ H ₁₀ N ₂ Se
Formula weight	212.11	199.11	213.14	229.14	299.23	329.25	1260.25	237.16
Temperature/K	150	149.95(10)	150(2)	100(2)	149.95(10)	293	293(2)	100(2)
Crystal system	triclinic	monoclinic	monoclinic	triclinic	monoclinic	monoclinic	triclinic	monoclinic
Space group	P-1	P2 ₁ /c	P2 ₁ /n	P-1	P2 ₁ /n	P2 ₁ /c	P-1	P2 ₁ /c
a/Å	6.7205(8)	5.5760(4)	5.4997(2)	6.8563(7)	5.82360(10)	15.743(4)	9.0766(3)	8.9398(5)
b/Å	7.2682(6)	15.3311(12)	8.7494(3)	8.6186(9)	14.8625(4)	14.932(3)	9.3878(3)	13.5971(8)
c/Å	9.6442(10)	8.9604(7)	18.1394(6)	8.9293(9)	28.3043(7)	6.025(2)	26.4138(9)	8.0283(4)
α/°	75.195(8)	90	90	64.562(2)	90	90	85.946(3)	90
β/°	77.439(9)	92.257(7)	95.204(3)	71.488(2)	92.380(2)	92.28(3)	86.233(3)	98.000(3)
γ/°	63.877(10)	90	90	82.846(2)	90	90	82.743(3)	90
Volume/Å ³	405.92(8)	765.40(10)	869.25(5)	451.79(8)	2447.72(10)	1415.1(8)	2223.42(13)	966.39(9)
Z	2	4	4	2	8	4	2	4
ρ _{calc} g/cm ³	1.735	1.728	1.6286	1.684	1.624	1.545	1.882	1.630
μ/mm ⁻¹	4.562	4.826	4.255	4.108	3.049	2.650	4.473	4.864
F(000)	208	392	423.8	228	1200	664.0	1188	472
Crystal size/mm ³	0.13 × 0.13 × 0.02	0.07 × 0.05 × 0.03	0.07 × 0.07 × 0.03	0.156 × 0.067 × 0.030	0.1 × 0.1 × 0.07	0.17 × 0.14 × 0.05	0.1 × 0.06 × 0.04	0.267 × 0.052 × 0.026
2Θ range for data collection/°	6.35 to 58.812	5.268 to 58.732	5.18 to 58.86	2.643 to 33.137	5.118 to 58.77	5.854 to 66.47	4.704 to 58.732	5.964 to 72.062
Reflections collected	3494	6596	4053	13695	13416	7840	22080	17433
Independent reflections	1862 [R _{int} = 0.0245]	1840 [R _{int} = 0.0246]	1979 [R _{int} = 0.0320]	3450 [R _{int} = 0.0300]	5718 [R _{int} = 0.0278]	4808 [R _{int} = 0.0384]	10309 [R _{int} = 0.0268]	1879 [R _{int} = 0.1044]
Data/restraints/parameters	1862/0/101	1840/0/91	1979/0/101	3450 / 0 / 110	5718/0/325	4808/0/182	10309/0/469	1879 / 0 / 124
Goodness-of-fit on F ²	1.023	1.067	1.036	1.073	1.117	1.047	1.027	1.169
Final R indexes [I>=2σ (I)]	R ₁ = 0.0279, wR ₂ = 0.0587	R ₁ = 0.0216, wR ₂ = 0.0469	R ₁ = 0.0335, wR ₂ = 0.0678	R ₁ = 0.0181, wR ₂ = 0.0441	R ₁ = 0.0363, wR ₂ = 0.0754	R ₁ = 0.612, wR ₂ = 0.1552	R ₁ = 0.0441, wR ₂ = 0.0945	R ₁ = 0.0440, wR ₂ = 0.1097
Final R indexes [all data]	R ₁ = 0.0351, wR ₂ = 0.0619	R ₁ = 0.0269, wR ₂ = 0.0487	R ₁ = 0.0559, wR ₂ = 0.0770	R ₁ = 0.0204, wR ₂ = 0.0448	R ₁ = 0.0534, wR ₂ = 0.0819	R ₁ = 0.1130, wR ₂ = 0.2038	R ₁ = 0.0655, wR ₂ = 0.1043	R ₁ = 0.0737, wR ₂ = 0.1264
Largest diff. peak/hole / e Å ⁻³	0.42/-0.41	0.33/-0.29	0.42/-0.54	0.6/-0.3	0.47/-0.55	0.74/-0.98	2.35/-1.10	0.9/-1.2

	10	HBr of 11	15	16	20	HBr of 20	21	22
Identification code	2082330	2082321	2082324	2082331	2082326	2082311	2082325	2082327
Empirical formula	C ₉ H ₈ N ₂ Se	C ₁₆ H ₁₅ BrN ₂ Se	C ₂₀ H ₁₆ N ₂ Se	C ₁₄ H ₁₈ N ₂ Se	C ₁₇ H ₁₆ N ₂ OSe	C ₁₇ H ₁₇ BrN ₂ OSe	C ₁₇ H ₁₆ N ₂ O ₂ Se	C ₂₂ H ₁₈ N ₂ OSe
Formula weight	223,13	394,17	363,31	293,26	343,28	424.19	359,28	405,34
Temperature/K	293(2)	293	293	293(2)	293(2)	100(2)	293(2)	293
Crystal system	monoclinic	monoclinic	monoclinic	monoclinic	monoclinic	monoclinic	orthorhombic	monoclinic
Space group	P2 ₁ /n	P2 ₁ /c	P2 ₁ /c	P2 ₁ /n	P2 ₁ /c	P2 ₁ /n	P2 ₁ 2 ₁ 2 ₁	P2 ₁ /c
a/Å	10.2757(10)	10.1315(7)	18.4368(11)	12.0668(8)	17.1141(12)	12.3164(16)	5.8504(6)	20.0700(15)
b/Å	7.4876(4)	16.5406(6)	15.0933(7)	5.9975(4)	14.9993(11)	8.9214(7)	14.9303(17)	15.2032(6)
c/Å	12.4378(9)	9.9513(7)	5.8505(3)	19.6436(10)	5.8375(3)	15.6592(8)	34.867(4)	5.8117(3)
α/°	90	90	90	90	90	90	90	90
β/°	113.119(10)	108.711(7)	97.977(5)	101.538(6)	90.174(6)	108.748(5)	90	91.309(6)
γ/°	90	90	90	90	90	90	90	90
Volume/Å ³	880.12(13)	1579.51(18)	1612.28(15)	1392.90(15)	1498.48(17)	1629.3(3)	3045.5(6)	1772.84(18)
Z	4	4	4	4	4	4	8	4
ρ _{calc} g/cm ³	1.684	1.658	1.497	1.398	1.522	1.729	1.567	1.519
μ/mm ⁻¹	4.207	4.898	2.329	2.677	2.506	4.760	2.474	2.131
F(000)	440	776	736	600	696	840	1456	824
Crystal size/mm ³	0.06 × 0.04 × 0.01	0.11 × 0.03 × 0.02	0.08 × 0.08 × 0.05	0.1 × 0.07 × 0.03	0.11 × 0.09 × 0.04	0.07 × 0.06 × 0.06	0.08 × 0.05 × 0.03	0.15 × 0.09 × 0.03
2θ range for data collection/°	6.504 to 58.596	4.908 to 59.098	5.214 to 58.868	6.592 to 66.622	4.76 to 58.97	2.664 to 33.157	4.674 to 59.054	4.864 to 58.87
Reflections collected	4228	7801	8388	7552	12900	33756	10985	9527
Independent reflections	2053 [R _{int} = 0.0252]	3648 [R _{int} = 0.0678]	3757 [R _{int} = 0.0287]	4758 [R _{int} = 0.0327]	3641 [R _{int} = 0.0954]	6206 [R _{int} = 0.0315]	6409 [R _{int} = 0.0267]	4183 [R _{int} = 0.0297]
Data/restraints/parameters	2053/0/109	3648/0/182	3757/0/209	4758/0/158	3641/0/192	6206 / 0 / 201	6409/0/402	4183/0/236
Goodness-of-fit on F ²	1.026	0.967	1.053	1.035	1.041	1.072	1.022	1.049
Final R indexes [I>=2σ (I)]	R ₁ = 0.0429, wR ₂ = 0.0867	R ₁ = 0.0519, wR ₂ = 0.1068	R ₁ = 0.0448, wR ₂ = 0.0869	R ₁ = 0.0416, wR ₂ = 0.0887	R ₁ = 0.0647, wR ₂ = 0.1626	R ₁ = 0.0219, wR ₂ = 0.0504	R ₁ = 0.0429, wR ₂ = 0.0689	R ₁ = 0.0506, wR ₂ = 0.0835
Final R indexes [all data]	R ₁ = 0.0781, wR ₂ = 0.1012	R ₁ = 0.1036, wR ₂ = 0.1455	R ₁ = 0.0720, wR ₂ = 0.0981	R ₁ = 0.0819, wR ₂ = 0.1093	R ₁ = 0.1118, wR ₂ = 0.2042	R ₁ = 0.0281, wR ₂ = 0.0530	R ₁ = 0.0714, wR ₂ = 0.0781	R ₁ = 0.1048, wR ₂ = 0.1001
Largest diff. peak/hole / e Å ⁻³	0.75/-0.54	0.54/-0.62	0.36/-0.33	0.41/-0.49	0.72/-0.56	0.6/-0.8	0.42/-0.36	0.30/-0.45
Flack parameter	-	-	-	-	-	-	0.360(12)	-

	35	36	37	38S	38	39Au	40	1x	1y
Identification code	2082312	2082313	2082315	2082319	2124335	2082316	2082317	2082318	2082314
Empirical formula	C ₁₇ H ₁₅ N ₃ O ₃ Se	C ₂₅ H ₁₈ N ₂ OSe	C ₂₂ H ₂₂ N ₂ OSeSi	C ₂₀ H ₁₈ HgN ₂ O ₃ S	C ₁₉ H ₁₆ HgN ₂ O ₃ Se	C ₂₂ H ₂₇ AuCl ₅ N ₃ OSe	C ₃₄ H ₂₆ N ₄ O ₂ Se ₂	C ₂₀ H ₁₅ N ₃ Se	C ₂₀ H ₁₅ N ₃ Se ₂
Formula weight	388.28	441.37	437.46	567.01	599.89	802.64	680.51	376.31	455.27
Temperature/K	100(2)	100(2)	150.00(10)	149.99(10)	100(2)	150.00(10)	150.00(10)	149.99(10)	100(2)
Crystal system	monoclinic	monoclinic	monoclinic	monoclinic	orthorhombic	triclinic	orthorhombic	monoclinic	monoclinic
Space group	P2 ₁ /n	P2 ₁ /c	P2 ₁ /c	P2 ₁ /n	Pna2 ₁	P-1	Fdd2	P2 ₁ /c	P2 ₁ /c
a/Å	6.5934(5)	10.4198(3)	9.7971(14)	16.6567(6)	6.707(6)	9.3257(3)	32.8581(13)	9.1913(5)	5.6550(7)
b/Å	15.4919(13)	20.7557(7)	9.649(5)	5.30189(19)	37.73(2)	15.8788(5)	19.1605(7)	15.8059(9)	21.4410(13)
c/Å	16.150(4)	9.4600(3)	22.573(5)	21.3913(11)	21.564(13)	19.2008(5)	9.2637(4)	11.5894(6)	14.4120(10)
α/°	90	90	90	90	90	89.872(2)	90	90	90
β/°	100.715(13)	96.5460(10)	94.575(18)	93.073(4)	90	87.129(2)	90	101.324(5)	94.671(5)
γ/°	90	90	90	90	90	82.845(2)	90	90	90
Volume/Å ³	1620.9(4)	2032.58(11)	2127.1(12)	1088.0	5456(7)	2817.57(15)	5832.2(4)	1650.89(16)	1741.6(3)
Z	4	4	4	4	12	4	8	4	4
ρ _{calc} g/cm ³	1.591	1.442	1.366	1.997	2.191	1.892	1.550	1.514	1.736
μ/mm ⁻¹	2.337	1.866	1.835	8.293	7.401	7.008	2.575	2.280	2.954
F(000)	784	896	896	1088.0	3384.0	1544.0	2736	760.0	896.0
Crystal size/mm ³	0.16 × 0.02 × 0.01	0.118 × 0.072 × 0.041	0.12 × 0.04 × 0.02	0.09×0.07×0.02	0.05 × 0.025 × 0.01	0.06 × 0.05 × 0.02	0.08 × 0.07 × 0.06	0.13 × 0.06 × 0.05	0.06 × 0.01 × 0.01
2Θ range for data collection/°	2.884 to 32.029	2.779 to 31.225	5.302 to 58.682	6.046 to 59.094	0.942 to 25.122	4.796 to 58.92	5.04 to 70.148	5.204 to 58.486	2.976 to 53.808
Reflections collected	17003	54159	11082	10250	91571	27875	11284	8150	36538
Independent reflections	5623 [R _{int} = 0.0690]	6553 [R _{int} = 0.0353]	4978 [R _{int} = 0.0371]	10250 [R _{int} = 0.0543]	14592 [R _{int} = 0.0584]	12825 [R _{int} = 0.0295]	4827 [R _{int} = 0.0356]	3810 [R _{int} = 0.0219]	5668 [R _{int} = 0.0441]
Data/restraints/parameters	5623/0/220	6553/0/263	4978/0/248	10250/0/248	14592/1/709	12825/56/646	4827/1/191	3810/0/217	5668/0/226
Goodness-of-fit on F ²	1,034	1,159	1.045	1.045	1.042	1.027	1.042	1.024	1.054
Final R indexes [I>=2σ (I)]	R ₁ = 0.0545, wR ₂ = 0.1099	R ₁ = 0.0445, wR ₂ = 0.1187	R ₁ = 0.0402. wR ₂ = 0.0894	R ₁ = 0.0392, wR ₂ = 0.0893	R ₁ = 0.0406. wR ₂ = 0.1079	R ₁ = 0.0306. wR ₂ = 0.0641	R ₁ = 0.0300. wR ₂ = 0.0640	R ₁ = 0.0284. wR ₂ = 0.0605	R ₁ = 0.0264. wR ₂ = 0.0619
Final R indexes [all data]	R ₁ = 0.0955, wR ₂ = 0.1261	R ₁ = 0.0551, wR ₂ = 0.1224	R ₁ = 0.0666. wR ₂ = 0.1017	R ₁ = 0.0555, wR ₂ = 0.0926	R ₁ = 0.0437. wR ₂ = 0.1098	R ₁ = 0.0426. wR ₂ = 0.0689	R ₁ = 0.0373. wR ₂ = 0.0668	R ₁ = 0.0374. wR ₂ = 0.0643	R ₁ = 0.0313. wR ₂ = 0.0645
Largest diff. peak/hole / e Å ⁻³	0.6/-1.6	1.9/-0.7	0.70/-0.48	1.48/-1.27	3.8/-1.2	2.25/-1.28	0.63/-0.28	0.35/-0.35	0.65/-0.76
Flack parameter	-	-	-	-	-	-	0.012(6)	-	-

Experimental details of the X-ray structure determinations

Diffraction data were collected at 150 K using a Rigaku Oxford Diffraction Gemini E Ultra diffractometer, equipped with an EOS CCD area detector and a four-circle kappa goniometer. For the data collection, the Mo source emitting graphite-monochromated Mo-K α radiation ($\lambda = 0.71073 \text{ \AA}$) was used. Data integration, scaling and empirical absorption correction was carried out using the CrysAlis Pro program package [1]. Crystals of compound **38** were very small. Data was therefore collected at beamline P11 with an energy of 20 keV ($\lambda = 0.619900 \text{ \AA}$) at PETRA III DESY Hamburg. For data integration XDS [2] and for scaling as well as absorption correction SADABS was used [3]. The structures were solved using Direct Methods and refined by Full-Matrix-Least-Squares against F2 using SHELXT [4] and SHELXL [5]. Non-hydrogen atoms were refined anisotropically and hydrogen atoms were placed at idealized positions and refined using the riding model. All calculations were carried out using the Olex2 graphical interface [6].

References

1. *CrysAlisPro 40.53, 40.53*; Rigaku Oxford Diffraction Ltd.: Oxford (U.K.), 2019.
2. Kabsch, W. *XDS. Acta Cryst.* **2010**, *D66*, 125-132.
3. Sheldrick, G.M. *SADABS 2.03*; Universität Göttingen, Germany: 2002.
4. Sheldrick, G.M. SHELXT - Integrated space-group and crystal-structure determination. *Acta Cryst.* **2015**, *A71*, 3-8.
5. Sheldrick, G.M. Crystal structure refinement with SHELXL. *Acta Cryst.* **2015**, *C71*, 3-8.
6. Dolomanov, O.V.; Bourhis, L.J.; Gildea, R.J.; Howard, J.A.K.; Puschmann, H. OLEX2: a complete structure solution, refinement and analysis program. *J. Appl. Cryst.* **2009**, *42*, 339-341.



Community for Open
Antimicrobial Drug Discovery

Hit-Confirmation

Antimicrobial screening, Cytotoxicity & Haemolysis

Procedure and Materials

Content

1.0 Summary	3
1.1 Study	3
1.2 Assay Parameters	3
1.3 Outcomes	3
1.4 Structural Novelty	4
1.5 Publishing CO-ADD Data	4
2.0 Methods	5
2.1 Sample Preparation.....	5
2.2 Antibacterial Assay	5
2.2.1 Procedure.....	5
2.2.2 Analysis.....	5
2.3 Antifungal Assay	6
2.3.1 Procedure.....	6
2.3.2 Analysis.....	6
2.4 Cytotoxicity Assay	7
2.4.1 Procedure.....	7
2.4.2 Analysis.....	7
2.5 Haemolysis Assay	7
2.5.1 Procedure.....	7
2.5.2 Analysis.....	7
2.6 Antibiotic, Cytotoxic and Haemolytic Standards Preparation and Quality Control.....	8
3.0 Materials	9
3.1 Assay Materials	9
3.2 Standards	9
3.3 Microbial strains and cell lines	9
4.0 Controls	10
4.1 Antimicrobial susceptibility of tested strains	10
4.1.1 Antibiotic standards	10
4.1.2 Antifungal standard	10
4.2 Susceptibility profile of cell lines	10
4.3 Susceptibility profile of human washed red cells	11
4.4 Outcome	11

1.0 Summary

1.1 Study

Hit Confirmation of active compounds by whole cell growth inhibition assays was conducted as an 8-point dose response to determine the Minimum Inhibitory Concentration (MIC), in duplicate (n=2). The inhibition of growth is measured against those microorganisms that showed susceptibility to the compounds tested in the Primary Screen.

Included in the Hit Confirmation were 5 bacteria: *Escherichia coli*, *Klebsiella pneumoniae*, *Acinetobacter baumannii*, *Pseudomonas aeruginosa* and *Staphylococcus aureus*, and 2 fungi *Candida albicans* and *Cryptococcus neoformans*.

In addition to determining MIC, active compounds were counter screened for cytotoxicity against a human embryonic kidney cell line, HEK293, by determining their CC₅₀ value. The compounds were also screened for haemolysis of human red blood cells.

1.2 Assay Parameters

Assay Parameters	Bacteria	Fungi	HEK293	Haemolysis
Test concentration	32 - 0.25 µg/mL or 20 – 0.15 µM ≤0.5% DMSO	32 - 0.25 µg/mL or 20 – 0.15 µM ≤0.5% DMSO	32 - 0.25 µg/mL or 20 – 0.15 µM ≤0.5% DMSO	32 - 0.25 µg/mL or 20 – 0.15 µM ≤0.5% DMSO
QC	Duplicate (n=2) Control MIC: Pass	Duplicate (n=2) Control MIC: Pass	Duplicate (n=2) Control CC ₅₀ : Pass	Duplicate (n=2) Control HC ₁₀ : Pass
Plates	Non-Binding Surface (NBS), 384-well plate	Non-Binding Surface (NBS), 384-well plate	TC, 384-well black wall/clear bottom	Polypropylene 384-well and polystyrene 384- well plates
Media	Cation-adjusted Mueller Hinton broth	Yeast Nitrogen Base	DMEM supplemented with 10% FBS	0.9% NaCl
Read Out	OD ₆₀₀	OD ₆₃₀ Resazurin OD ₆₀₀₋₅₇₀	Resazurin F _{560/590}	OD ₄₀₅

1.3 Outcomes

Hit Confirmation outcomes are detailed in individual Project reports, personalised for each Project Submission for each CO-ADD user.

Please see your data sheet with file extension **P0XXX_HC_data.xlsx**, for example
CO-ADD Project **P0100**, **P0100_HC_data.xlsx**

1.4 Structural Novelty

As per the T&C's of CO-ADD, structures for all submitted compounds for antimicrobial screening should be disclosed to CO-ADD following Primary Screening. Without structures for all submitted compounds, Hit Confirmation assays will not be triggered.

If you have not already done so, please **provide CO-ADD with the chemical structure** of the full sample set in this study (both for compounds showing activity and those that do not), which will allow CO-ADD to filter out future samples with the same, or highly similar structure. In addition, please **notify CO-ADD** if you agree to publish the data (*i.e.* structures and activity) in the public bioactive database ChEMBL (www.ebi.ac.uk/chembl/). CO-ADD aims to increase the public knowledge of antimicrobial research, including data about non-active compounds.

All confirmed hits, without cytotoxicity or haemolytic activity, will be considered for further Hit-Validation, after a detailed analysis of structure-activity relationship and antimicrobial novelty, within CO-ADD samples, as well as, within public antimicrobial activity databases, like ChEMBL (www.ebi.ac.uk/chembl/).

1.5 Publishing CO-ADD Data

If you wish to publish data provided by CO-ADD, we kindly ask that you acknowledge CO-ADD appropriately with the following reference:

Helping Chemists Discover New Antibiotics
M.A. Blaskovich, J. Zuegg, A.G. Elliott, M.A. Cooper
ACS Infect. Dis., **2015**, 1(7), 285-287.
DOI: [10.1021/acsinfecdis.5b00044](https://doi.org/10.1021/acsinfecdis.5b00044); PMID: [27622818](https://pubmed.ncbi.nlm.nih.gov/27622818/)

as well as an acknowledgement for the funding of CO-ADD:

“The antimicrobial screening performed by CO-ADD (The Community for Antimicrobial Drug Discovery) was funded by the Wellcome Trust (UK) and The University of Queensland (Australia).”

Please advise CO-ADD at your earliest convenience that you have used provided data for publication purposes. This information is extremely helpful in keeping track of the outputs from the CO-ADD initiative and supports the program in renewed funding possibilities to continue CO-ADD as a free screening service available to the academic community.

CO-ADD also asks, that where possible you publish your data in an Open Access journals.

2.0 Methods

2.1 Sample Preparation

Samples were provided by the collaborator and stored frozen at -20 °C. Samples were prepared in DMSO and water to a final testing concentration of 32 µg/mL or 20 µM (unless otherwise indicated in the data sheet) and serially diluted 1:2 fold for 8 times. Each sample concentration was prepared in 384-well plates, non-binding surface plate (**NBS**; Corning 3640) for each bacterial/fungal strain, tissue-culture treated (**TC-treated**; Corning 3712/3764) black for mammalian cell types and polypropylene 384-well (**PP**; Corning 3657) for haemolysis assays, all in duplicate (n=2), and keeping the final DMSO concentration to a maximum of 0.5%. All the sample preparation was done using liquid handling robots.

Compounds that showed notable solubility issues during stock solution preparation are detailed in the **Data sheet** for the individual Project.

2.2 Antibacterial Assay

2.2.1 Procedure

All bacteria were cultured in Cation-adjusted Mueller Hinton broth (**CAMHB**) at 37 °C overnight. A sample of each culture was then diluted 40-fold in fresh broth and incubated at 37 °C for 1.5-3 h. The resultant mid-log phase cultures were diluted (CFU/mL measured by OD₆₀₀), then added to each well of the compound containing plates, giving a cell density of 5×10⁵ CFU/mL and a total volume of 50 µL. All the plates were covered and incubated at 37 °C for 18 h without shaking.

2.2.2 Analysis

Inhibition of bacterial growth was determined measuring absorbance at 600 nm (OD₆₀₀), using a Tecan M1000 Pro monochromator plate reader. The percentage of growth inhibition was calculated for each well, using the negative control (media only) and positive control (bacteria without inhibitors) on the same plate as references.

The percentage of growth inhibition was calculated for each well, using the negative control (media only) and positive control (bacteria without inhibitors) on the same plate. The MIC was determined as the lowest concentration at which the growth was fully inhibited, defined by an inhibition ≥ 80%. In addition, the maximal percentage of growth inhibition is reported as D_{Max}, indicating any compounds with partial activity.

Hits were classified by MIC ≤ 16 µg/mL or MIC ≤ 10 µM in either replicate (n=2 on different plates).

2.3 Antifungal Assay

2.3.1 Procedure

Fungi strains were cultured for 3 days on Yeast Extract-Peptone Dextrose (YPD) agar at 30 °C. A yeast suspension of 1×10^6 to 5×10^6 CFU/mL (as determined by OD₅₃₀) was prepared from five colonies. The suspension was subsequently diluted and added to each well of the compound-containing plates giving a final cell density of fungi suspension of 2.5×10^3 CFU/mL and a total volume of 50 µL. All plates were covered and incubated at 35 °C for 36 h without shaking.

2.3.2 Analysis

Growth inhibition of *C. albicans* was determined measuring absorbance at 630 nm (OD₆₃₀), while the growth inhibition of *C. neoformans* was determined measuring the difference in absorbance between 600 and 570 nm (OD₆₀₀₋₅₇₀), after the addition of resazurin (0.001% final concentration) and incubation at 35 °C for 2 h. The absorbance was measured using a Biotek Multiflo Synergy HTX plate reader.

In both cases, the percentage of growth inhibition was calculated for each well, using the negative control (media only) and positive control (fungi without inhibitors) on the same plate. The MIC was determined as the lowest concentration at which the growth was fully inhibited, defined by an inhibition ≥ 80% for *C. albicans* and an inhibition ≥ 70% for *C. neoformans*. Due to a higher variance in growth and inhibition, a lower threshold was applied to the data for *C. neoformans*. In addition, the maximal percentage of growth inhibition is reported as D_{Max}, indicating any compounds with marginal activity.

Hits were classified by MIC ≤ 16 µg/mL or MIC ≤ 10 µM in either replicate (n=2 on different plates).

2.4 Cytotoxicity Assay

2.4.1 Procedure

HEK293 cells were counted manually in a Neubauer haemocytometer and then plated in the 384-well plates containing the compounds to give a density of 5000 cells/well in a final volume of 50 µL. **DMEM** supplemented with **10% FBS** was used as growth media and the cells were incubated together with the compounds for 20 h at 37 °C in 5% CO₂.

2.4.2 Analysis

Cytotoxicity (or cell viability) was measured by fluorescence, ex: 560/10 nm, em: 590/10 nm (F_{560/590}), after addition of 5 µL of 25 µg/mL resazurin (2.3 µg/mL final concentration) and after incubation for further 3 h at 37 °C in 5% CO₂. The fluorescence intensity was measured using a Tecan M1000 Pro monochromator plate reader, using automatic gain calculation.

CC₅₀ (concentration at 50% cytotoxicity) were calculated by curve fitting the inhibition values vs. log(concentration) using a sigmoidal dose-response function, with variable fitting values for bottom, top and slope. In addition, the maximal percentage of cytotoxicity is reported as D_{Max}, indicating any compounds with partial cytotoxicity.

The curve fitting was implemented using Pipeline Pilot's dose-response component, resulting in similar values to curve fitting tools such as GraphPad's Prism and IDBS's XIFit. Any value with > indicate sample with no activity (low D_{Max} value) or samples with CC₅₀ values above the maximum tested concentration (higher D_{Max} value).

Cytotoxic samples were classified by CC₅₀ ≤ 32 µg/mL or CC₅₀ ≤ 10 µM in either replicate (n=2 on different plates). In addition, samples were flagged as partial cytotoxic if D_{Max} ≥ 50%, even with CC₅₀ > the maximum tested concentration.

2.5 Haemolysis Assay

2.5.1 Procedure

Human whole blood was washed three times with 3 volumes of 0.9% NaCl and then resuspended in same to a concentration of 0.5 × 10⁸ cells/mL, as determined by manual cell count in a Neubauer haemocytometer. The washed cells were then added to the 384-well compound-containing plates for a final volume of 50 µL. After a 10 min shake on a plate shaker the plates were then incubated for 1 h at 37 °C. After incubation, the plates were centrifuged at 1000g for 10 min to pellet cells and debris, 25 µL of the supernatant was then transferred to a polystyrene 384-well assay plate.

2.5.2 Analysis

Haemolysis was determined by measuring the supernatant absorbance at 405 nm (OD₄₀₅). The absorbance was measured using a Tecan M1000 Pro monochromator plate reader.

HC₁₀ and HC₅₀ (concentration at 10% and 50% haemolysis, respectively) were calculated by curve fitting the inhibition values vs. log(concentration) using a sigmoidal dose-response function with variable fitting values for top, bottom and slope. In addition, the maximal

percentage of haemolysis is reported as D_{Max} , indicating any compounds with partial haemolysis.

The curve fitting was implemented using Pipeline Pilot's dose-response component, resulting in similar values to curve fitting tools such as GraphPad's Prism and IDBS's XIFit. Any value with > indicate sample with no activity (low D_{Max} value) or samples with HC_{10} values above the maximum tested concentration (higher D_{Max} value).

Haemolysis samples were classified by $HC_{10} \leq 32 \mu\text{g/mL}$ or $HC_{10} \leq 10 \mu\text{M}$ in either replicate ($n=2$ on different plates). In addition, samples were flagged as partial haemolytic if $D_{Max} \geq 50\%$, even with $HC_{10} >$ the maximum tested concentration.

2.6 Antibiotic, Cytotoxic and Haemolytic Standards Preparation and Quality Control

Colistin and Vancomycin were used as positive bacterial inhibitor standards for Gram-negative and Gram-positive bacteria, respectively. Fluconazole was used as a positive fungal inhibitor standard for *C. albicans* and *C. neoformans*. Tamoxifen was used as a positive cytotoxicity standard. Melittin was used as a positive haemolytic standard.

Each antibiotic standard was provided in 4 concentrations, with 2 above and 2 below its MIC or CC_{50} value, and plated into the first 8 wells of column 23 of the 384-well NBS plates. Tamoxifen and melittin was used in 8 concentrations in 2 fold serial dilutions with 50 $\mu\text{g/mL}$ highest concentration.

The quality control (QC) of the assays was determined by Z'-Factor, calculated from the Negative (media only) and Positive Controls (bacterial, fungal or cell culture without inhibitor), and the Standards. Plates with a Z'-Factor of ≥ 0.4 and Standards active at the highest and inactive at the lowest concentration, were accepted for further data analysis.

3.0 Materials

3.1 Assay Materials

Material	Code	Brand/Supplier	Cat No.
Compound preparation plate, Polypropylene	PP	Corning	3364
Assay Plates – Antimicrobial Non-binding surface	NBS 384w	Corning	3640
Assay Plates – Cytotoxicity Tissue culture treated	Black/Clear bottom 384w	Corning	3712
Assay Plates - Haemolysis	PP-Haem	Corning	3657
Reading Plates - Haemolysis	Clear 384w	Corning	3680
Growth media - bacteria	CAMHB	Bacto Laboratories	212322
Culture agar - fungi	YPD	Becton Dickinson	242720
Growth media - fungi	YNB	Becton Dickinson	233520
Resazurin		Sigma-Aldrich	R7017
Dulbecco's Modified Eagle Medium	DMEM	Life Technologies	11995-073
Foetal Bovine Serum	FBS	Bovogen	FFBS-500
0.9% NaCl	Saline	Baxter	AHF7124

3.2 Standards

Sample Name	Sample ID	Full MW	Stock Conc. (mg/mL)	Solvent	Source
Colistin - Sulfate	MCC_000094:02	1400.63	10.0	DMSO	Sigma; C4461
Vancomycin - HCL	MCC_000095:02	1485.71	10.0	DMSO	Sigma; 861987
Fluconazole	MCC_008383:01	306.27	2.56	DMSO	Sigma; F8929
Tamoxifen	MCC_000096:01	371.50	10	DMSO	Sigma; T5648
Melittin	MCC_008868:02	2846.46	10	Water	Sigma; M2272

3.3 Microbial strains and cell lines

ID	Batch	Organism	Strain	Description
GN_001	02	<i>Escherichia coli</i>	ATCC 25922	FDA control strain
GN_003	02	<i>Klebsiella pneumoniae</i>	ATCC 700603	MDR
GN_034	02	<i>Acinetobacter baumannii</i>	ATCC 19606	Type strain
GN_042	02	<i>Pseudomonas aeruginosa</i>	ATCC 27853	Quality control strain
GP_020	02	<i>Staphylococcus aureus</i>	ATCC 43300	MRSA
FG_001	01	<i>Candida albicans</i>	ATCC 90028	CLSI reference
FG_002	01	<i>Cryptococci neoformans</i>	ATCC 208821	H99, Type strain
MA_007	02	<i>Homo sapiens</i> embryonic kidney cells	ATCC CRL-1573	HEK 293
HA_150	-	<i>Homo sapiens</i>	ARCBS 5400 00150	Whole blood

4.0 Controls

4.1 Antimicrobial susceptibility of tested strains

Values are the average of ≥ 6 independent biological replicates. All values are within the expected range as per CLSI guidelines.

4.1.1 Antibiotic standards

MIC determined by BMD method, CA-MHB, Corning 3640 384 NBS plates		GN_001:02 <i>Escherichia coli</i> FDA Control ATCC 25922	GN_003:02 <i>Klebsiella pneumoniae</i> ESBL ATCC 700603	GN_034:02 <i>Acinetobacter baumannii</i> Type strain ATCC 19606	GN_042:02 <i>Pseudomonas aeruginosa</i> QC strain ATCC 27853
Compound	Compound Type	MIC ($\mu\text{g/mL}$)			
Colistin - sulfate	Antibiotic	0.125	0.25	0.25	0.25

MIC determined by BMD method, CA-MHB, Corning 3640 384 NBS plates		GP_020:02 <i>Staphylococcus aureus</i> MRSA ATCC 43300
Compound	Compound Type	MIC ($\mu\text{g/mL}$)
Vancomycin - HCl	Antibiotic	1

4.1.2 Antifungal standard

MIC determined by BMD method, YNB, Corning 3640 384 NBS plates		FG_001:02 <i>Candida albicans</i> CLSI reference ATCC 90028	FG_002:02 <i>Cryptococcus neoformans H99</i> Type strain ATCC 208821
Compound	Compound Type	MIC ($\mu\text{g/mL}$)	
Fluconazole	Antifungal	0.125	8

4.2 Susceptibility profile of cell lines

Values are the average of > 6 independent biological replicates. CC ₅₀ is the concentration at 50% cytotoxicity.		MA_007 HEK293 ATCC CRL-1573
Compound	Compound Type	CC ₅₀ ($\mu\text{g/mL}$)
Tamoxifen	PKC inhibitor	9
		2.2

4.3 Susceptibility profile of human washed red cells

		HA_150 Human Whole blood ARCBS 00150			
Compound	Compound Type	HC ₁₀ (µg/mL)		HC ₅₀ (µg/mL)	
Average	Stdev	Average	Stdev		
Melittin	Haemolytic peptide	2.7	0.9	8.5	2.5

4.4 Outcome

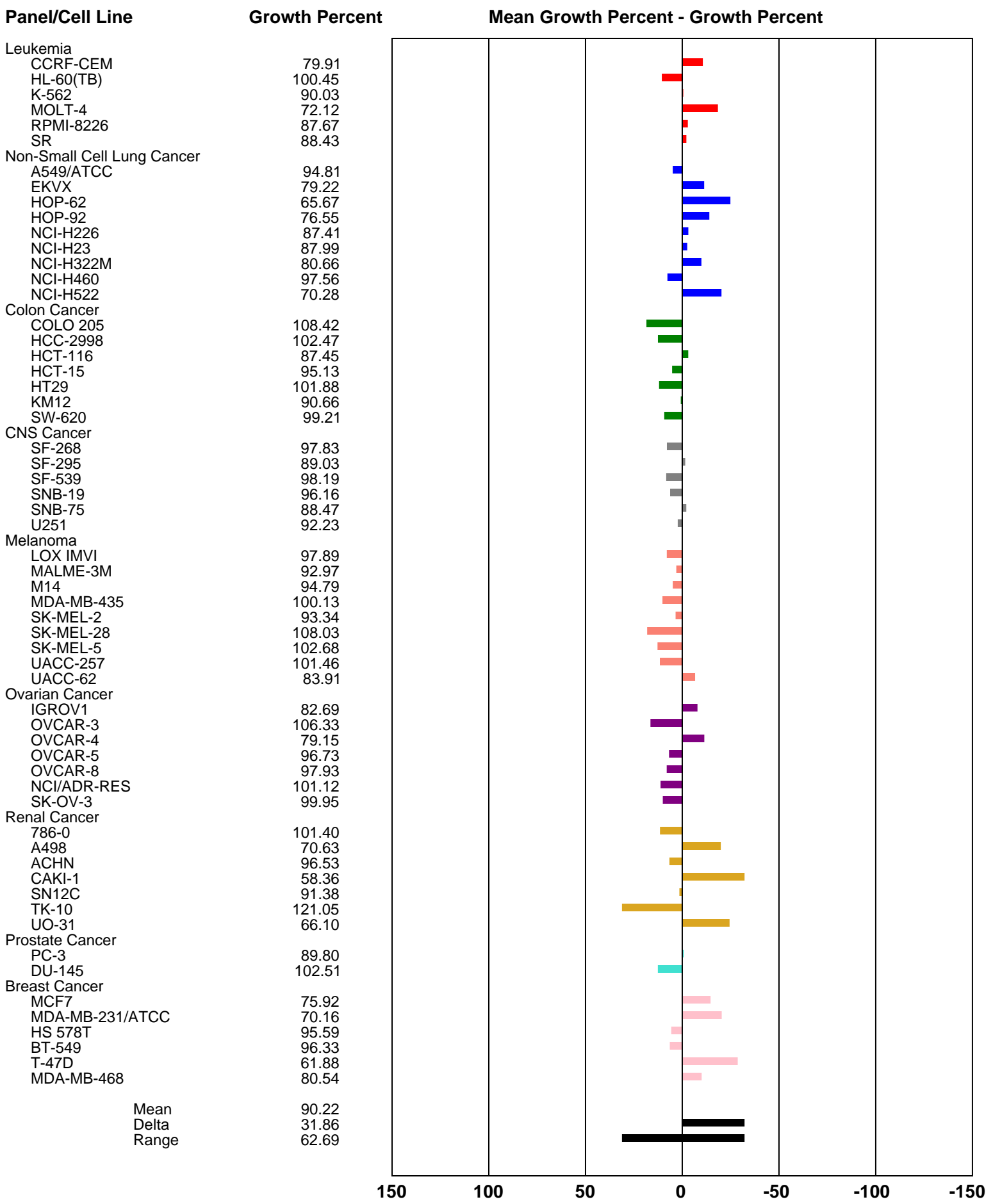
All standard compound controls displayed inhibitory values within the expected range for each assay type and each organism tested. For further information please contact the CO-ADD team at support@co-add.org.

Strain ID	Species	Standard positive inhibitor control	Pass/Fail
GN_001:02	<i>E. coli</i>	Colistin	Pass
GN_003:02	<i>K. pneumoniae</i> (MDR)	Colistin	Pass
GN_034:02	<i>A. baumannii</i>	Colistin	Pass
GN_042:02	<i>P. aeruginosa</i>	Colistin	Pass
GP_020:02	<i>S. aureus</i> (MRSA)	Vancomycin	Pass
FG_001:01	<i>C. albicans</i>	Fluconazole	Pass
FG_002:01	<i>C. neoformans</i> (H99)	Fluconazole	Pass
MA_007:02	<i>Homo sapiens</i> HEK293	Tamoxifen	Pass
HA_150	<i>Homo sapiens</i>	Melittin	Pass

One Dose Mean Graph

Experiment ID: 1812OS48

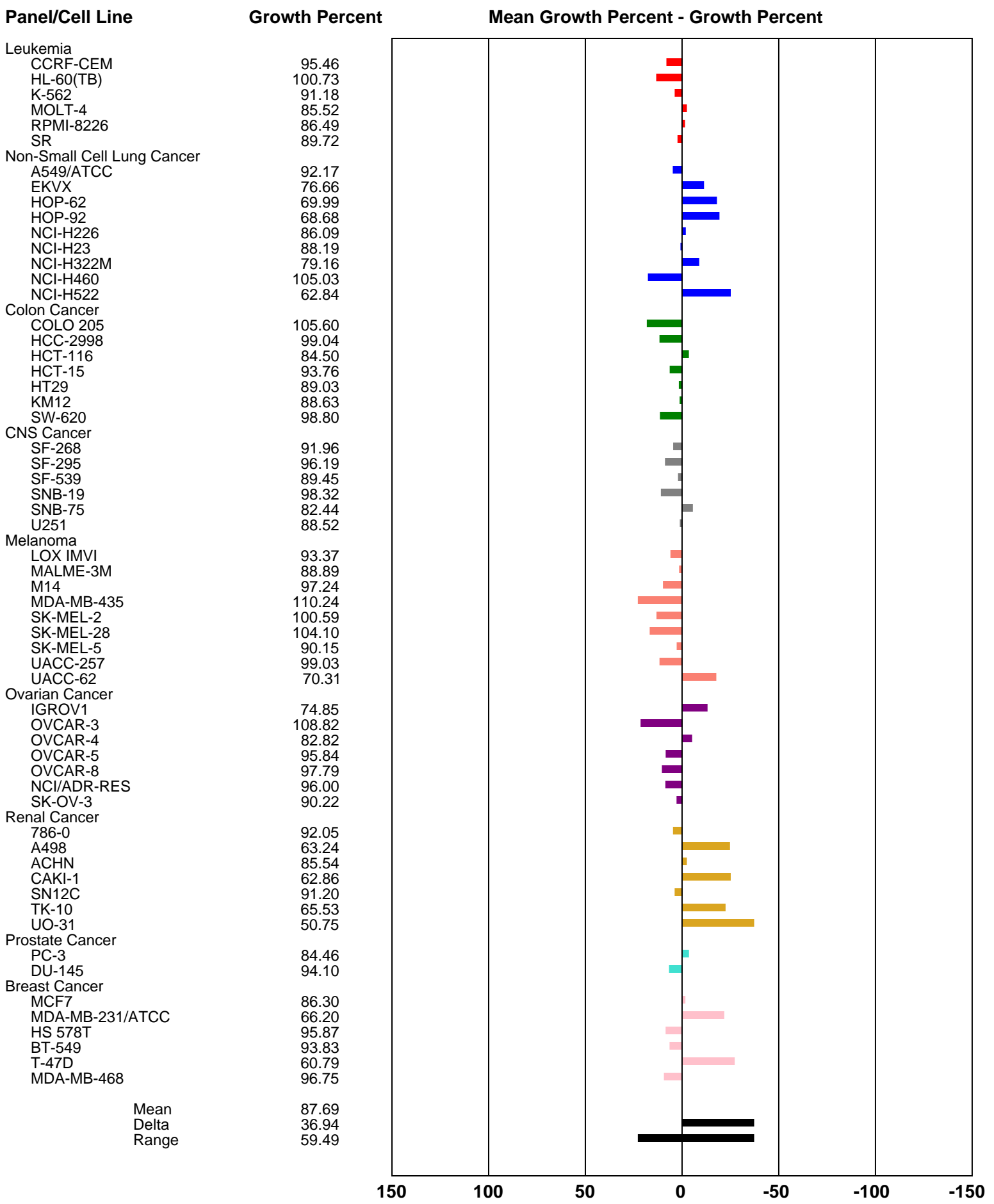
Report Date: Jan 14, 2019



One Dose Mean Graph

Experiment ID: 1812OS48

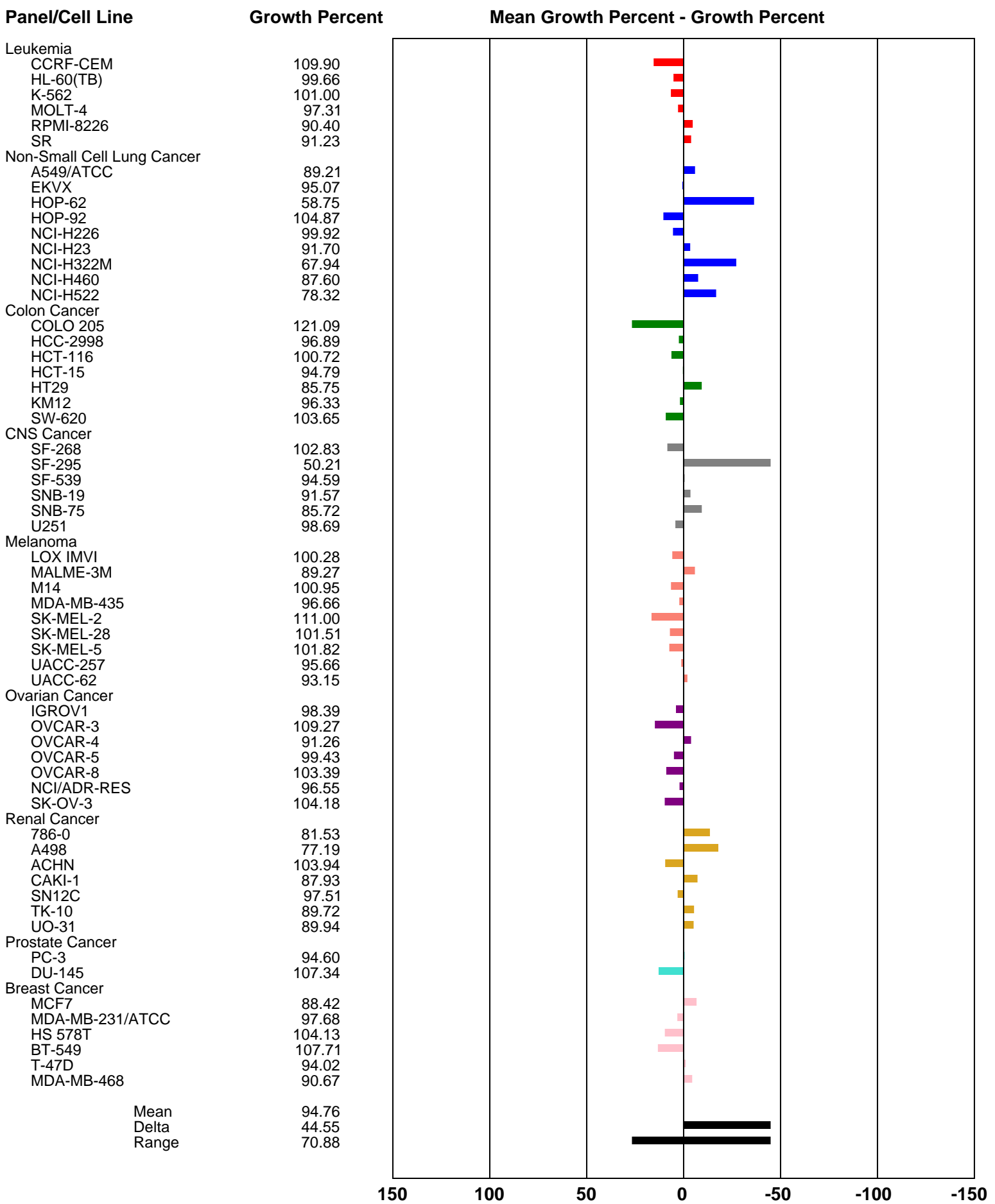
Report Date: Jan 14, 2019



One Dose Mean Graph

Experiment ID: 1812OS48

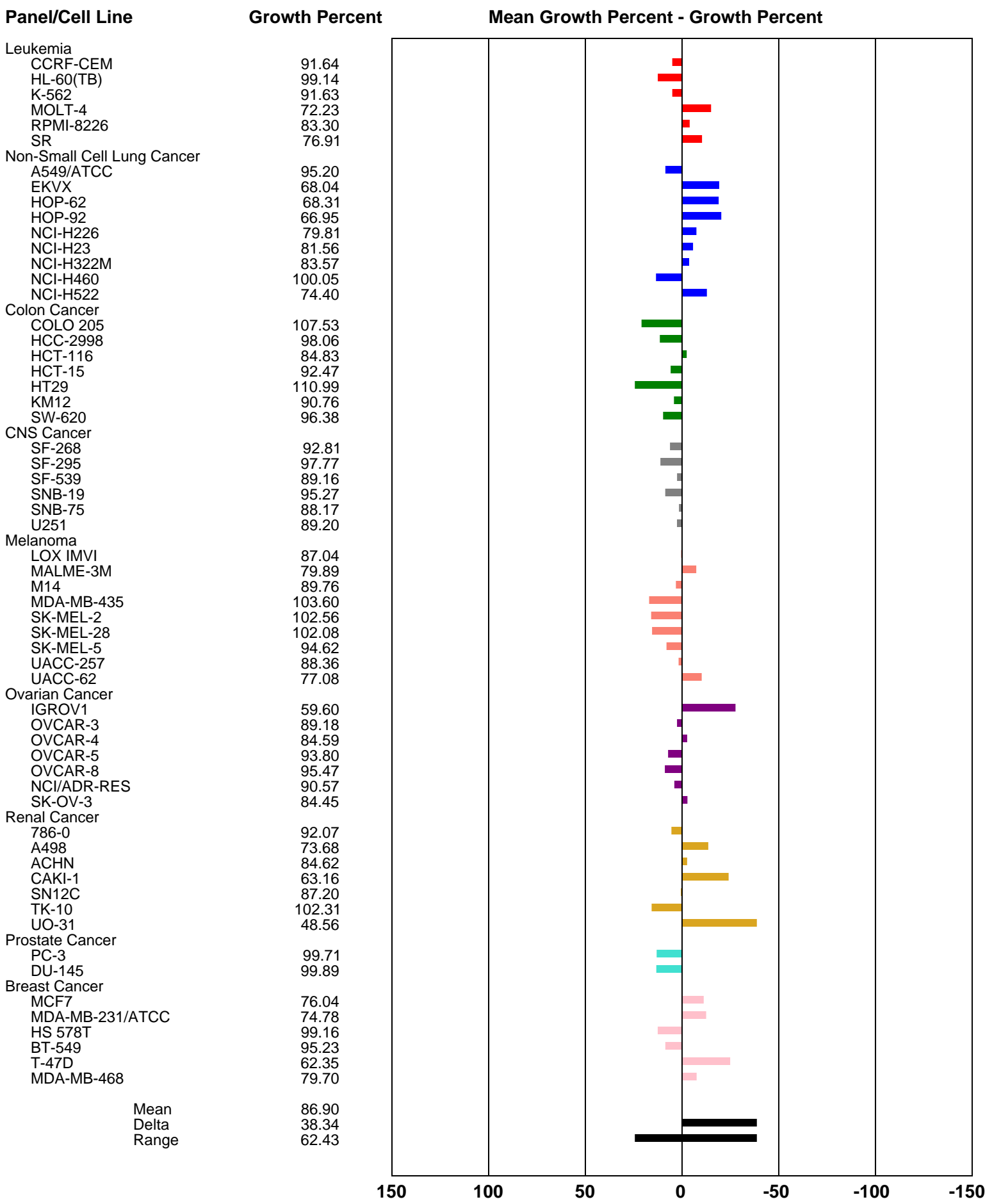
Report Date: Jan 14, 2019



One Dose Mean Graph

Experiment ID: 1812OS48

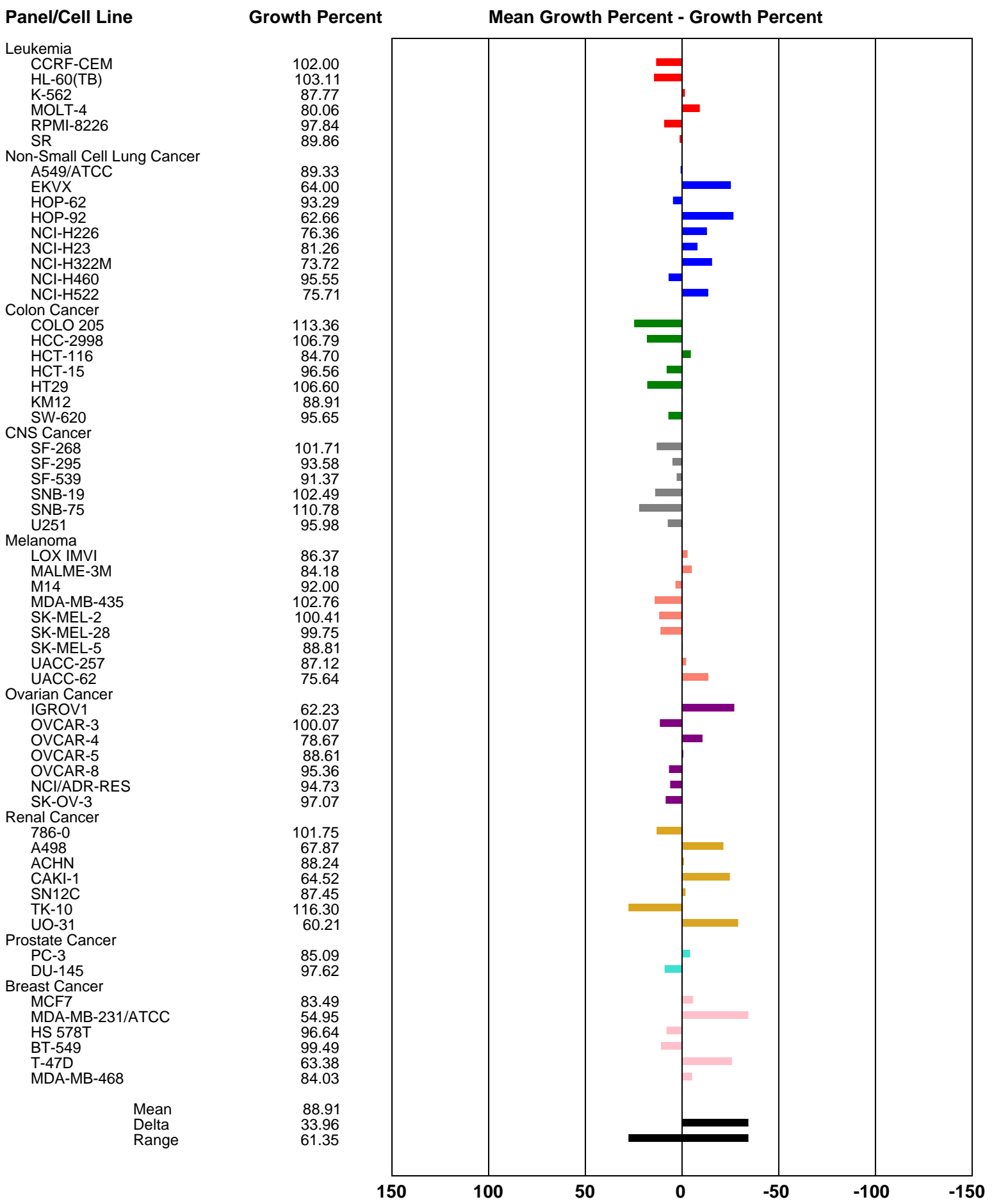
Report Date: Jan 14, 2019



One Dose Mean Graph

Experiment ID: 1812OS48

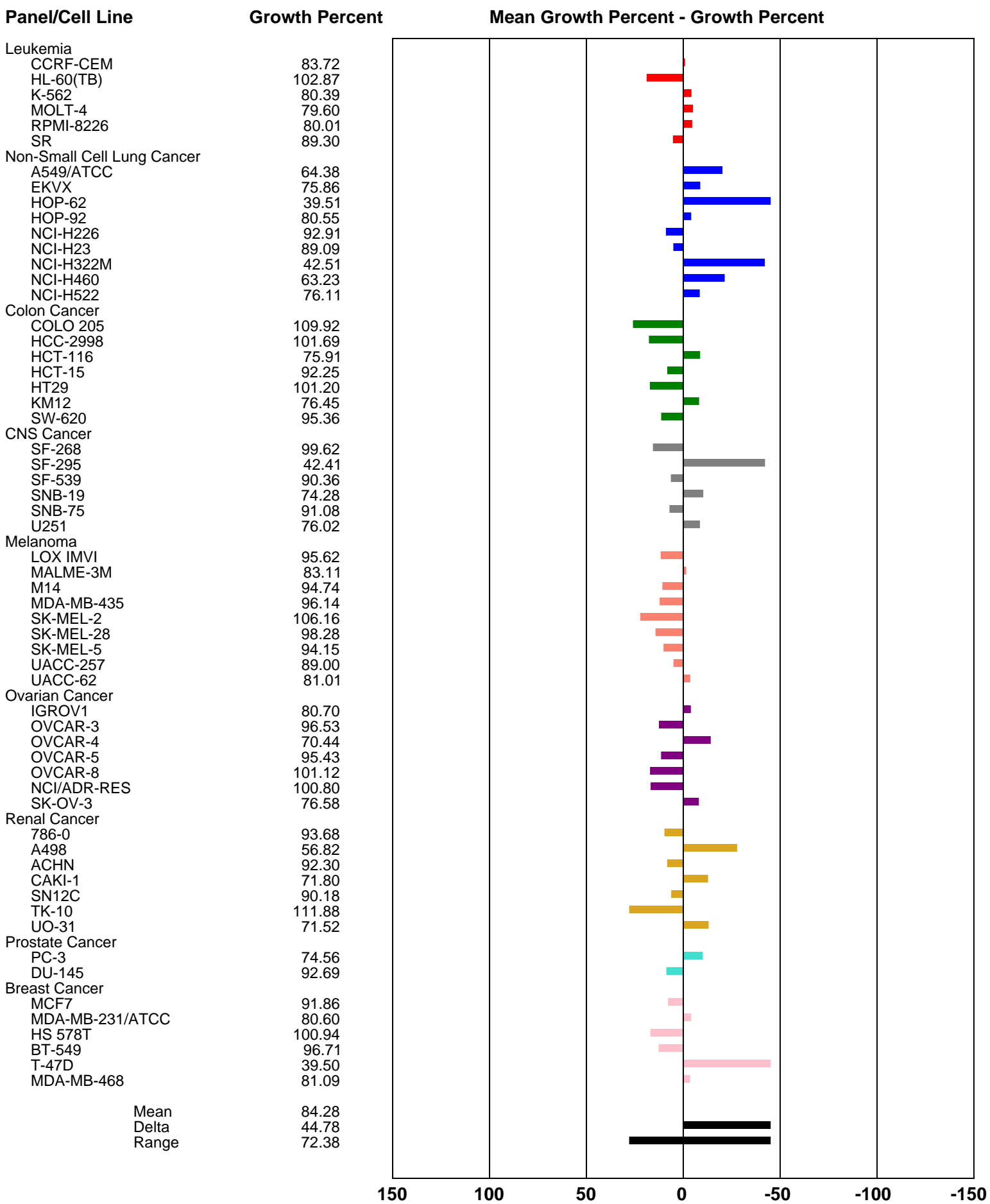
Report Date: Jan 14, 2019



One Dose Mean Graph

Experiment ID: 1812OS48

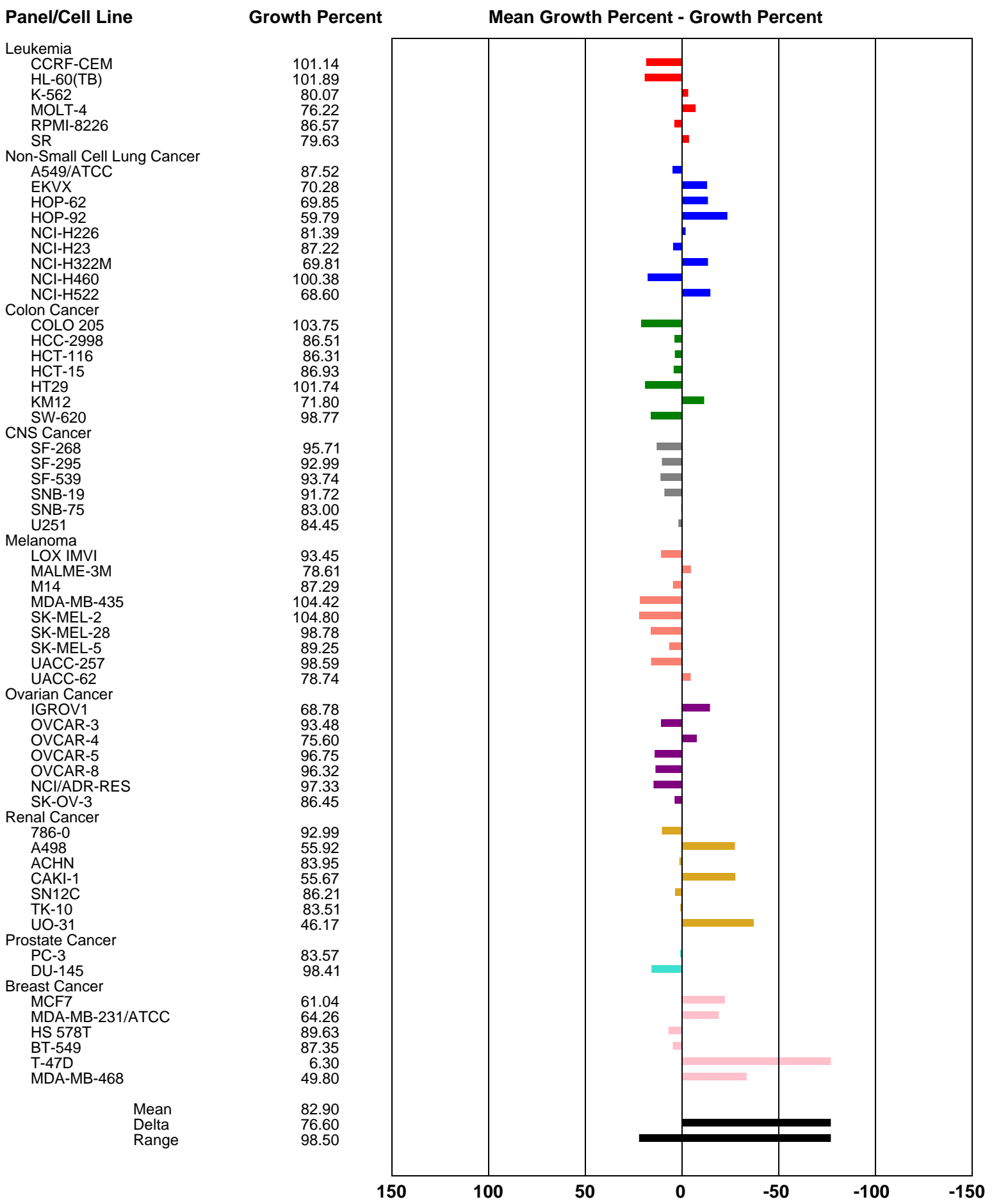
Report Date: Jan 14, 2019



One Dose Mean Graph

Experiment ID: 1812OS48

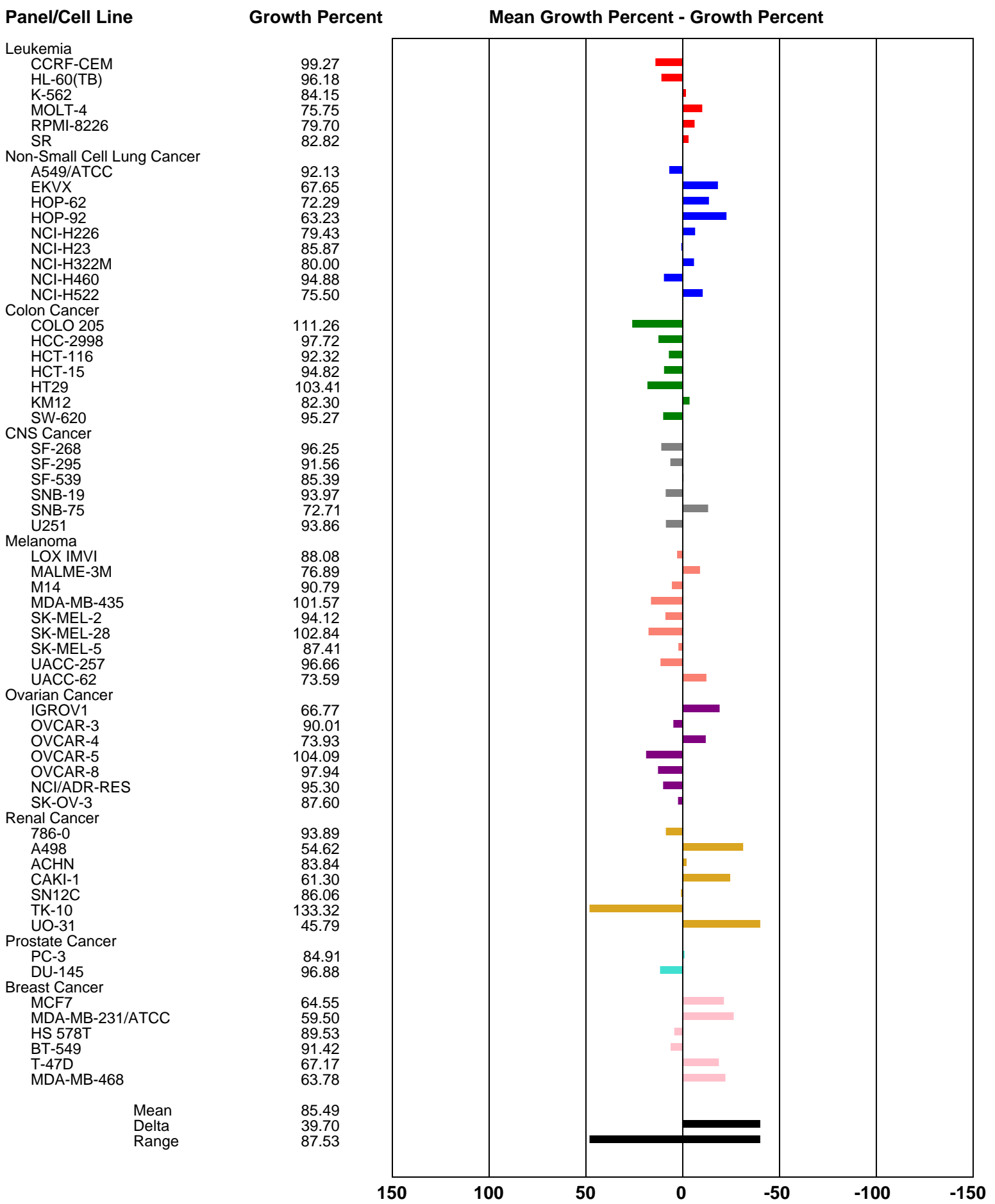
Report Date: Jan 14, 2019



One Dose Mean Graph

Experiment ID: 1812OS48

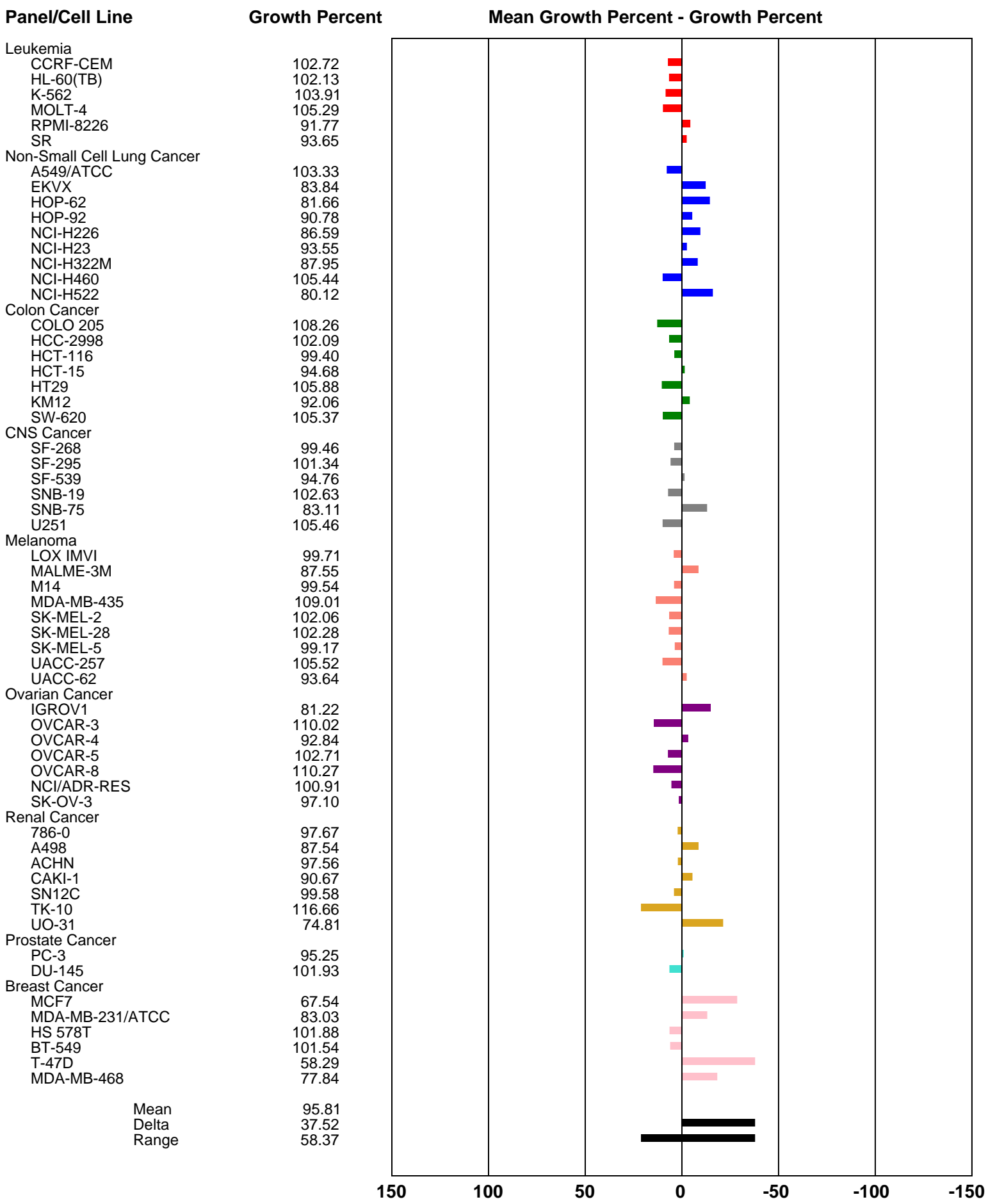
Report Date: Jan 14, 2019



One Dose Mean Graph

Experiment ID: 1812OS48

Report Date: Jan 14, 2019



One Dose Mean Graph

Experiment ID: 1812OS48

Report Date: Jan 14, 2019

